

PL ISSN 0028-3894

arg 2

C 165

ASSOCIATION OF POLISH  
NEUROPATHOLOGISTS  
and  
MEDICAL RESEARCH CENTRE,  
POLISH ACADEMY OF SCIENCES

# NEUROPATHOLOGIA POLSKA

A-23

337, Dwon

VOLUME 30

1992

NUMBER 2

---

WROCLAW · WARSZAWA · KRAKÓW  
ZAKŁAD NARODOWY IM. OSSOLIŃSKICH  
WYDAWNICTWO POLSKIEJ AKADEMII NAUK

<http://rcin.org.pl>

# NEUROPATHOLOGIA POLSKA

## QUARTERLY

---

VOLUME 30

1992

NUMBER 2

---

### EDITORIAL COUNCIL

Maria Dąmbska, Jerzy Dymecki, Krystyna Honczarenko, Danuta  
Maślińska, Mirosław J. Mossakowski, Halina Weinrauder

### EDITORS

Editor-in-Chief: Irmina B. Zelman

Co-editors: Wiesława Biczyskova, Halina Kroh, Mirosław J. Mossakowski,  
Mieczysław Wender

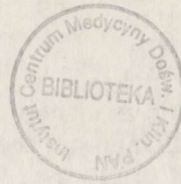
Secretary: Anna Taraszewska

Technical Secretary: Teresa Miodowska

### EDITORIAL OFFICE

Medical Research Centre  
Dworkowa 3, 00-784 Warszawa, Poland, Phone: 49-54-10

The typescript of the present issue was delivered to the publisher 15.05.1992 r.



MARIA DĄMBSKA

## PERINATAL DAMAGE OF BRAIN STEM DEPENDING ON THE MATURITY OF ITS STRUCTURES

Laboratory of Developmental Neuropathology, Medical Research Centre, Polish Academy of Sciences, Warsaw, Poland

The aim of this study was to discuss the interaction between the maturation of the brain stem and its susceptibility to perinatal lesion. Many observations indicate that the last months of pregnancy and the perinatal period are the time of intensive maturation of these structures. Lesions of the brain stem were many times found after acute anoxia as well as after chronic asphyxia during this period. This indicates the importance of prevention of the pathology of pregnancy. Occurring in the last trimester of gestation it can induce damage of brain stem centers important for the fetus to survive the stress of birth and adaptation for individual life.

*Key words: brain stem, perinatal pathology.*

The interdependence between the stage of the central nervous system (CNS) development and the character of structural abnormalities appearing during the first trimester of intrauterine life is well known. The prolonged morpho- and histogenesis of the CNS depending upon the phylogenetical age of their structures results in protraction of the teratogenic period until the second half of pregnancy. This period overlaps the next stage of development characterized by intensive maturation of nerve tissue with its increased metabolism and energetic requirements. This makes several brain structures particularly susceptible to damaging factors inducing severe lesions.

Such susceptibility of the brain stem in the pre- and postnatal period, higher than when its maturation became accomplished, was observed in some neuropathological examinations (Norman 1972; Griffiths, Laurence 1974). Nevertheless correlations between the maturation process and changes found in the examined cases are difficult to analyse, because of the complexity of the brain stem organization.

Only summarizing the results of investigations concerning particular structures can we follow the course of brain stem maturation. This exhibits a high intensity during the second half of pregnancy and in the perinatal period. At that time oxygen consumption increases markedly testifying to the activity of metabolism. The maturation processes follow basic morphogenesis which takes place in the brain stem during the first three months of intrauterine

life. The cranial nerve nuclei are well discernible as early as the end of the second month, but their neurons are still very immature. In the course of the consecutive process — the large neurons develop faster than the small ones. Their axons arise and grow, the amount of cytoplasm increases in comparison with the volume of the nucleus, the organelles and the dendritic tree develop as visible even in routine examination (Figs 1a, b).

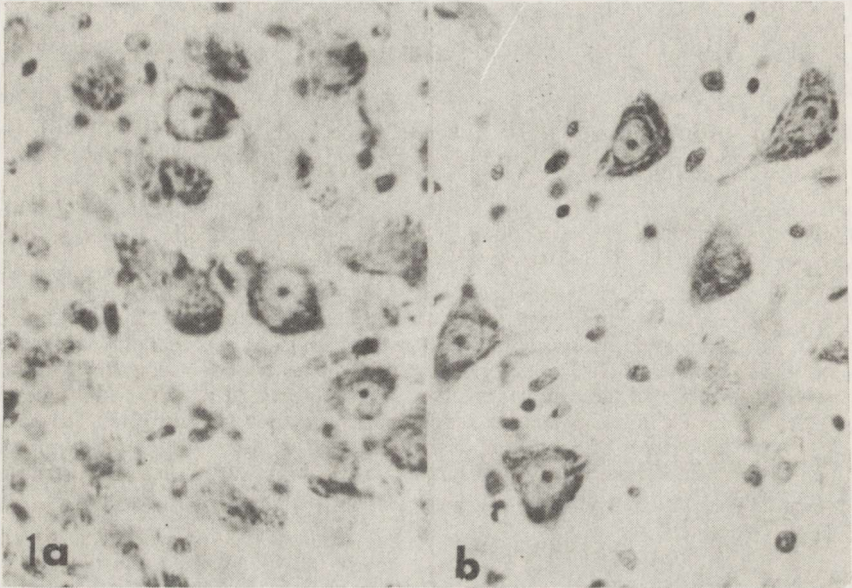


Fig. 1. Neurons of facial nerve: a) 26<sup>th</sup> week of gestation, b) 38<sup>th</sup> week of gestation. Cresyl-violet.  $\times 400$

More detailed analysis of the maturation process was performed in some structures. Inagaki et al. (1987) used the histo-morphometric method of nerve cells examination and found intensive maturation of the acoustic nucleus during 28–32 weeks of gestation. Examination of synaptic development, according to morphometric estimation of the number of dendritic spines visualized by Golgi impregnation, revealed the development of neurons in the hypoglossal nucleus between 20–40 weeks of gestation (Takashima, Becker 1986). The same authors also found a rapid increase of the number of dendritic spines in bulbar 'respiratory centres' during a similar period, a decrease and then stabilization after birth. In the magnocellular nucleus of the reticular formation a higher number of spines was found during 34–36 weeks of gestation, in both nuclei of the vagal nerve (motor and of solitary tract) this peak was observed between the 36<sup>th</sup> and 40<sup>th</sup> week of intrauterine life (Fig. 2).

The myelination process examined by Yakovlev and Lecours (1967), Rorke and Riggs (1969), Larroche (1977), Gilles et al. (1983) seemed to be parallel with nerve cells maturation. The review of brain stem pathways myelination presented in Table 1 indicates that it starts at the 24<sup>th</sup> week of gestation. Being differentiated in various tracts this process barely begins in some of them before

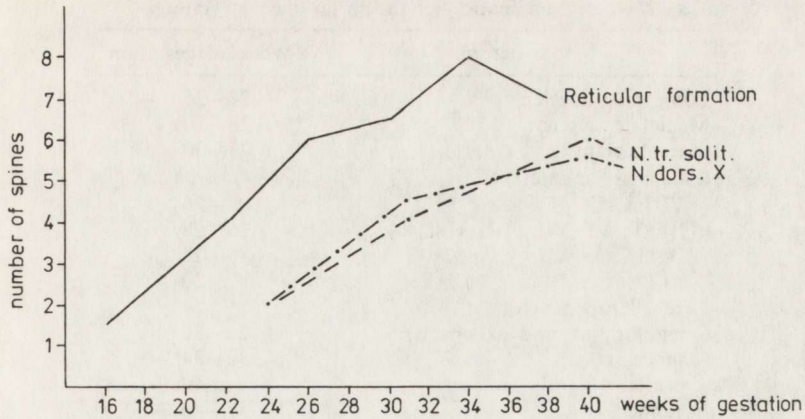


Fig. 2. Developmental changes in dendritic spine density in "respiratory centers". According to Takshina and Becker (1986)



Fig. 3. Medulla oblongata of mature newborn. Klüver-Barrera.  $\times 3$

birth, in others it is protracted for a long time after birth. In the newborn this uneven myelination of the brain stem pathways is well visible (Fig. 3).

The observations concerning brain stem lesions during maturation are parallel to the results of detailed investigations of its development. Gilles (1969) found that "hypotensive brain stem necrosis" defined by Janzer and Friede (1980) as "cardiac arrest encephalopathy" occurs much more frequently

Table 1. Myelination of the brain stem structures

Structure	Week of gestation
Long. med. fasciculi	24–26
Medial lemniscus	26–30
Lateral lemniscus	26–30
Radicles of cranial nerves	
VIII audit.	24–26
III, V, VI, VII, VIII vest.	26–28
IV, IX, X, XII	28
XI	30
Cerebellar peduncles	
inferior (int. and ext. parts)	26–36
superior	32–34 →
medial	40 →
Pyramid	38–40 →
Reticular formation	40 →

in the CNS of the newborn and very young infants than in mature brains.

The damage of brain stem structures was seen also after prolonged asphyxia. The first casuistic observations appeared about 20 years ago (Brand, Bignami 1969; Norman 1974). Then, investigations concerning the threat caused by the pathology of pregnancy for the CNS of the fetus furnished similar observations. Laure-Kamionowska (1980) examined the noxious influence of gestosis on the fetal brain. She found that, if long-lasting and leading to subacute asphyxia, gestosis results in damage of the brain stem. A similar type of lesions was observed after other types of pathology in the third trimester of pregnancy, particularly after repeated bleedings (Kamionowska, Dąbska 1979). The results cited above inclined the authors to examine the brains of newborn infants born from pregnancies complicated by placental pathology leading to prolonged fetal asphyxia. In premature newborns the brain stem lesions were generalized, including neurons of cranial nerve nuclei (Fig. 4). After 34 weeks of gestation and in infants at term the most pronounced lesions were seen in the reticular formation (Dąbska et al. 1987). A case with similar type of changes was observed earlier by Norman (1972). The time of damage coinciding with intensive formation of synapses and myelination of pathways of the reticular formation seems to be critical for its lesion.

Quattrochi et al. (1985) analysed the CNS changes in 61 infants which died with diagnosis of sudden infant death syndrome (SIDS). They found a higher than in control brains number of dendritic spines (impregnated by Golgi method) in the respiratory centers of the brain stem and admitted that this was the syndrome of brain stem immaturity of unknown origin.

Finally we examined the brains of newborns and small infants which died because of respiratory deficiency, including the classical respiratory distress syndrome (RDS). Lesions of the brain stem, particularly within the reticular formation were found in the examined cases (Fig. 5). In one half of them the neuropathological picture allowed to consider the changes as prior to the appearance of respiratory deficiency. In other cases the lesions increased

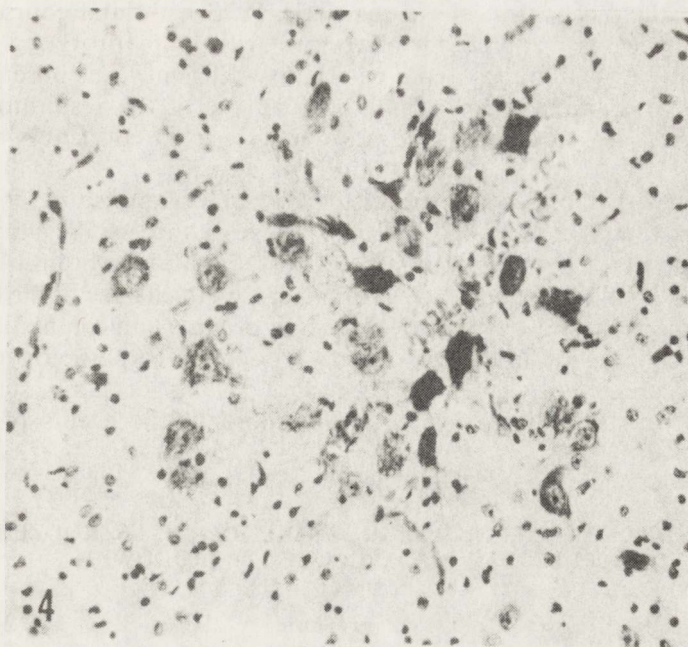


*Fig. 4. Damage of neurons of N VII. Cresyl violet.  $\times 200$*

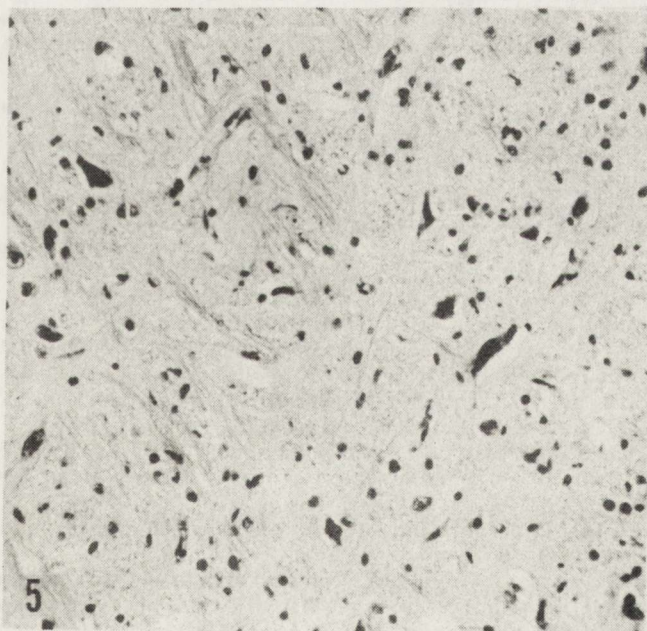


*Fig. 5. Reticular formation. Loss and lesions of neurons. Cresyl violet.  $\times 200$*

probably by the mechanism of vicious circle. RDS with fatal course occurred in a part of cases in preterm newborns with immaturity of surfactant production in lungs. In our material respiratory deficiency was observed also in newborns near term. We can admit that damage of the respiratory centers contributed to a lack of efficacy of appropriate, classical treatment of respiratory insufficiency.

The review of accidental and systematic observations presented above allows stress that the general opinion of the resistance of the brain stem to prolonged asphyxia is not true in respect to the maturing brain. At the time when the CNS has survived the stress of birth, a good efficacy of the brain stem with its respiratory and circulatory centers is of great importance. We would like to underline how important is the prevention of the pathology of the last trimester of pregnancy, which could induce lesions of brain stem centers responsible for good adaptation of the newborn to the events of birth and individual life.

#### STAN DOJRZAŁOŚCI PNIA MÓZGU JAKO PODŁOŻE USZKODZEŃ JEGO STRUKTUR W OKRESIE OKOŁOPORODOWYM

##### Streszczenie

Praca poświęcona jest omówieniu zależności między stanem dojrzałości struktur pnia mózgu a ich podatnością na uszkodzenia okołoporodowe. Przegląd wyników badań nad rozwojem pnia wskazuje, że ostatnie miesiące życia płodowego i okres okołoporodowy charakteryzuje intensywne dojrzewanie jego struktur. W tym okresie stwierdzono wielokrotnie uszkodzenie ośrodków pniowych w następstwie nie tylko ostrego niedotlenienia, ale również przewlekłej asfiksji. Podatność pnia mózgu na uszkodzenie w okresie intensywnego metabolizmu związanego z dojrzewaniem wskazuje jak ważnym jest zapobieganie patologii ciąży. Jej wpływ może bowiem na drodze asfiksji doprowadzić do uszkodzeń ośrodków pniowych o zasadniczym znaczeniu dla przeżycia porodu i adaptacji noworodka do samodzielnego życia.

##### REFERENCES

1. Brand M, Bignami A: The effect of chronic hypoxia on the neonatal and infantile brain. *Brain*, 1969, 92, 233–255.
2. Dąbska M, Laure-Kamionowska M, Liebhart M: Brainstem lesions in the course of chronic fetal asphyxia. *Clin Neuropathol*, 1987, 6, 110–115.
3. Gilles FH: Hypotensive brainstem necrosis. *Arch Pathol*, 1969, 88, 32–41.
4. Gilles FH, Shankle W, Dooling EC: Myelinated tracts: Growth patterns. In: *Developing Human Brain. Growth and Epidemiologic Neuropathology*. Ed: J. Wright, PSG Inc, Boston, London, 1983, pp 117–184.
5. Griffiths AD, Laurence KM: The effect of hypoxia and hypoglycemia on the brain of the newborn human infant. *Dev Med Child Neurol*, 1974, 16, 308–319.
6. Inagaki M, Tomita Y, Takashima S, Ohtani K, Andoh G, Takeshita K: Functional and morphometrical maturation of the brainstem auditory pathways. *Brain Dev*, 1987, 9 (6), 597–601.
7. Janzer RC, Friede RL: Hypotensive brainstem necrosis or cardiac arrest encephalopathy? *Acta Neuropathol (Berl)*, 1980, 50, 53–56.
8. Kamionowska M, Dąbska M: Ocena neuropatologiczna mózgow noworodków z cięż powikłanych patologią ostatniego trymestru. *Mat XIX Ogólnopolskiego Zjazdu Pediatrów*, Poznań, 1979, 104–105.
9. Larroche JC: *Developmental pathology of neonate*. Excerpta Med Amsterdam, London, New York, 1977.



10. Laure-Kamionowska M: Wpływ gestozy na mózg płodu. *Neuropatol Pol*, 1980, 18, 239–257.
11. Norman MC: Antenatal neuronal loss and gliosis of the reticular formation, thalamus and hypothalamus. *Neurobiology*, 1972, 22, 910–916.
12. Norman M: Unilateral encephalomalacia in cranial nerve nuclei in neonates. Report of two cases. *Neurology*, 1974, 24, 424–427.
13. Quattrochi JJ, McBride PT, Yates AJ: Brainstem immaturity in sudden infant death syndrome: A quantitative rapid Golgi study of dendritic spines in 95 infants. *Brain Res*, 1985, 325, 39–48.
14. Rorke LB, Riggs HE: Myelination of the brain in the newborn. Ed: JB Lippincott, Philadelphia-Toronto, 1969.
15. Takashima S, Becker LE: Prenatal and postnatal maturation of medullary “respiratory centres”. *Dev Brain Res*, 1986, 26, 173–177.
16. Yakovlev P, Lecours A: The myelogenetic cycles of regional maturation of the brain. In: *Regional development of the brain in early life*. Ed: A Minkowski, Oxford, Edinburgh, 1967, pp 3–70.

Author's address: Laboratory of Developmental Neuropathology, Medical Research Centre, Polish Academy of Sciences, 3 Pasteura Str, 02-093 Warsaw, Poland

GRAŻYNA SZUMAŃSKA, ROMAN GADAMSKI

LECTIN HISTOCHEMISTRY AND ALKALINE  
PHOSPHATASE ACTIVITY IN THE PIA MATER VESSELS  
OF SPONTANEOUSLY HYPERTENSIVE RATS (SHR)

Department of Neuropathology, Medical Research Centre, Polish Academy of Sciences, Warsaw,  
Poland

Some lectins were used to study the localization of sugar residues on the endothelial cell surface in the pia mater blood vessels of control (WKY) and hypertensive rats (SHR). The lectins tested recognized the following residues: beta-D-galactosyl (*Ricinus communis* agglutinin 120, RCA-1), alpha-L-fucosyl (*Ulex europaeus* agglutinin, UEA-1), N-acetylglucosaminyl and sialyl (Wheat germ agglutinin, WGA), N-glycolyl-neuraminic acid (*Limax flavus* agglutinin, LFA), and N-acetyl-D-galactosaminyl (*Helix pomatia* agglutinin, HPA). Several differences were revealed in the presence of sugar receptors on the surface of endothelial cells between the control and the hypertensive rats. Our studies showed also differences in the localization of the tested glycoconjugates between pial capillaries, small, medium-size and large pial arteries. The histochemical evaluation of alkaline phosphatase revealed an increased activity of the enzyme in the pial vessels of SHRs as compared with control rats, with a similar localization of the enzyme activity. Some differences in the distribution of lectin binding sites and alkaline phosphatase activity could be associated with the different functions of particular segments of the pial vascular network.

Key words: *lectins, glycoconjugates, pia mater vessels, rats, hypertension.*

The blood-brain barrier (BBB), a specific system controlling bidirectional exchange between the vascular bed and brain parenchyma is a well known and extensively studied biological phenomenon. Processes of intensive metabolic exchange are located mostly at the level of endothelial cells (ECs) of brain microvessels, including capillaries, precapillary arterioles and postcapillary venules. The transport across ECs, showing in most instances features of active transport, is controlled and mediated by special mechanisms, in which specific enzymatic systems are involved (Joó 1969, 1971; Oldendorf 1977; Betz, Goldstein 1978; Bradbury 1979; Betz et al. 1980; Kreutzberg, Toth 1983; Joó et al. 1983; Vorbrodtt et al. 1983). Structural and functional brain abnormalities are frequently related to the disturbances of BBB mechanisms in which the function of these enzymatic systems, located both in the cytoplasm and on the surface of ECs is either disturbed or damaged. Numerous histochemical and ultrastructural studies of recent years documented such abnormalities in

various pathological conditions (Joó et al. 1983; Vorbrodt et al. 1983, 1985; Lossinsky, Wiśniewski 1986; Szumańska, Mossakowski 1985, 1988; Szumańska 1986). However, most of the above studies indicating the important role of the vascular network in metabolic processes in the brain concerned those brain regions which are protected by the BBB, and only few of them dealt with blood vessels from those brain regions and structures which are lacking the BBB system (Mchedlishvili, Baramidze 1971; Gadamski, Baramidze 1979; Vorbrodt et al. 1984; Gadamski et al. 1989).

Several essential features distinguish cerebral microvessels in non-barrier brain regions from those characterized by the presence of the barrier system. They concern both the structure of ECs and their interrelations (presence of fenestrations, lack of intercellular tight junctions) as well as histochemical and permeability properties. This indicates that the mechanism of transport across the ECs in non-BBB regions and in pia mater vessels may be characterized by different metabolic and functional properties of their endothelial lining. This inclined us to apply a histochemical technique revealing the distribution of some chosen monosaccharide residues on the surface of the ECs in pia mater vessels both in normal and hypertensive rats. Their arrangement and distribution were compared with the localization of alkaline phosphatase (AP) activity, the enzyme participating in the active transport processes through the vessel walls (Samorajski, McCloud 1961; Vorbrodt et al. 1983).

#### MATERIAL AND METHODS

The investigations were performed on two rat strains: normal (Wistar Kyoto) (WKY) and spontaneously hypertensive (SHR) one. Animals in ether anesthesia were sacrificed by intracardiac perfusion with a fixative containing 2% paraformaldehyde and 1% glutaraldehyde in 0.1 M cacodylate buffer, pH 7.4. After 15 min of perfusion, the brains were removed from the skulls and pieces of pia mater were stripped off from the brain in Krebs-Ringer solution and placed into ice-cold fixative for 1.5 h. Pia mater specimens were then washed in PBS, pH 7.4. Part of the fixed material was used for evaluation of the AP activity according to Mayahara et al. (1967) in Vorbrodt's et al. (1981) modification in a medium containing beta-glycerophosphate as substrate. Control medium contained 0.5 mM levamisole hydrochloride as an inhibitor of AP activity.

The remaining part of fixed pia mater specimens were exposed to avidin biotinylated-horseradish peroxidase-labeled lectins for detection of specific sugar residues (methodological details in papers of Szumańska et al. 1986, 1987). Lectins revealing the following sugar residues were used: 1. Beta-D-galactosyl (*Ricinus communis* agglutinin 120) (RC-1), 2. Alpha-L-fucosyl (*Ulex europaeus* agglutinin) (UEA-1), 3. N-acetylglucosaminyl and sialyl (Wheat germ agglutinin) (WGA), 4. N-glycolyl-neuraminic acid (*Limax flavus* agglutinin) (LFA), and 5. N-acetyl-D-galactosaminyl (*Helix pomatia* agglutinin) (HPA).

After the reaction the specimens were embedded in glycerogel and examined in a light microscope concentrating especially on large (diameter above 130  $\mu\text{m}$ ), medium-size (60–130  $\mu\text{m}$ ) and small (25–60  $\mu\text{m}$ ) arteries and on what is called sphincters of offshoots (diameter about 50  $\mu\text{m}$ ).

## RESULTS

## Alkaline phosphatase (AP)

In WKY (control) rats the strongest AP reaction was observed in sphincters of offshoots of large, medium-size and small pial arteries and in the walls of capillaries, precortical and radial arterioles (Figs 1, 2). Larger arteries and other structural elements of pia mater did not exhibit AP activity. The positive reaction was completely inhibited when levamisole was added to the incubation medium. In the group of SHR rats the localization of AP activity was similar to that mentioned above, but its intensity was higher (Fig. 3). The vessel walls of SHR pia mater seemed thicker than in WKY rats. The positive reaction revealed also loosely scattered, melanine-containing cells not observed in WKY rats. In the remaining structural pial elements, AP reaction was negative.

## Lectins

In the WKY rats the majority of precortical and radial arterioles as well as large and medium-size vessels did not show even a trace reaction with RCA-1, whereas small arterioles (12–18  $\mu\text{m}$ ) were occasionally decorated with RCA-1 (Fig. 4). Pia mater vessels of SHR rats revealed moderately positive staining with this lectin. The walls of vessels about 40  $\mu\text{m}$  diameter and their offshoot sphincters showed intense labeling in the form of a homogeneously diffusional reaction (Fig. 5). Therefore, the number of galactosyl binding site receptors in the vessel walls of SHR rats was evidently greater than in WKY rats.

When UEA-1 was used to investigate the labeling of alpha-L-fucosyl residues, the localization and intensity of the staining reaction was similar to that with RCA-1. While UEA-1 agglutinin showed almost negative staining in pial vessels of WKY rats, in the SHR group the radial arterioles and arteries of 30–50  $\mu\text{m}$  diameter showed a positive homogeneous reaction of low intensity (Fig. 6). In the case of nonperfused animals the additional strong reaction with UEA-1 revealed morphotic blood elements (Fig. 7).

Monosaccharide receptors recognized by LFA agglutinin (neuraminic acid residues) were found in WKY rats in trace amounts in precortical and radial arterioles and larger size vessels (Fig. 8). In a group of SHR rats the amount of neuraminic acid receptors in the walls of pia mater vessels seemed greater: the staining reaction was more pronounced (Fig. 9). This applied mainly to the radial arterioles (compare Figs 8 and 9).

Of the five lectins tested the most intensive reaction of pia mater vessels in WKY rats was observed after incubation of the tested tissue with WGA. A characteristic feature of this reaction was its maximal intensity in precortical and radial arterioles (of 12–18  $\mu\text{m}$  diameter), while most of the remaining vessels were negative (Fig. 10). In a group of SHR rats the reaction with WGA was similar as in control rats, only somewhat stronger. An additional difference was the appearance of binding sites for WGA in the walls of vessels of about 30–60  $\mu\text{m}$  diameter (Fig. 11) and in the fiber-like structures surrounding larger pial vessels (60–130  $\mu\text{m}$ ). Under the conditions of the applied technique it was not possible to recognize whether these fibers were of collagen or elastic type.

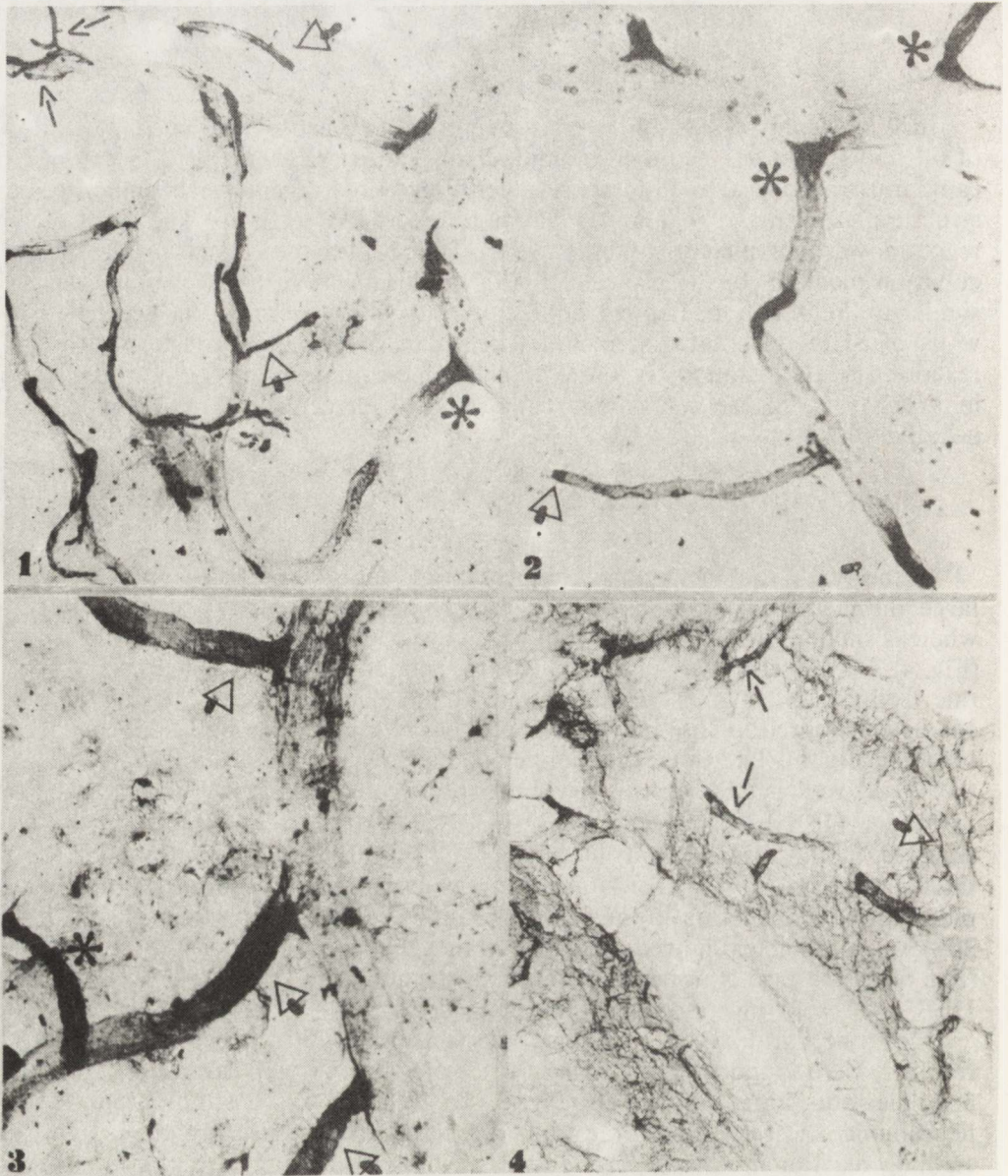


*Fig. 1.* Control rat. Reaction for AP activity. Strong staining in capillaries (arrows), radial arterioles (arrowheads) and offshoot sphincters (star).  $\times 100$

*Fig. 2.* WKY rat. Strong AP activity in radial arterioles (arrowhead) and offshoot sphincters (stars).  $\times 200$

*Fig. 3.* SHR. Very strong AP activity in offshoot sphincters (arrowheads) and in radial arterioles (star). The reaction is much stronger than in control rat (compare *Fig. 2*).  $\times 400$

*Fig. 4.* WKY rat. Moderate intensity of RCA-1 labeling in the vessel walls with diameter above 12–28  $\mu\text{m}$  (arrows). Larger vessels are unlabeled (arrowhead).  $\times 100$

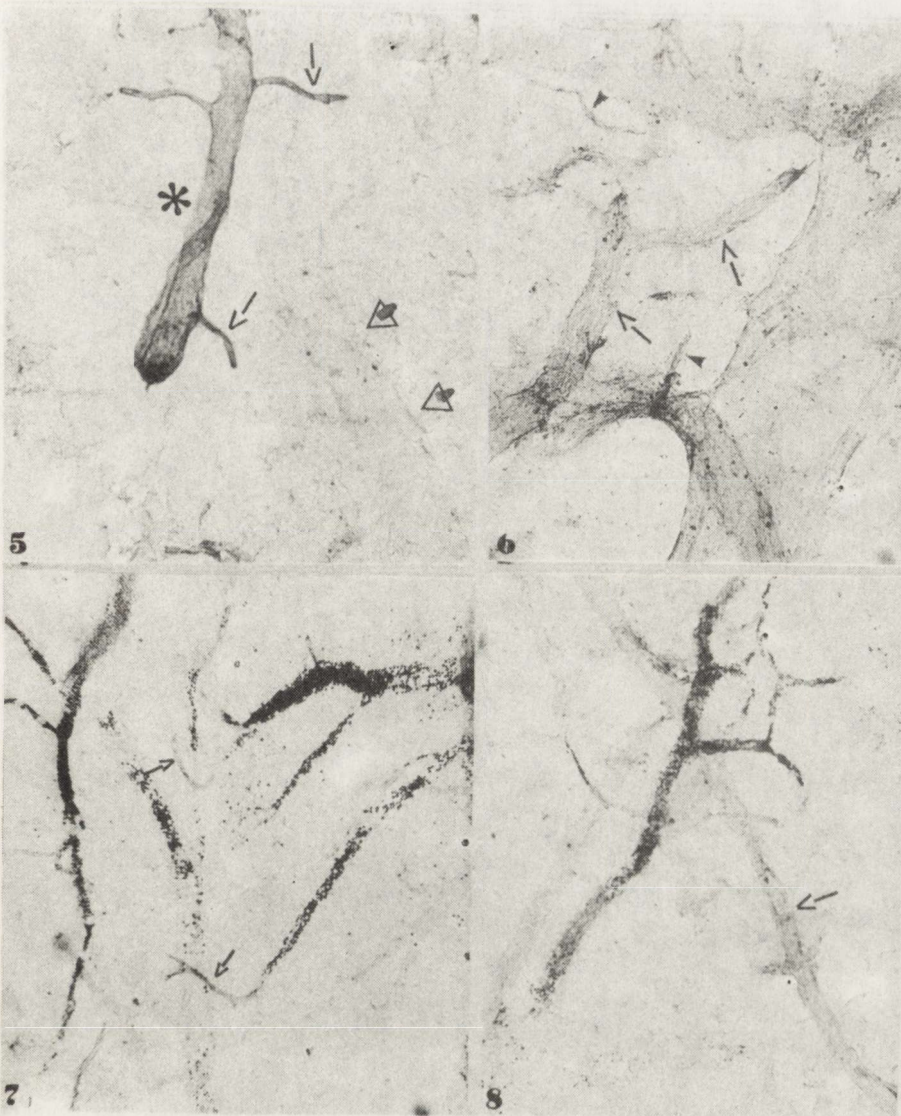


*Fig. 5.* SHR. Positive staining reaction with RCA-1 in radial arterioles (arrows) and medium size vessels (star). Vessels of larger caliber (arrowheads) are unlabeled with this lectin. Sphincters of offshoots, contrary to AP activity, do not show stronger reaction.  $\times 100$

*Fig. 6.* SHR. Labeling with UEA-1 is equally weak in the walls of radial arterioles (arrowheads) and larger vessels (arrows).  $\times 100$

*Fig. 7.* SHR. Unperfused animal. High labeling with UEA-1 of the blood morphotic elements and only negligible in the radial arteriole walls (arrows).  $\times 100$

*Fig. 8.* WKY rat. Staining reaction with LFA revealed sialic acid receptors in the walls of medium size arteries with diameter above  $30 \mu\text{m}$  (arrow). Smaller vessels remained unstained. Strong LFA binding to red blood cells.  $\times 100$

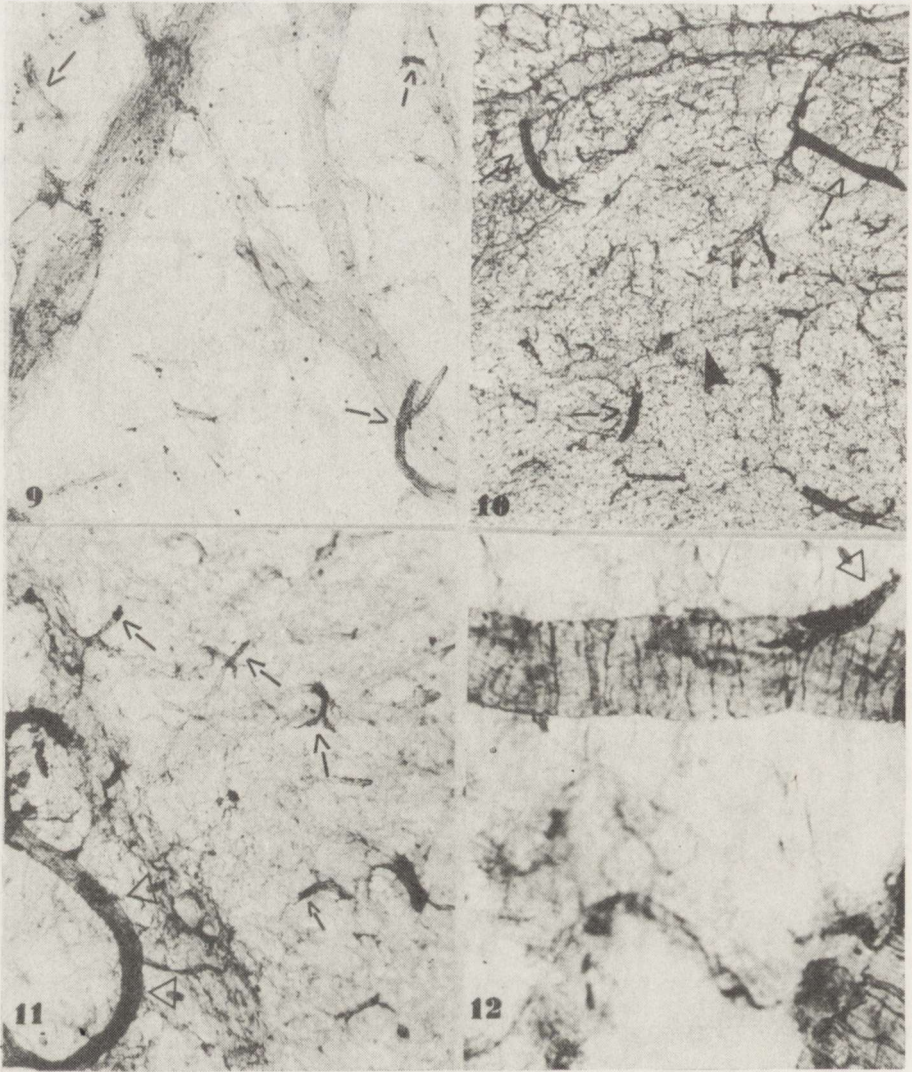


*Fig. 9.* SHR. Increased intensity of staining reaction with LFA in radial arterioles (arrows) and larger vessels as compared with the control (*Fig. 8*).  $\times 100$

*Fig. 10.* WKY rat. Very intensive staining reaction with WGA in radial arterioles (arrows). Larger vessels remained unstained (arrowhead). Positive staining of fibrous elements of pia mater shows WGA binding sites also present there.  $\times 60$

*Fig. 11.* SHR. WGA staining reaction much more intensive than in control animals (*Fig. 10*). WGA binding sites appear in the walls of the vessels of 30–60  $\mu\text{m}$  diameter (arrowheads). Strong staining in radial arterioles (arrows) and on the fibrous elements surrounding larger vessels.  $\times 100$

*Fig. 12.* SHR. WGA staining reaction. Strong labeling in the fibrous elements on the walls of medium size and large arteries. Very strong reaction in radial arterioles (arrowhead).  $\times 400$

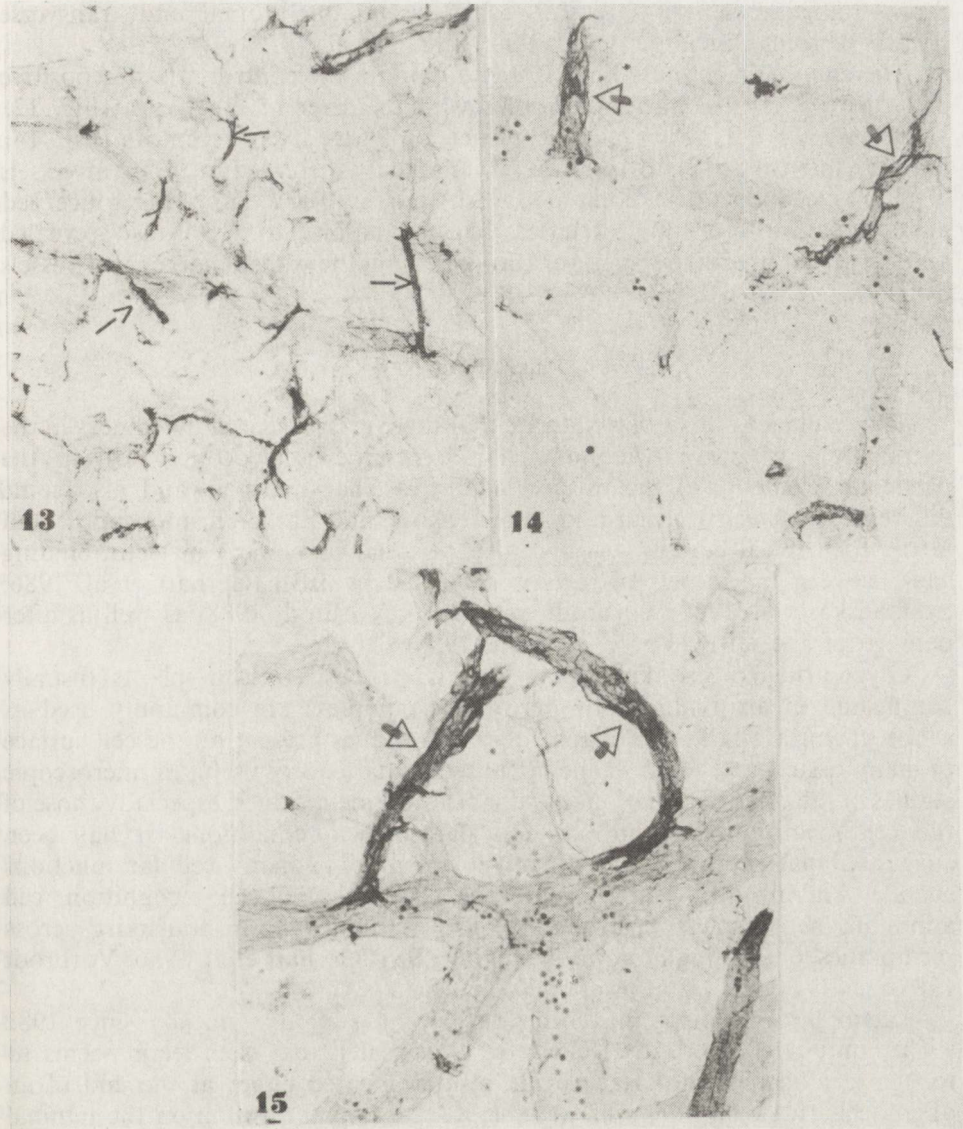


*Fig. 13.* WKY rat. Positive staining with HPA in radial arterioles (arrows). Larger vessels are negative.  $\times 100$

*Fig. 14.* WKY rat. HPA staining reaction. The walls of radial arterioles are labeled (arrowheads). Larger vessels remain unstained.  $\times 200$

*Fig. 15.* SHR. Labeling with HPA is more pronounced than in control animals (*Fig. 14*), particularly in the small arteries (8–15  $\mu\text{m}$ ) (arrows). Positive reaction is also exhibited by the fibrous elements in larger vessels (with diameter above 65  $\mu\text{m}$ ).  $\times 400$



Strong labeling with WGA showed precisely longitudinal and transverse stripes surrounding larger pial vessel (Fig. 12).

The staining reaction with HPA agglutinin in the control rats was positive in larger vessels and radial arterioles with diameter of 6–15  $\mu\text{m}$  (Fig. 13). Larger vessels did not reveal the presence of this sugar receptors (Fig. 14). Staining intensity of HPA residues was markedly increased in SHR in vessels of the same diameter as compared with that in WKY rats. This concerned mainly the walls of small arteries, but the affinity to HPA also revealed a longitudinal fiber-like structures running along the walls of larger pial vessels (Fig. 15).

#### DISCUSSION

The results of our studies indicate that there exist essential differences in the localization of different monosaccharide residues (glycoconjugates) in the particular elements of the rat pia mater vascular network, and also some differences between normal and hypertensive rats. Earlier histochemical and ultracytochemical studies revealed also essential differences in lectin-binding sites between the vessels of regions protected by BBB (Gerhart et al. 1986; Szumańska et al. 1986; Vorbrodt et al. 1986; Vorbrodt 1988) as well as after damage of the BBB (Vorbrodt et al. 1986).

Glycoproteins, also known as lectins, synthesized from plants (usually conjugated in an avidin-biotin-peroxidase complex) are commonly used as a histochemical marker of oligosaccharide residues present on the cell surface of many tissues and organs. The lectin technique is very useful in microscopic studies of the distribution of many monosaccharide residues, especially those of the cell membranes in normal and pathological conditions. It has been suggested that glycoconjugates may be involved in many cellular functions such as stabilization of the membrane structure, cell-cell recognition, cell adhesion, neoplastic transformation, growth control, ion transport across membranes, or binding of hormones (Pino 1984; Gerhart et al. 1986; Vorbrodt 1988).

Lectin histochemistry has been developing very dynamically since 1982 when Simionescu et al. and Palade et al. revealed that each lectin seems to recognize a specific monosaccharide residue located either at the end of an oligosaccharide chain or in an accessible subterminal position on the luminal surface of the vascular endothelium. Most lectins have more than one binding site and some have an affinity for more than one residue.

In the passage of various macromolecules across vascular endothelium are involved both luminal and albuminal surfaces of ECs with all kinds of receptors located there, as well as a negative charge (anionic sites) in all vessels of the central nervous system (Palade et al. 1982; Simionescu et al. 1982; Vorbrodt et al. 1984; Alroy et al. 1987).

Presence of sugar receptors of many lectins has been detected in endothelial cells with changes in their configuration and chemical content in various pathological conditions (Hennigar et al. 1985; Schulte, Spicer 1985; Gerhart et al. 1986; Szumańska et al. 1986, 1987; Vorbrodt 1986, 1987; Alroy et al. 1987; Fatehi et al. 1987).

The almost total lack of beta-D-galactosyl residues detected with RCA-1 in pial ECs of WKY (control) rats is very surprising since in the animal brain endothelia so high an intensity of reaction with this lectin was found, that it could be considered a marker of these cells (Szumańska et al. 1986). The high concentration of beta-D-galactosyl residues in the ECs of the BBB-vessels and fenestrated ones (Pino 1984; Alroy et al. 1987; Vorbrodt 1988) makes us conclude that the RCA-1 receptor is typical for all animal endothelia but it should not be associated with the BBB mechanisms.

In the control material tested also important was the noted negative result of the reaction with UEA-1, indicating lack of fucosyl residues. This confirms the hypothesis of Holthöfer et al. (1988) that UEA-1 is a marker of human blood microvessels only, although some alpha-l-fucosyl residues have been observed in the pial endothelia of SHR. Furthermore, in the vascular network of SHR the staining intensity of WGA, LFA and HPA was markedly increased as compared with the control. Very surprising was the presence in pial microvessels of RCA-1 and UEA-1 sugar residues in a group of SHR, but not in control rats. The methodology used by us (light microscopy) does not allow to recognize the differences revealed by the EM technique, nevertheless, we can state that the differences in a number of receptors of particular lectins between control and hypertensive rats are unquestionable.

We have also revealed differences in histochemical staining intensity of the tested glycoconjugates depending on the type of microvessels (capillaries, arterioles and venules). The structural and functional differences between these three types of vessels have been known for a long time. Nag and Arseneau (1983) observed in hypertensive rats an increased permeability and negative charge, but only in some segments of the arterioles, whereas capillaries and venules remained unpermeable to the tracer. Similar observations have been made by Vorbrodt et al. (1986) and Vorbrodt (1988) who found after BBB injury reverse transport (abluminal one) of extravasated edematous fluid across the walls of metarterioles and venules, but not across the capillary walls. Such reverse transport is accompanied by changes in polar distribution of alkaline phosphatase in luminal and albuminal EC plasmalemma. That is why we have decided to evaluate AP activity in our material and compare its localizatin and intensity with the pattern of some monosaccharide receptors on the endothelia of the pia mater vessels of normal and hypertensive rats. AP is considered to be a marker of plasma membranes in capillary endothelia. It is one of the enzymes located there and participating in active transport across vessel walls.

The results of our study indicate that only small pial arterioles and sphincters of offshoots show high AP activity, which is stronger in SHR than in control rats. This can be treated also as an exponent of increased BBB permeability in the ECs of hypertensive rats. Yet it must be stressed that very high AP activity was found not only in the small pial arterioles, but also in offshoots which do not correspond to what is called "active segments" (Mchedlishvili, Baramidze 1971) and to the distribution of dehydrogenase and nucleotidase enzyme activity (Gadamski et al. 1980). Also the distribution of binding sites of the tested lectins does not correspond to the spots of intensive AP activity in the pial vasculature. The hypothesis of Sokolova et al. (1985) concernig the rarefaction of arterioles and capillary network in the brain of rats

with different forms of hypertension needs separate comment. The above mentioned authors considered the decrease of vessel diameters due to thickening of their walls and dilution of the pial vascular network as a result of hypertension. An essential role in the process of autoregulation under these pathological conditions is played by the sphincters of offshoots. Increased AP activity at those particular sites in our hypertensive rats may also confirm this hypothesis.

The results of our study suggest therefore, that not only particular enzyme systems, but also glycoconjugates are important components of the cell surface, participating in transport phenomena in the endothelia of the brain and pia mater vascular network.

#### HISTOCHEMIA LEKTYN ORAZ AKTYWNOŚĆ FOSFATAZY ZASADOWEJ W NACZYNIACH OPONY MIĘKKIEJ U SZCZURÓW Z WRODZONYM NADCIŚNIENIEM TĘTNICZYM

##### Streszczenie

Lektyny, których receptory cukrowe zlokalizowane są na błonach komórek śródbłonkowych, użyto do badań histochemicznych glikokoniugatów występujących w sieci naczyń oponowych mózgu szczurów kontrolnych (WKY) i szczurów z wrodzonym nadciśnieniem tętniczym (SHR). Do badań użyto lektyny, które rozpoznają następujące zakończenia cukrowe:  $\beta$ -D-galaktozę (*Ricinus communis* agglutinin – RCA-1),  $\alpha$ -L-fukozę (*Ulex europaeus* agglutinin – UEA-1), N-acetyl-glukozaminę i kwas sialowy (Wheat germ agglutinin – WGA), N-acetyl oraz N-glikolyl-kwas sialowy (neuroaminowy) (*Limax flavus* agglutinin – LFA) i N-acetyl-D-galaktozaminę (*Helix pomatia* agglutinin – HPA). Wykazano różnice w składzie receptorów cukrowych w komórkach śródbłonna u szczurów kontrolnych i nadciśnieniowych oraz różnice w ich lokalizacji pomiędzy kapilarami, tętniczkami i naczyniami żylnymi.

Wykonano również badanie histochemiczne aktywności fosfatazy zasadowej, enzymu uczestniczącego w mechanizmie zaburzeń bariery naczyniowo-mózgowej. Stwierdzono wzrost aktywności enzymu u szczurów z nadciśnieniem, przy podobnej lokalizacji aktywności fosfatazy zasadowej, jak u zwierząt kontrolnych.

Wykazane różnice sugerują możliwość zróżnicowania funkcji metabolicznych w poszczególnych odcinkach drzewa naczyniowego opony miękkiej szczura.

##### REFERENCES

1. Alroy J, Goyal V, Skutelsky E: Lectin histochemistry of mammalian endothelium. *Histochemistry*, 1987, 86, 603–607.
2. Betz AL, Firth JA, Goldstein GW: Polarity of the blood-brain barrier: distribution of enzymes between the luminal and antiluminal membranes of brain capillary endothelium. *Brain Res*, 1980, 192, 17–28.
3. Betz AL, Goldstein GW: Polarity of the blood-brain barrier: neutral amino acid transport into isolated brain capillaries. *Science*, 1978, 202, 225–226.
4. Bradbury M: The concept of a blood-brain barrier. *J Wileyand and Sons, New York, Toronto*, 1979, pp 60–83.
5. Fatehi MI, Gerhart D, Meyers TG, Drewes LR: Characterization of the blood-brain barrier: glycoconjugate receptors of 14 lectins in canine brain cultured endothelial cells and blotted membranes. *Brain Res*, 1987, 415, 30–39.
6. Gadamski R, Baramidze DG: Unerwienie wegetatywne opony miękkiej królika w warunkach normy i niedotlenienia ośrodkowego układu nerwowego. *Neuropatol Pol*, 1979, 17, 505–521.
7. Gadamski R, Kuridze N, Mamaladze A, Mchedlishvili G: Pattern of vegetative innervation of the pia mater vessels in phylogeny. *Neuropatol Pol*, 1989, 27, 127–140.

8. Gadamski R, Szumańska G, Baramidze D: Enzymatic activity of pial arterial blood vessels of the rabbit in normal and ischemic conditions. *Neuropatol Pol*, 1980, 18, 569–581.
9. Gerhart D, Zlonis MS, Drewes LR: Light and electron microscopic localization of D-galactosyl residues in capillary endothelial cells of the canine cerebral cortex. *J Histochem Cytochem*, 1986, 34, 641–648.
10. Hennigar RA, Sens DA, Spicer SS, Schulte RA, Newman V, Sens MA, Garvin AJ: Lectin histochemistry of nephroblastoma (Wilm's tumour). *Histochem J*, 1985, 17, 1091–1110.
11. Holthöfer H, Virtanen T, Kariniemi AL, Hormia M, Linder E, Miettinen I: *Ulex europaeus* I lectin as a marker for vascular endothelium in human tissues. *Lab Invest*, 1982, 47, 60–66.
12. Joó F: Electron histochemical structure of capillaries in the rat brain. *Acta Biol (Szeged)*, 1969, 15, 78–88.
13. Joó F: Increased production of coated vesicles in the brain capillaries during enhanced permeability of the blood-brain barrier. *Br J Exp Pathol*, 1971, 52, 646–649.
14. Joó F, Temesvari P, Dux E: Regulation of the macromolecular transport in the brain macrovessels: the role of cyclic GMP. *Brain Res*, 1983, 278, 165–174.
15. Kreutzberg GW, Toth I: Enzyme cytochemistry of cerebral microvessel wall. In: *Cerebrovascular transport mechanisms*. Eds: K-A Hossmann, I Klatzo. *Acta Neuropathol (Berl)*, suppl 8, 1983, 35–41.
16. Lossinsky AS, Wiśniewski HM: A comparative ultrastructural study of endothelial cell tubular structures from injured mouse blood-brain barrier and normal hepatic sinusoid demonstrated after perfusion fixation with osmium tetroxide. *Microvasc Res*, 1986, 31, 333–344.
17. Mayahara H, Hirano H, Saito T, Ogawa K: The new lead citrate method for the ultracytochemical demonstration of nonspecific alkaline phosphatase. *Histochemie*, 1967, 1, 88–96.
18. Mchedlishvili GJ, Baramidze DG: Functional behaviour of the precortical arteries under conditions of experimental hypo- and hypertension. *Bull Exp Biol Med*, 1971, 72, 14–16.
19. Nag S, Arseneau R: Alteration of endothelial surface charge in hypertension. *J Cereb Blood Flow Metab*, suppl 1, 1983, 624–625.
20. Oldendorf WH: The blood-brain barrier: the ocular and cerebrospinal fluids. Eds: LZ Bito, H Davson, JD Ferstenmacher. Academic Press, London, 1977, pp 177–190.
21. Palade GE, Simionescu M, Simionescu N: Differentiated microdominants in the vascular endothelium. In: *Pathology of the endothelial cell*. Eds: HL Nossel, HJ Vogel. Academic Press, New York, London, 1982, pp 23–33.
22. Pino R: Ultrastructural localization of lectin receptors on the bone marrow sinusoidal endothelium of the rat. *Am J Anatomy*, 1984, 169, 259–272.
23. Samorajski T, McCloud J: Alkaline phosphomonoesterase and blood-brain permeability. *Lab Invest*, 1961, 10, 492–501.
24. Schulte BA, Spicer SS: Histochemical methods for characterizing secretory and cell surface sialoglycoconjugates. *J Histochem Cytochem*, 1985, 33, 427–438.
25. Simionescu M, Simionescu N, Palade GE: Differentiated microdominants on the luminal surface of capillary endothelium: distribution of lectin receptors. *J Cell Biol*, 1982, 95, 406–413.
26. Sokolova IA, Manukhina EB, Blinkov S, Koshelev VB, Pinelis VG, Rodinov IM: Rarefaction of the arterioles and capillary network in the brain of rats with different forms of hypertension. *Microvasc Res*, 1985, 30, 1–9.
27. Szumańska G, Mossakowski MJ: Aktywnść cykazy adenylowej i fosfatazy zasadowej w naczyniach mózgu szczura w doświadczalnym zatruciu tlenkiem manganawym. *Neuropatol Pol*, 1985, 23, 297–314.
28. Szumańska G, Mossakowski MJ, Januszewski S: Zmiany aktywności fosfatazy zasadowej i cykazy adenylowej w sieci naczyń mózgu w doświadczalnym zespole poreanimacyjnym. *Neuropatol Pol*, 1988, 26, 335–357.
29. Szumańska G, Vorbrodth AW, Mandybur HM, Wiśniewski HM: Lectin histochemistry of plaques and tangles in Alzheimer disease. *Acta Neuropathol (Berl)*, 1987, 73, 1–11.
30. Szumańska G, Vorbrodth AW, Wiśniewski HM: Lectin histochemistry of scrapie amyloid plaques. *Acta Neuropathol (Berl)*, 1986, 69, 205–212.
31. Vorbrodth AW: Changes in the distribution of endothelial surface glycoconjugates associated with altered permeability of brain micro-blood vessels. *Acta Neuropathol (Berl)*, 1986, 70, 103–111.

32. Vorbrodt AW: Ultrastructural cytochemistry of blood-brain endothelia. *Prog Histochem Cytochem*, 1988, 18, 1–97.
33. Vorbrodt AW, Dobrogowska DH, Lossinsky AS, Wiśniewski HM: Ultrastructural localization of lectin receptors on the luminal and albuminal aspects of brain micro-blood vessels. *J Histochem Cytochem*, 1986, 34, 251–261.
34. Vorbrodt AW, Lossinsky AS, Wiśniewski HM: Enzyme cytochemistry of blood-brain barrier (BBB) disturbances. *Acta Neuropathol (Berl)*, suppl 8, 1983, 43–57.
35. Vorbrodt AW, Lossinsky AS, Wiśniewski HM: Ultrastructural studies of concanavalin A receptors and 5-nucleotidase localization in normal and injured mouse cerebral microvasculature. *Acta Neuropathol (Berl)*, 1984, 63, 210–217.
36. Vorbrodt AW, Lossinsky AS, Wiśniewski HM, Moretz RC, Iwanowski L: Ultrastructural cytochemical studies of cerebral microvasculature in scrapie infected mice. *Acta Neuropathol (Berl)*, 1981, 53, 203–211.
37. Vorbrodt AW, Lossinsky AS, Wiśniewski HM, Suzuki R, Yamaguchi T, Masonaka H, Klatzo I: Ultrastructural observations on the vascular route of protein removal in vasogenic brain edema. *Acta Neuropathol (Berl)*, 1985, 66, 265–273.

Authors' address: Department of Neuropathology, Medical Research Centre, Polish Academy of Sciences, 3 Dworkowa Str, 00-784 Warsaw, Poland

BARBARA GAJKOWSKA, MIROSŁAW J. MOSSAKOWSKI

## CALCIUM ACCUMULATION IN SYNAPSES OF THE RAT HIPPOCAMPUS AFTER CEREBRAL ISCHEMIA

Department of Neuropathology and Laboratory of Ultrastructure of the Nervous System, Medical Research Centre, Polish Academy of Sciences, Warsaw, Poland

The ultrastructural localization of calcium deposits in the synapses of rat hippocampus after 10 min global cerebral ischemia was evaluated. Oxalate-pyroantimonate technique was applied. After 24 hours of postischemic recirculation enhancement of intracellular (pre- and postsynaptic parts) and extracellular (synaptic clefts) calcium deposits was found in great proportion of synapses in CA<sub>1</sub> sector. Abundant Ca-precipitates appeared specially in synaptic clefts and in the postsynaptic parts near synaptic densities. Increased calcium deposits in some changed mitochondria were also observed. The results presented in this paper suggest synaptic modulation of Ca<sup>2+</sup> homeostasis, disturbed after ischemic incident. Presence of Ca-precipitates in synaptic clefts and postsynaptic parts seems to be a sensitive indicator of increased calcium influx from the extracellular to the intracellular compartments.

**Key words:** *hippocampus, synapses, Ca-pyroantimonate technique, ischemia.*

Delayed neuronal death is a characteristic type of irreversible nerve cell injury resulting from cerebral ischemia. It appears in some selectively vulnerable neuronal groups of the brain, among which pyramidal cells of the CA<sub>1</sub> sector of Ammon's horn have been most extensively studied. Delayed neuronal death, first described by Ito et al. (1975) in Mongolian gerbils as an exponent of the maturation phenomenon, was later shown to occur both in gerbils and rats in various experimental models of cerebral ischemia (Kirino 1982; Kirino et al. 1984; Kirino, Sano 1984; Yamaguchi, Klatzo 1984; Suzuki et al. 1985; Mossakowski et al. 1989). It is generally accepted that delayed neuronal death results from the excitotoxic action of aminoacid neurotransmitters, mostly glutamate and aspartate (Olney et al. 1983; Griffith et al. 1984).

Two main mechanisms of neuronal changes due to the action of excitatory aminoacid neurotransmitters (EAAs) are postulated (Rothman, Olney 1986; Siesjö, Bengtsson 1989). The first is represented by acute cellular swelling, resulting from abnormal ions and water influx into neurons, following opening of ion channels by EAAs (Choi 1985, 1987; Rothman 1985). The second type is represented by a delayed mechanism mediated by the increased intracellular level of free calcium, which activates a number of metabolic processes leading

to cell disintegration and death (Choi 1987, 1988; Siesjö, Bengtsson 1989). Two major features distinguish both cellular responses to the action of EAAs. These are selectivity and reversibility. Delayed neuronal death is known to be selective and irreversible. Acute cellular swelling accompanied by a transient increase of cytosolic  $\text{Ca}^{++}$  concentration is totally reversible and involves all types of neurons and dendritic fields, which receive excessive EAAs stimulation (Olney et al. 1983; Griffith et al. 1984). The synaptic mechanism operated by EAAs in the hippocampus interacts with other neurotransmitter systems, in which GABA, acetylcholine, adenosine, serotonin, noradrenaline, histamine and/or neuropeptides are involved. Functional balance between inhibitory and excitatory stimulation plays an important role in preventing cellular damage due to ischemia. It seems, therefore, possible that the pathological process ending as delayed neuronal death of CA<sub>1</sub> hippocampal pyramidal neurons may at least be initiated by disturbances of this balance caused by the decreased inhibition appearing against the background of normal or enhanced excitation by EAAs during the postischemic period. Our previous electron-microscope studies revealed features of an early and reversible alteration of CA<sub>1</sub> sector interneurons, which may result in insufficiency of GABA-ergic inhibitory processes (Gajkowska et al. 1989). Yasumoto et al. (1988) described a decrease of GABA content in the CA<sub>1</sub> sector after cerebral ischemia and postulated that reduced inhibitory processes may be one of the factors responsible for neuronal damage. The delayed neuronal death of pyramidal neurons in the CA<sub>1</sub> hippocampal sector is preceded by accumulation of calcium in the tissue (van Reempts et al. 1986; Deshpande et al. 1987). Its cellular compartmentation has so far not been clarified. These alterations of calcium homeostasis evoked by excitatory synaptic stimulation in the selectively vulnerable area of Ammon's horn in cerebral ischemia inclined us to perform ultrastructural and cytochemical studies of synaptic contacts in the CA<sub>1</sub> hippocampal sector in case of global cerebral ischemia resulting from temporary cardiac arrest in rats. Application of the highly sensitive oxalate-pyroantimonate histochemical technique of Borges et al. (1977) as modified by Mata et al. (1987) seemed to be most appropriate for specific visualization of calcium distribution of various compartments of the synaptic system.

#### MATERIAL AND METHODS

Studies were carried out on 10 male Wistar rats, weighing 160–180 g. In the experimental animals cardiac arrest was achieved for 10 min according to Korpachev et al. (1982). A detailed description of experimental procedure and pathophysiological data were presented previously (Mossakowski et al. 1986).

24 h after resuscitation 5 experimental animals were sacrificed by transcardiac perfusion with a 2.5% solution of glutaraldehyde in 0.1 M cacodylate buffer, pH 7.4. Blocks of brain tissue containing the CA<sub>1</sub> sector of dorsal hippocampus were taken and additionally fixed for 1 h in 2.5% of glutaraldehyde solution, washed in 0.1 M cacodylate buffer and postfixed in 2.0% osmium tetroxide in cacodylate buffer. They were dehydrated routinely in alcohol solutions and propylene oxide and embedded in Epon 812. Ultrathin

sections were counterstained with uranyl acetate and lead citrate, and examined in a JEOL 1200E electron microscope.

The remaining 5 experimental animals were 24 h after resuscitation perfused transcardially for 2 min with 90 mM potassium oxalate in 1.9% sucrose, adjusted to pH 7.4 with KOH at 37°C. This was followed by perfusion with a solution composed of 3% glutaraldehyde 0.5% paraformaldehyde, 90 mM potassium oxalate and 1.9% sucrose adjusted to pH 7.4 with KOH. Perfusion lasting approximately 1 h was performed at a constant rate. At the end of perfusion, the tissue samples containing the CA<sub>1</sub> sector of dorsal hippocampus were taken and kept in the fixative solution for 2 h at 4°C. Then they were rinsed in 90 mM potassium oxalate in 1.9% sucrose, pH 7.4, postfixed in 1% osmium tetroxide and 2% potassium pyroantimonate for 2 h at room temperature. Unbound potassium pyroantimonate was washed out by rinsing the tissue samples for 15 min in water adjusted with KOH to pH 10. Subsequently, samples were dehydrated in graded ethanol solutions and embedded in Epon 812. Ultrathin sections, counterstained with uranyl acetate and lead citrate were examined in a JEM 1200E electron microscope.

In order to check the specificity of the reaction, ultrathin sections mounted on grids were washed in 10 mM EGTA (ethylene glycol-bis-β-aminoethyl-ether) – N,N,N',N'-tetraacetic acid), the calcium chelating agent, for 1 h at 60°C. EGTA-treatment in turn was controlled by incubation of the sections in distilled water for 1 h at 60°C.

Two animals not subjected to any experimental procedures served as control material. Tissue blocks containing the CA<sub>1</sub> sector of dorsal hippocampi were processed identically as those from the experimental animals.

## RESULTS

### Ultrastructural observations.

The great majority of the synaptic contacts in the CA<sub>1</sub> sector examined 24 h after the ischemic incident were ultrastructurally unchanged. This concerned symmetric and asymmetric synapses of axo-somatic and axo-dendritic types. No abnormalities were observed either in the axonal endings, synaptic clefts or postsynaptic areas (Figs 1, 2). However, among the dominating ultrastructurally unchanged synaptic population, some synapses revealed obvious abnormalities, concerning both the pre- and postsynaptic parts.

Some presynaptic bags were swollen, they were devoid of synaptic vesicles or contained a remarkably reduced number of them (Fig. 3). Abnormal arrangement of synaptic vesicles in the direct vicinity of the synaptic cleft was a common feature. In some cases swollen mitochondria represented the only organelles of swollen axonal endings. So changed synaptic contacts were located mostly on ultrastructurally altered perikarya of pyramidal cells and their dendritic shafts or spines (Figs 3, 4). Some of the pyramidal cells revealed marked dilatation of channels of the rough endoplasmic reticulum and disaggregation of polyribosomes and cytoskeleton elements. However, most of



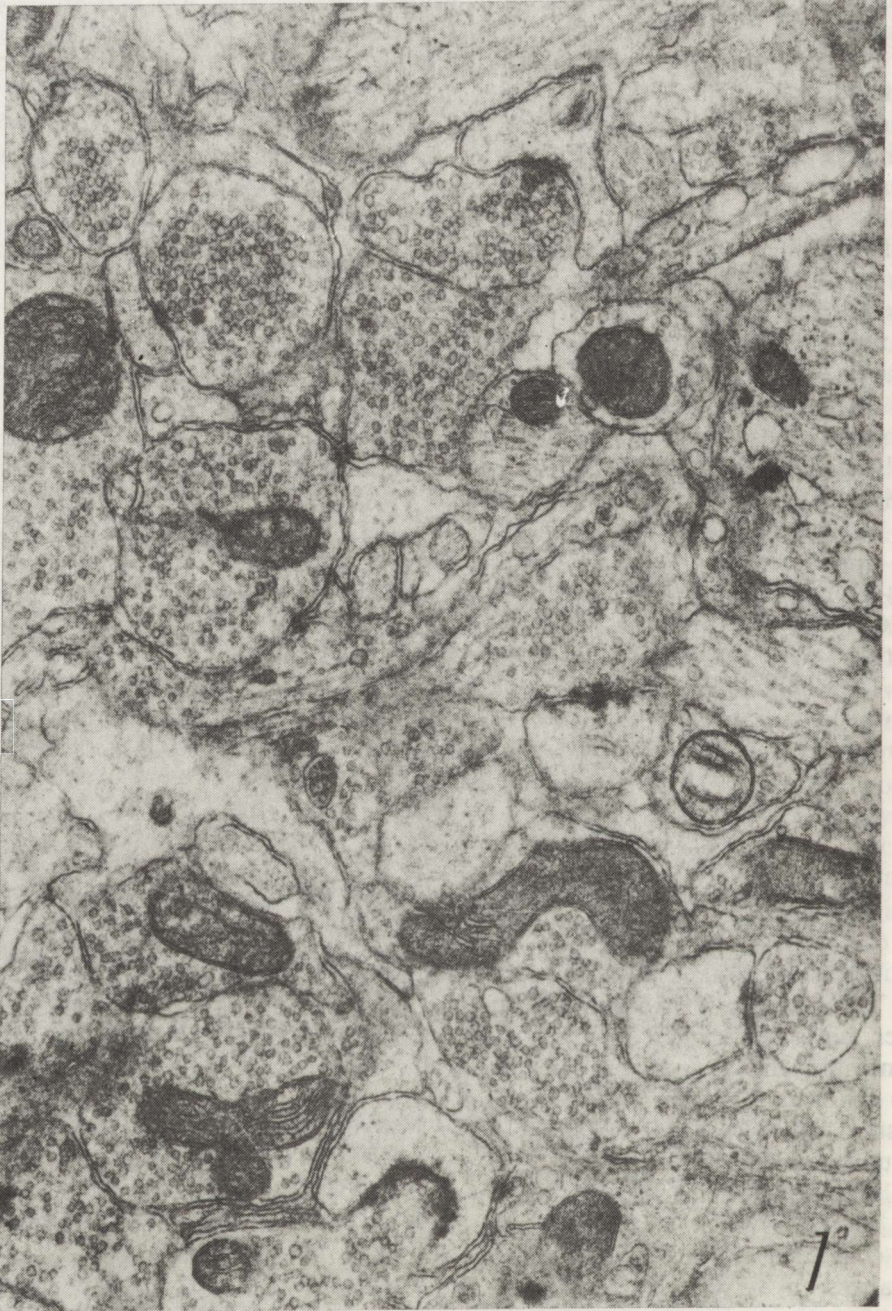


*Fig. 1.* CA<sub>1</sub> sector, 24 h after cerebral ischemia. Fragment of neuropil with ultrastructurally unchanged synapses both in pre- and postsynaptic parts.  $\times 30\,000$

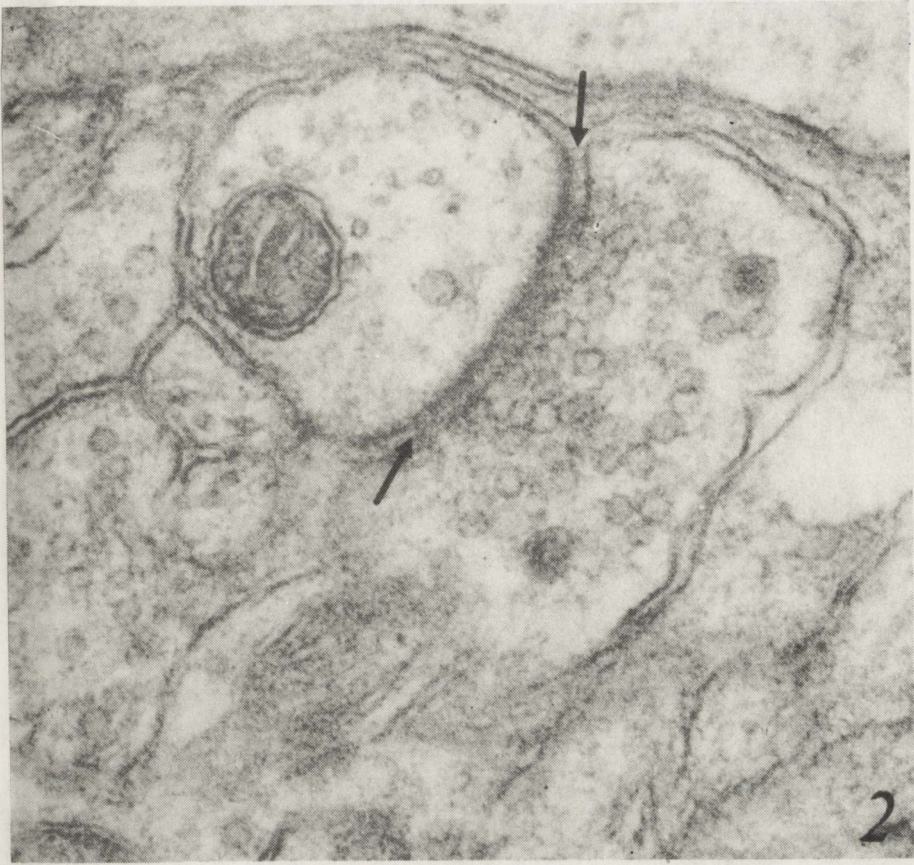


Fig. 2. CA<sub>1</sub> sector, 24 h after ischemia. Unchanged axo-dendritic asymmetric synapse. Note clearly visible synaptic cleft, filled with delicate floccular filaments (arrows).  $\times 90\,000$

the mitochondria and other cytoplasmic organelles seemed to be relatively well preserved. Some of the dendritic profiles in the neuropile of the CA<sub>1</sub> sector were greatly swollen, containing distended vacuolar structures (Fig. 3).

#### Cytochemical observations.

In control animals, not subjected to any experimental procedure, cytochemical pictures resembled that described previously by Probst in 1986. Delicate, fine calcium deposits were present mostly in the extracellular compartment first of all within the synaptic clefts. Some fine granular material was also visible in the cytoplasm of both pre- and postsynaptic parts (Fig. 5). Intramitochondrial calcium deposition was a rather unfrequent feature.

The only difference between control and experimental animals as far as cytochemical picture is concerned consisted in significant increase of calcium deposition within the synaptic compartments in animals which survived the ischemic incident. In quite a large proportion of the synapses abundant calcium aggregates were present. Most of them were localized within synaptic clefts and in the postsynaptic parts (Figs 6, 7, 8, 9). In the latter location they were either

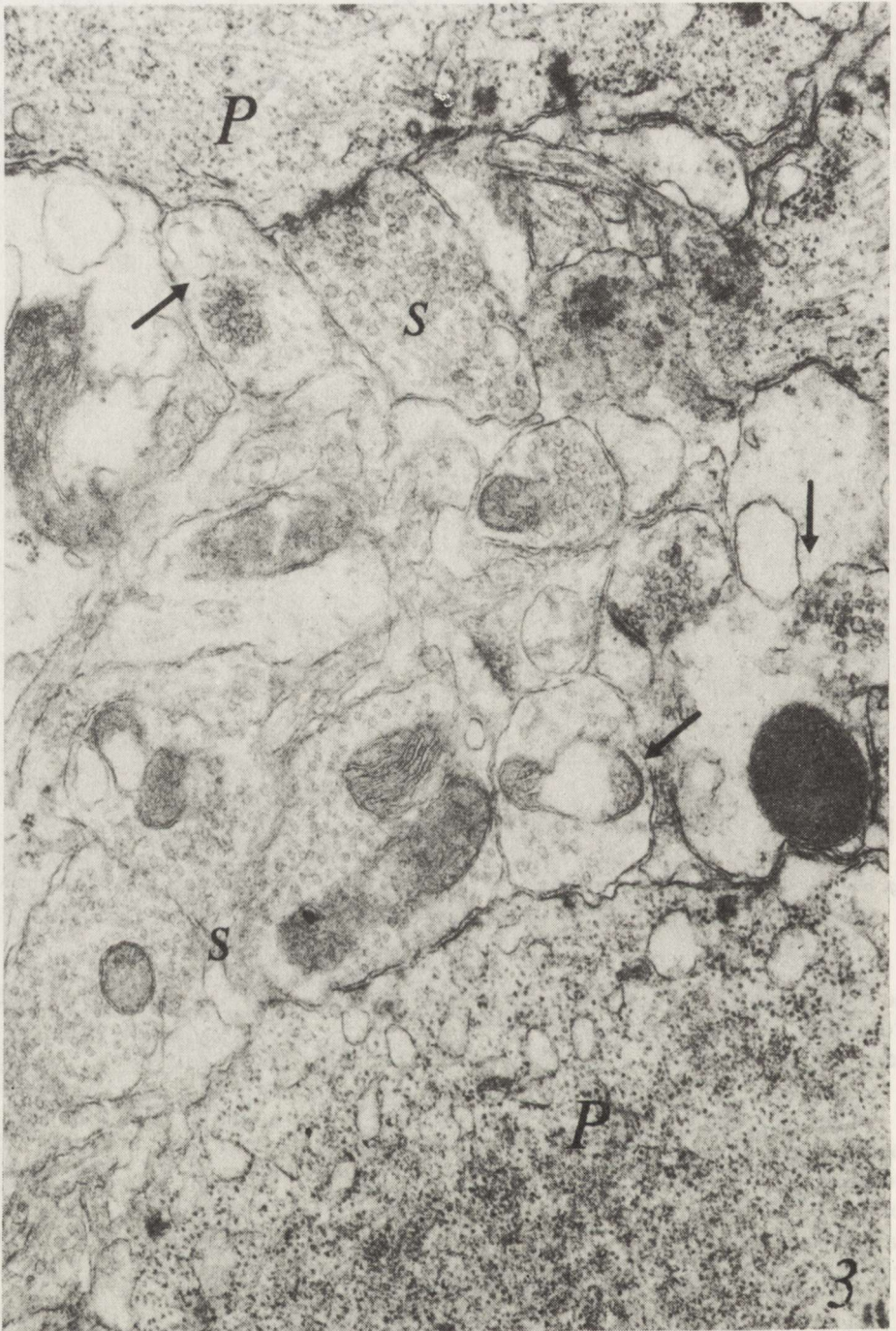


*Fig. 3.* CA<sub>1</sub> sector, 24 h after ischemia. Numerous synaptic contacts are present on the perikarya of two ultrastructurally altered pyramidal cells (P). Among apparently normal synapses (S), some display considerable swelling, reduction in number of synaptic vesicles and abnormal arrangement as well as appearance of large vesicular structures (arrows).  $\times 30\ 000$

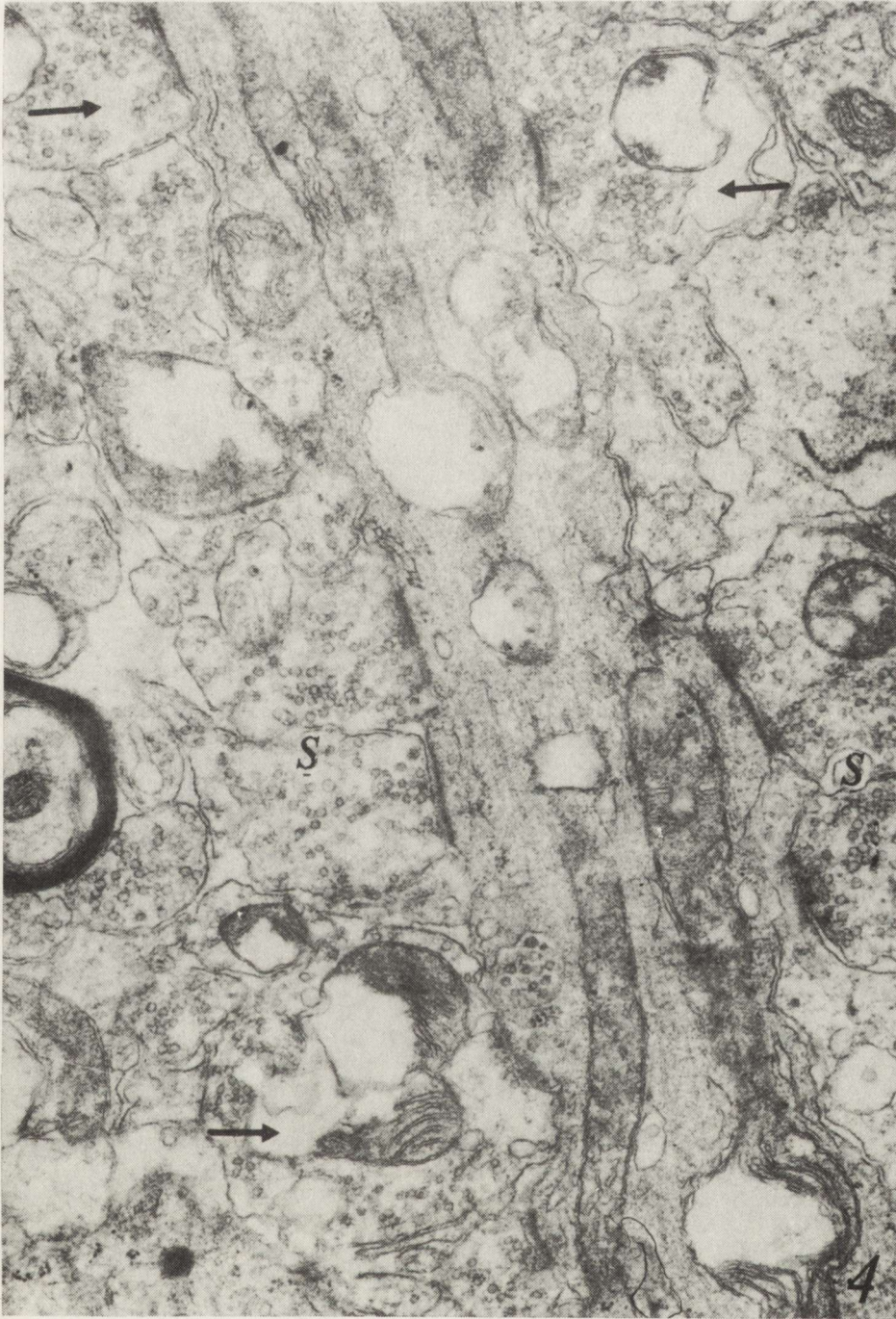


*Fig. 4.* CA<sub>1</sub> sector, 24 h after ischemia. Slightly abnormal dendritic shaft surrounded by mostly unchanged synaptic bags (S). Some of them are swollen and display abnormalities concerning number and arrangement of synaptic vesicles (arrows).  $\times 30\ 000$

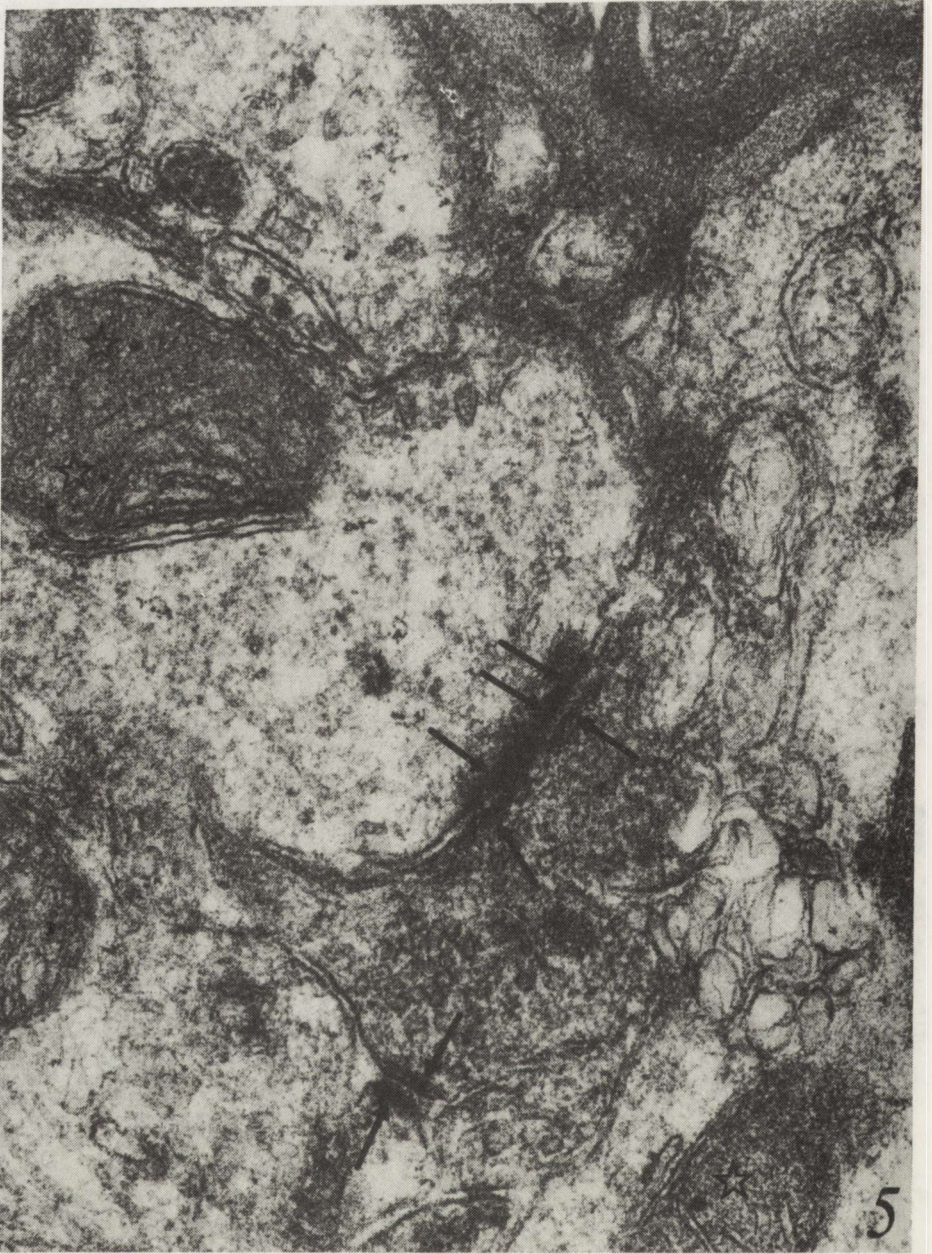


*Fig. 5.* CA<sub>1</sub> sector, control animal. Oxalate-pyroantimonate reaction. Fine-granular calcium deposits are spread in both pre- and postsynaptic parts in the vicinity of the synaptic densities (arrows). Calcium deposits are also visible in some mitochondria (asterisk).  $\times 60\ 000$

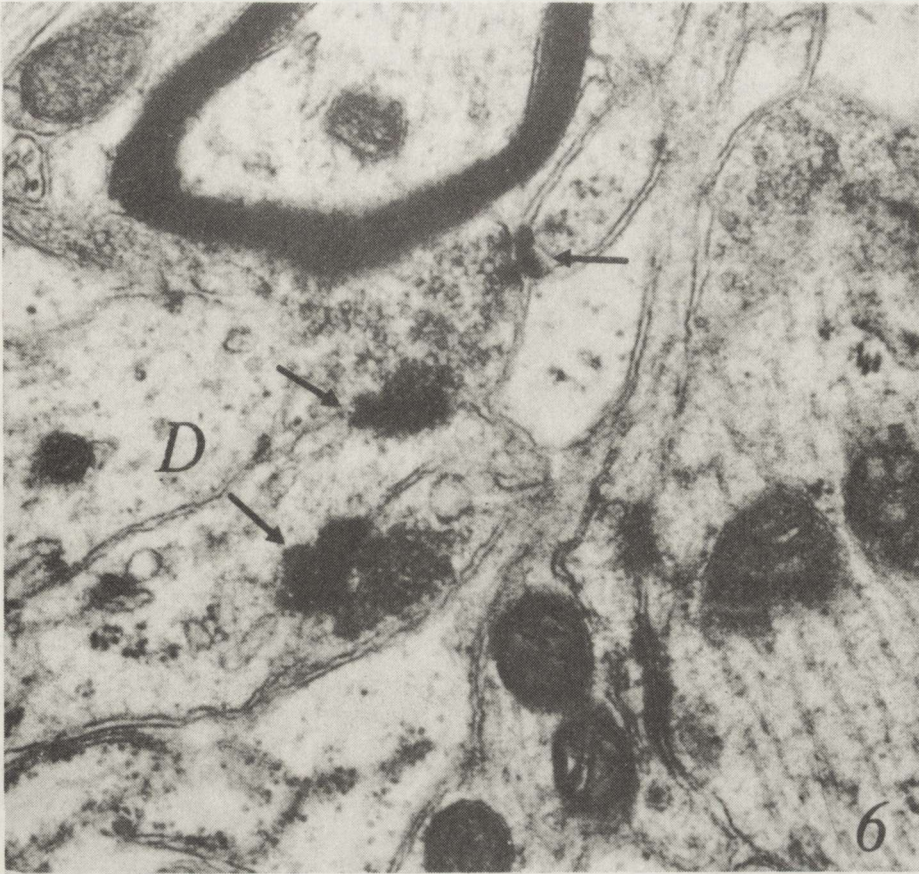
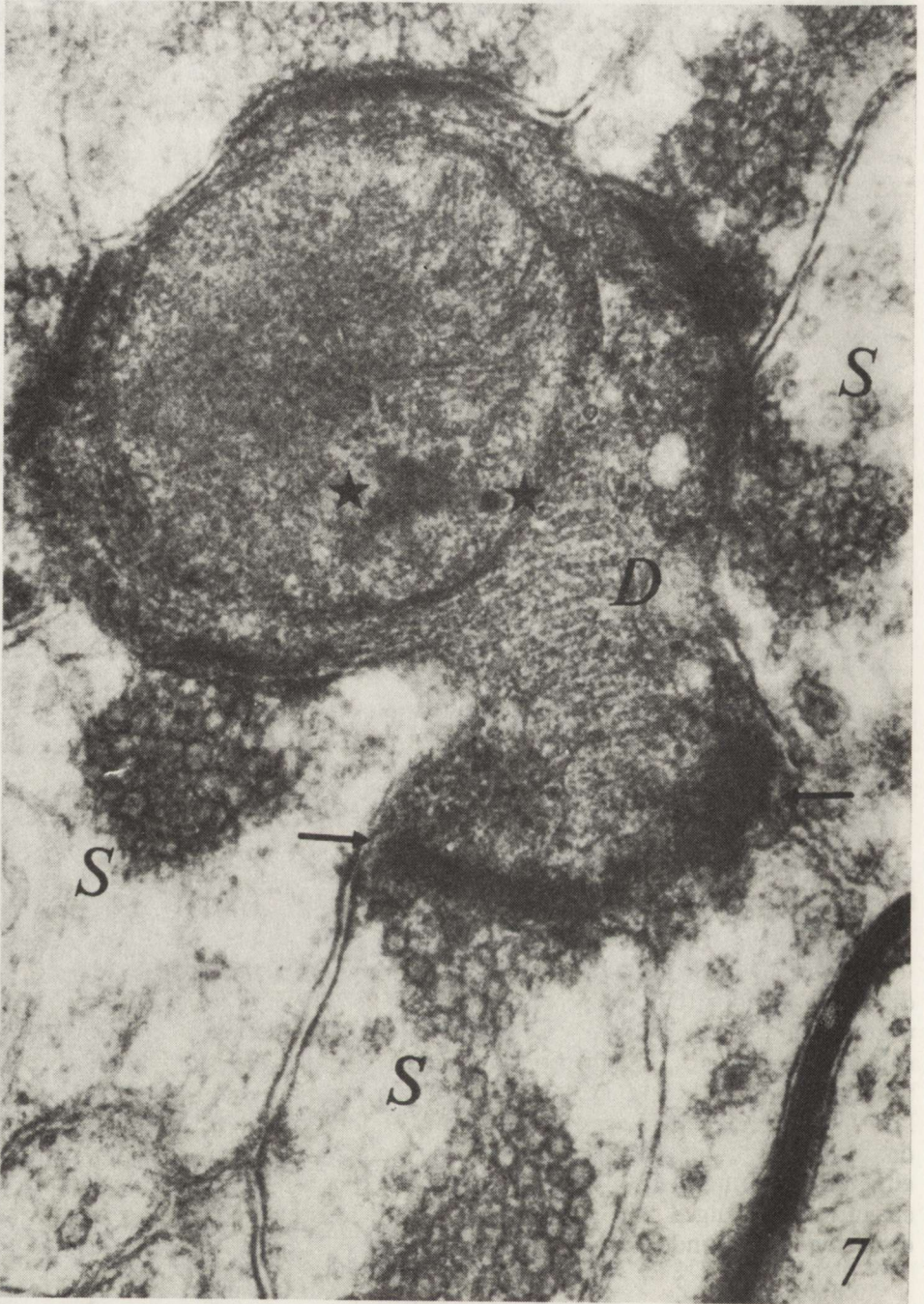


Fig. 6. CA<sub>1</sub> sector, 24 h after ischemia. Oxalate-pyroantimonate reaction. Dense calcium deposits (arrows) are present within the synaptic clefts and in the postsynaptic parts of swollen dendritic shafts (D).  $\times 50\,000$

diffusely spread or clumped in larger accumulations (Fig. 6). It is noteworthy that the direct vicinity of postsynaptic density was the most common site of calcium aggregation in intracellular synaptic compartments. Occasionally mitochondria displaying ultrastructural alterations contained either fine granular or dense calcium deposits (Figs 7, 9). Presynaptic bags very seldom displayed calcium aggregation. Synaptic structures containing calcium deposits either in synaptic clefts or postsynaptic parts were usually contacting ultrastructurally changed perikarya of the pyramidal neurons or their abnormal dendritic shafts and spines.

#### DISCUSSION

Our cytochemical observations showed that application of the oxalate-pyroantimonate technique of Borges et al. (1977) permits reproducible demonstration of tissue calcium deposits in the central nervous system in both



*Fig. 7.* CA<sub>1</sub> sector, 24 h after ischemia, oxalate-pyroantimonate reaction. High magnification of synaptic contacts. Accumulation of calcium deposits within synaptic clefts (arrows) and in postsynaptic part in the vicinity of synaptic density. Note swollen nerve endings with aggregations of synaptic vesicles. Granular and diffuse calcium precipitates are present within mitochondrion (asterisk) of postsynaptic part (D).  $\times 75\ 000$

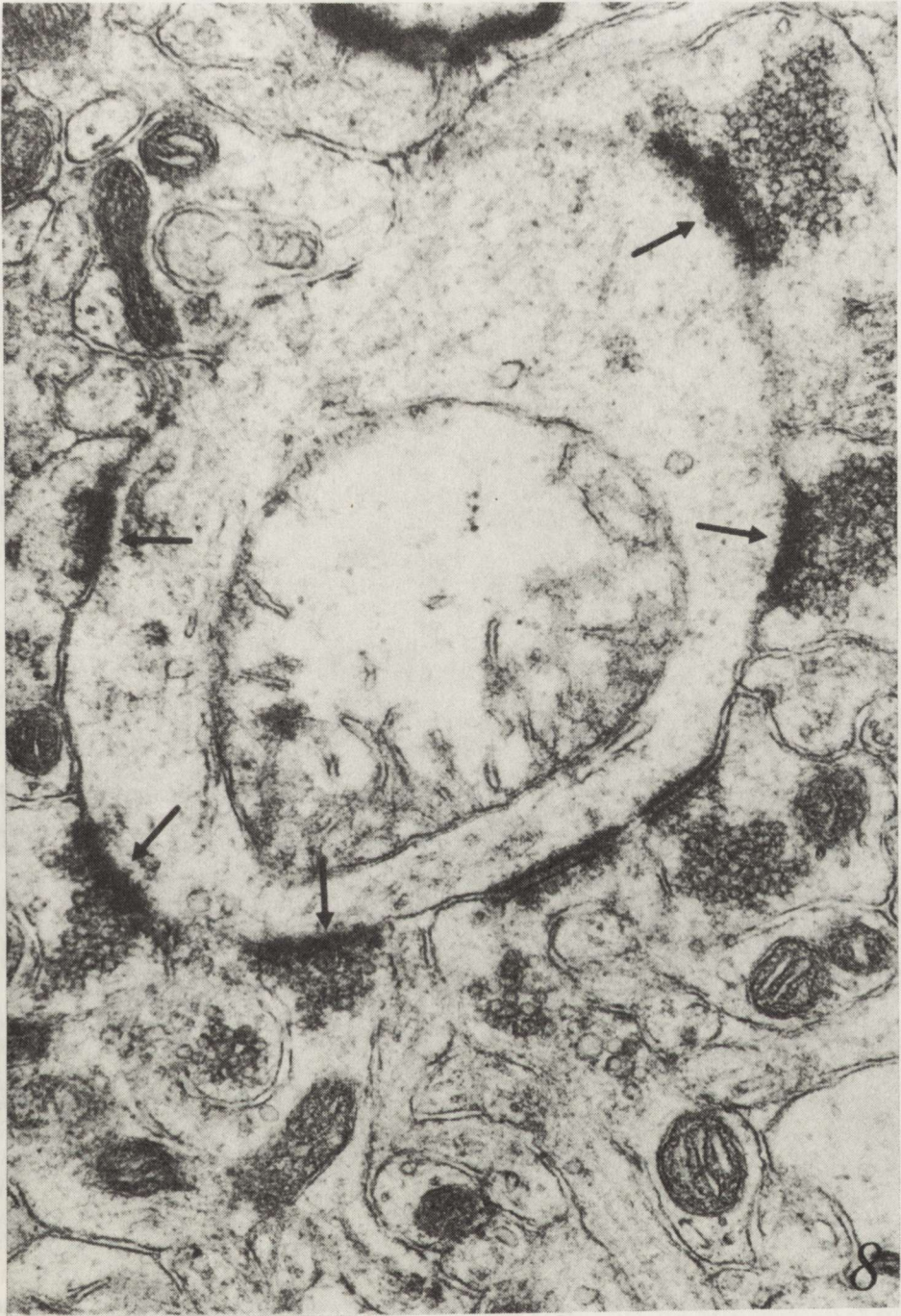


*Fig. 8.* CA<sub>1</sub> sector, 24 h after ischemia, oxalate-pyroantimonate reaction. Large swollen dendrite surrounded by slightly swollen synaptic bags with irregular aggregations of synaptic vesicles. Some synaptic contacts show dense calcium deposits within synaptic clefts (arrows).  $\times 45\ 000$



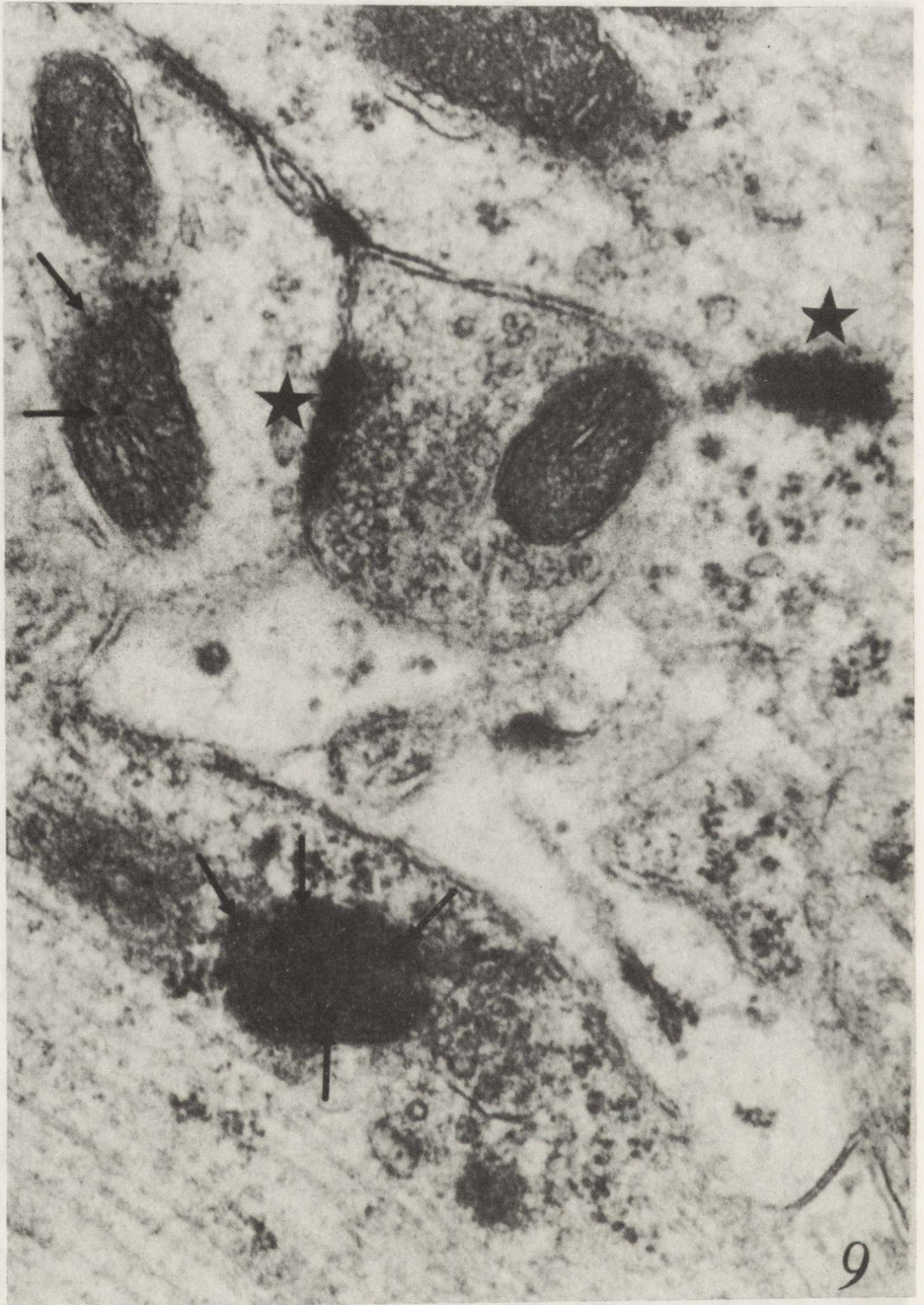


*Fig. 9.* CA<sub>1</sub> sector, 24 h after ischemia, oxalate-pyroantimonate reaction. Dendritic profiles containing mitochondria with large (ultrastructurally changed) and granular (ultrastructurally normal) calcium deposits (arrows). Note calcium precipitates within synaptic clefts (asterisk).  
× 60 000

normal and pathological conditions. In the presented series of studies we concentrated our attention on the CA<sub>1</sub> sector of Ammon's horn under conditions of global cerebral ischemia resulting from experimentally induced cardiac arrest in rats, on the basis of the generally accepted hypothesis concerning the damaging effect of intracellular influx of calcium following the excitatory action of amino acid neurotransmitters operating in this particular brain area (Choi 1988; Siesjö, Bengtsson 1989).

The specific target of our observations were synaptic contacts in this region 24 h after restoration of the cerebral blood flow. Selection of this particular postischemic period was connected with earlier literature data indicating the beginning of increased tissue calcium content within 24–48 h following temporary brain ischemia (Deshpande et al. 1987). According to their observations maximal calcium concentration was concomitant with progression or irreversible neuronal changes. The other reason of this choice were our electron microscopic observations indicative that ultrastructural exponents of calcium deposition in the cytoplasm of sector CA<sub>1</sub> neurons after short lasting forebrain ischemia in Mongolian gerbils started to appear 24 h after restoration of normal cerebral blood flow (Mossakowski et al. 1989). In earlier postischemic stages ultrastructural abnormalities of CA<sub>1</sub> interneurons suggested insufficiency of GABA-ergic inhibition. This inclined us to postulate that the process leading finally to delayed neuronal death may result from imbalance between inhibitory and excitatory stimulation of the CA<sub>1</sub> pyramidal neurons, the former due to temporary insufficiency of GABA-ergic interneurons, the latter — following excessive glutaminergic stimulation *via* Schaffer's collaterals (Gajkowska et al. 1989).

Our cytochemical studies showed that the essential difference between control and experimental studies was basically quantitative and consisted in more abundant calcium precipitation in animals which survived the ischemic insult. The second feature distinguishing both animal groups was distribution of calcium deposits. In the control animals calcium aggregates were more or less equally distributed in the pre- and postsynaptic parts of synapses with marked accentuation in the synaptic clefts. This calcium distribution was previously described by Ohara et al. (1979) and more recently by Probst (1986). In our experimental animals most of the calcium deposits were localized either in the synaptic clefts or in postsynaptic parts, with relatively slight accumulation in presynaptic bags. The increased postsynaptic calcium content indicates its massive influx from the extracellular space to intracellular compartment, related with reduced energy metabolism and damage of transport mechanisms (Siesjö, Wieloch 1985; Wieloch, Westerberg 1989). Postsynaptic calcium deposition confirmed the previous observation of van Reempts et al. (1986), who described this phenomenon in another model of cerebral brain ischemia. Very slight calcium accumulation in presynaptic bags in the ischemic animals, lower than in the control ones seems to be related with the examined stage of postischemic events. It has been established by Blaustein et al. (1978) that in the presynaptic terminal calcium influx leads to the fusion of synaptic vesicles with the membranes and to release of neurotransmitters to the synaptic clefts. Vesicles clumping in the direct vicinity of presynaptic densities and significant reduction of the amount of the synaptic vesicles in the axonal endings

may suggest that we were observing final stages of the neurotransmitter secretion. It seems, however, impossible to exclude that swollen and empty synaptic bags belong to damaged inhibitory interneurons, as described in our previous studies (Gajkowska et al. 1989). This hypothesis finds support in their location on the cell bodies of the pyramidal neurons, which is the typical site of inhibitory nerve endings in this part of the hippocampus.

#### LOKALIZACJA JONÓW WAPNIA W SYNAPSACH HIPOKAMPA SZCZURA PO ISCHEMII

##### Streszczenie

Oceniono ultrastrukturalną lokalizację złogów wapnia w synapsach hipokampa szczura po 10 min całkowitym niedokrwieniu, stosując cytochemiczną metodę pyroantymonową. Stwierdzono wzrost wewnątrzkomórkowych (w odcinkach pre- i postsynaptycznych) oraz zewnątrzkomórkowych (w szczelinach synaptycznych) złogów wapnia w większości badanych synaps odcinka CA<sub>1</sub> hipokampa. Obfitość złogów wapnia była szczególnie zaznaczona w szczelinach synaptycznych oraz w odcinkach postsynaptycznych. Mitochondria wykazywały również nagromadzenie w nadmiarze złogów Ca. Przedstawione wyniki sugerują zaburzenie synaptycznej homeostazy wapnia po przebytych incydencie niedokrwieniowym i wzmożony napływ jonów Ca z przetrzeni zewnątrzkomórkowych do wewnątrzkomórkowych.

##### REFERENCES

1. Blaustein MP, Ratzloff RV, Kendrick NC, Schweitzer ES: Calcium buffering in presynaptic nerve terminals. Evidence for involvement of a nonmitochondrial ATP-dependent sequestration mechanism. *J Gen Physiol*, 1978, 72, 15–41.
2. Borges M, de Brabander M, van Reempts J, Awanter F, Jacob WA: Intercellular microtubules in lung mast cells of guinea pig in anaphylactic shock. *Lab Invest*, 1977, 37, 1–7.
3. Deshpande JK, Siesjö BK, Wieloch T: Calcium accumulation and neuronal damage in the rat hippocampus following cerebral ischemia. *J Cereb Blood Flow Metab*, 1987, 7, 89–95.
4. Choi DW: Glutamate neurotoxicity in cortical cell cultures is calcium-dependent. *Neurosci*, 1985, 58, 293–297.
5. Choi DW: Ionic dependence of glutamate neurotoxicity. *J Neurosci*, 1987, 7, 369–379.
6. Choi DW: Glutamate neurotoxicity and diseases of the central nervous system. *Neuron*, 1988, 1, 623–634.
7. Gajkowska B, Gadamski R, Mossakowski MJ: Wpływ krótkotrwałego niedokrwienia na ultrastrukturę zakrętu hipokampa chomików mongolskich. II. Obraz mikroskopowo-elektro-nowy synaps we wczesnym okresie poniedokrwieniowym. *Neuropatol Pol*, 1989, 27, 339–366.
8. Griffith T, Evans MC, Meldrum BS: Status epilepticus: the reversibility of calcium loading and acute neuronal pathological changes in the rat hippocampus. *Neuroscience*, 1984, 12, 557–567.
9. Ito U, Spatz M, Walker JT, Klatzo I: Experimental cerebral ischemia in Mongolian gerbils. I. Light microscope observations. *Acta Neuropathol (Berl)*, 1975, 32, 209–223.
10. Kirino T: Delayed neuronal death in gerbil hippocampus following ischemia. *Brain Res*, 1982, 239, 57–69.
11. Kirino T, Sano K: Selective vulnerability in the gerbil hippocampus following transient ischemia. *Acta Neuropathol (Berl)*, 1984, 62, 269–278.
12. Kirino T, Tamura A, Sano K: Delayed neuronal death in rat hippocampus following transient forebrain ischemia. *Acta Neuropathol (Berl)*, 1984, 64, 139–147.
13. Korpatchev WG, Lysenkov SP, Thiel LZ: Modelowanie klinicznej smierci i postreanimacji choroby u krys. *Patol Fiziol Exper Ter*, 1982, 3, 78–80.
14. Mata M, Staple J, Fink DJ: Ultrastructural distribution of Ca<sup>++</sup> within neurons. An oxalate-pyroantimonate study. *Histochemistry*, 1987, 87, 339–349.
15. Mossakowski MJ, Hilgier W, Januszewski S: Morphological abnormalities in the central

- nervous system of rats in experimental postresuscitation period. *Neuropatol Pol*, 1986, 24, 471–489.
16. Mossakowski MJ, Gajkowska B, Tsitsishvili A: Ultrastructure of neurons from the CA<sub>1</sub> sector of Ammon's horn in short-term cerebral ischemia in Mongolian gerbils. *Neuropatol Pol*, 1989, 27, 39–53.
  17. Ohara PT, Wade CR, Lieberman AR: Calcium storage sites in axon terminals and other components of intact c.n.s. tissue: studies with a modified pyroantimonate technique. *J Anat*, 1979, 129, 869–873.
  18. Olney JW, de Gubareff T, Sloviter RS: "Epileptic" brain damage in rats induced by sustained electrical stimulation of the perforant path. II. Ultrastructural analysis of acute hippocampal pathology. *Brain Res Bull*, 1983, 10, 699–712.
  19. Probst W: Ultrastructural localization of calcium in the CNS of vertebrates. *Histochemistry*, 1986, 85, 231–239.
  20. Rothman SM: The neurotoxicity of excitatory amino acid is produced by passive chloride influx. *J Neurosci*, 1985, 5, 1483–1489.
  21. Rothman SM, Olney JW: Glutamate and the pathophysiology of hypoxic-ischemic brain damage. *Ann Neurol*, 1986, 19, 105–111.
  22. Siesjö BK, Bengtsson F: Calcium fluxes, calcium antagonists, and calcium-related pathology in brain ischemia, hypoglycemia, and spreading depression: a unifying hypothesis. *J Cereb Blood Flow Metab*, 1989, 9, 127–140.
  23. Siesjö BK, Wieloch T: Cerebral metabolism in ischemia: neurochemical basis for therapy. *Br J Anaesth*, 1985, 57, 47–62.
  24. Suzuki R, Yamaguchi T, Inaba V, Wagner HG: Microphysiology of selectively vulnerable neurons. *Prog Brain Res*, 1985, 63, 59–68.
  25. Van Reempts J, Haseldonck M, Van Deuren B, Wouters L, Borges M: Structural damage of the ischemic brain: involvement of calcium and effects of posts ischemic treatment with calcium entry blockers. *Drug Dev Res*, 1986, 8, 387–395.
  26. Wieloch T, Westerberg E: Mechanism of glutamate neurotoxicity in cerebral ischemia. In: *Neurotransmission and cerebrovascular function. II*. Eds: J Scylaz, R Sercombe. Elsevier, Amsterdam, 1989, pp 87–94.
  27. Yamaguchi T, Klatzo I: Maturation of cell damage following transient ischemia in gerbils. In: *Cerebral ischemia*. Eds: A Bes, P Braquet, R Paoletti, BK Siesjö. Elsevier, Amsterdam, New York, Oxford, 1984, pp 13–24.
  28. Yasumoto Y, Passonneau JR, Feussner G, Lust WP: Metabolic alterations in fiber layers of CA<sub>1</sub> region of the gerbil hippocampus following short-term ischemia: high energy phosphates, glucose-related metabolites and amino-acids. *Metab Brain*, 1988, 3, 133–149.

Authors' address: Medical Research Centre, Polish Academy of Sciences, 3 Dworkowa Str, 00-784 Warsaw, Poland

ANDRZEJ KAPUŚCIŃSKI

## CHANGES IN ENDOGENOUS PROSTACYCLIN IN THE RAT BRAIN DURING CLINICAL DEATH AND AFTER RESUSCITATION

Department of Neuropathology, Medical Research Centre, Polish Academy of Sciences, Warsaw

By means of the radioimmunologic method changes of concentration of 6-keto-prostaglandin  $F_{1\alpha}$  ( $PGF_{1\alpha}$ ) — the stable metabolite of prostacyclin in the rat brain have been evaluated during 5-min clinical death and up to 2 hrs after resuscitation. Ischemia did not produce significant changes of 6-keto- $PGF_{1\alpha}$  concentration in the brain. In the early postresuscitation period the concentration of 6-keto- $PGF_{1\alpha}$  in the and 7-fold control values. Later the concentration of 6-keto- $PGF_{1\alpha}$  in the brain decreased reaching in 30 min a 3-fold the control level, and in 60 and 120 min after resuscitation control values. The reasons of unsuccessful therapy of ischemic stroke with prostacyclin are discussed.

Key words: *Prostacyclin, ischemia, rat brain.*

A diverse array of mammalian cells and tissues enzymatically oxidize arachidonic acid to physiologically active compounds. These compounds include prostacyclin, thromboxanes, prostaglandins and leukotrienes. Prostacyclin, also known as prostaglandin  $I_2$  ( $PGI_2$ ) is an unstable vinyl ether formed from the prostaglandin endoperoxide, prostaglandin  $H_2$ . This conversion of  $PGH_2$  to prostacyclin is catalyzed by prostacyclin synthetase and the two primary sites of synthesis are the veins and arteries. Prostacyclin has biological properties opposing the effect of thromboxane  $A_2$ . Prostacyclin is a vasodilator and a potent inhibitor of platelet aggregation (Gryglewski et al. 1976; Moncada, Vane 1979) while thromboxane  $A_2$  is a vasoconstrictor and promoter of platelet aggregation (Hamberg et al. 1975; Svensson et al. 1975). A physiological balance between the activities of these two effectors is probably important for maintaining a healthy vascular bed.

Prostacyclin is unstable and undergoes spontaneous hydrolysis to 6-keto-prostaglandin  $F_{1\alpha}$ . Study of this reaction *in vitro* established that prostacyclin has a half-life of about 3 min (Cho, Allen 1978). This half-life increases to 9–23 min in platelet-poor plasma (Orchard, Robinson 1981). Due to this spontaneous hydrolysis of prostacyclin, quantitation of 6-keto-prostaglandin  $F_{1\alpha}$  is accepted by many researchers as a measure of prostacyclin formation (Fitzpatrick et al. 1979).

The deleterious effect of thromboxane and prostaglandins on cerebral blood flow, including vasospasm and platelet aggregation, and the opposite properties of PGI<sub>2</sub> have been a theoretical basis for the treatment of ischemic stroke in the clinic (Gryglewski et al. 1982; Huczyński et al. 1985) and experimental investigations (Hallenbeck, Furlow 1979; Kerckhoff et al. 1983; Pluta 1985, 1986, 1988, 1990; Mossakowski, Gadamski 1987). The use of PGI<sub>2</sub> (Pluta 1985, 1986) and/or the cyclooxygenase inhibitor indomethacin (Mossakowski, Gadamski 1985, 1987) have been shown to have a protective effect on restoring of bioelectric activity after complete brain ischemia in rabbit and CA<sub>1</sub> hippocampal histologic damage in gerbil.

Nevertheless, the results of several studies were found to be negative in therapeutic effects of PGI<sub>2</sub> in ischemic stroke in experimental studies (Kerckhoff et al. 1983; Pluta 1988, 1990) as well as in clinical practice (Huczyński et al. 1985).

We examined the effect of clinical death and recovery after resuscitation on the content of deleterious eicosanoids PGD<sub>2</sub>, PGF<sub>2α</sub> and TxB<sub>2</sub> in the rat brain (Kapuściński, Hilgier 1989). It seemed useful to find out how intensive is the synthesis of PGI<sub>2</sub>, and its dynamics as a potential protective agent in the same experimental model.

The purpose of the present study was to evaluate the content of endogenous PGI<sub>2</sub> in the rat brain during clinical death and after resuscitation.

#### MATERIAL AND METHODS

Under ether anesthesia 5-min clinical death was induced in 35 adult female Wistar rats, weighing 170–180 g, by intrathoracic compression of the cardiac vessels bundle at the base of the heart, with a hook-like device without major surgery (Korpachev et al. 1982). Cardio-pulmonary resuscitation was achieved by external cardiac massage and artificial ventilation with air. The animals were sacrificed in groups of five at the end of ischemia and 5, 15, 30, 60 and 120 min after resuscitation. Five animals served as a control group in which under ether anesthesia a sham-operation was performed.

Preparation of brain samples and extraction procedures: the brains were removed from the skull in less than 30 sec, frozen in liquid nitrogen and stored at –70°C until analysed. Brain samples were cut off, weighed (approximately 400 mg) and homogenized in 0.1 N phosphate buffer pH 7.4 (5ml/g) in a Teflon homogenizer at 0°C. The homogenates were diluted 1:4 in 1M HCl, centrifuged at 10,000g at 4°C for 10 min. (<sup>3</sup>H) 6-keto-PGF<sub>1α</sub> with a radioactivity of 1,000 cpm, was added to each supernatant for calculation of recovery. The solid phase extraction developed by Powell (1980) was modified according to protocol for Amprep minicolumns (RPN 1903) and Amprep Manifold-10 (Amersham). The supernatants were applied to C<sub>2</sub> 100 mg minicolumns prewashed with 2 ml methanol and 2 ml water. After application of the supernatants interference elution was performed with 5 ml water, 5 ml 10% ethanol and 5 ml hexane, followed by analyte elution with 5 ml methyl formate. The eluates were concentrated under nitrogen gas and resuspended with 250 μl of phosphate-buffered saline with gelatin and thimerosal (assay buffer). The typical recovery was about 90%.

The sensitive and specific ( $^3\text{H}$ ) 6-keto-prostaglandin  $\text{F}_{1\alpha}$  radioimmunoassay (RIA) system (Amersham) was used. The sensitivity was within the range 14–500 pg/tube. RIA was performed according to the recommended protocol. All samples were assayed in duplicate with appropriate standards to construct the standard curve for calculations. Sample extracts, radiolabeled tracer, antiserum and standards were incubated at room temperature for 1 hour and then at  $4^\circ\text{C}$  for 20 hours. Separation of the unbound radioactive ligand was achieved by adsorption on dextrane-coated, charcoal, followed by centrifugation. The radioactivity was counted for 10 min in Bray's scintillant in an LS 5000TA Beckman beta scintillation counter. Results were expressed as mean  $\pm$  S.D. and analysed by Student's test.

## RESULTS

The dynamics of changes of 6-keto-PGF $_{1\alpha}$  content in the rat brain in the control group, at the end of the 5-min clinical death and during the postresuscitation period up to two hours is presented in Table 1.

Table 1. 6-keto-prostaglandin  $\text{F}_{1\alpha}$  in the rat brain during clinical death and after resuscitation

Control	End of clinical death	Period after resuscitation				
		5 min	15 min	30 min	60 min	120 min
92.2 $\pm$ 13.0	94.8 $\pm$ 11.8	717.6* $\pm$ 162.1	633.4* $\pm$ 99.7	308.6* $\pm$ 122.6	96.6 $\pm$ 21.2	91.4 $\pm$ 19.7

Values represent means  $\pm$  S.D. from 5 animals in pg/g of wet tissue

\* Significance in reference to control –  $p < 0.01$

As seen in the Table 1, in the control sham-operated group, the mean level of 6-keto-PGF $_{1\alpha}$  in the brain was 92.2 pg/g of wet tissue. At the end of the 5-min clinical death this level did not differ significantly from the control and was on the average 103%. In the early period after resuscitation the concentration of 6-keto-PGF $_{1\alpha}$  significantly and quickly increased reaching in 5 min on the average 778%. In the 15 min recovery period the concentration slightly decreased being still very high, presenting on the average 687%. In the later period after resuscitation the level of 6-keto-PGF $_{1\alpha}$  significantly and quickly decreased reaching in 30 min of recovery 335% and in 60 and 120 min the control values 105% and 99% respectively.

## DISCUSSION

The reversible increase of several prostaglandins including 6-keto-PGF $_{1\alpha}$  in the brain was observed by other authors in ischemic models on gerbils (Gaudet, Levine 1979; Gaudet et al. 1980; Kempinski et al. 1987) and rats (Minamisawa et al. 1988). The important implication from the present study together with the results of the above named authors is that synthesis and release of endogenous PGI $_2$  in brain ischemia is efficient, relatively

short-lasting, and appears in the early postischemic period. Actually, the massive accumulation of arachidonic acid during the ischemic episode, allows for its conversion into an eicosanoids cascade, including prostacyclin, during the recovery period. The biological opposite effect of individual eicosanoids should not be described by concentration units. Nevertheless, in our experimental model the 6-keto-PGF<sub>1 $\alpha$</sub>  concentration increased maximally 8-fold and that of thromboxane B<sub>2</sub> (TxB<sub>2</sub>) 15-fold (Kapuściński, Hilgier 1989). In the studies of Minamisawa et al. (1988) 6-keto-PGF<sub>1 $\alpha$</sub>  level rose 5-fold and TxB<sub>2</sub> 11-fold. The concentration of other deleterious prostaglandins rises enormously during that time (Kapuściński, Hilgier 1989), and one might assume that there is a relative deficiency of endogenous prostacyclin as a vasodilator and inhibitor of platelet aggregation.

It should be emphasized that in this particular experimental model after 5 min of ischemia, in the early recovery period, there is no platelet aggregation and no vasospasm, on the contrary, cerebral vessels are maximally dilated during postischemic reactive hyperemia (Kapuściński 1987). Thus, the application of PGI<sub>2</sub> as medication for ischemic stroke, in the early postischemic period, when the concentration of endogenous PGI<sub>2</sub> is significantly elevated, can produce result opposite to those expected with the known systemic hypotensive effect of prostacyclin (Armstrong et al. 1978; Pluta 1986; Mossakowski, Gadamski 1987).

The author assumes that the molecular mechanisms concerning alterations in the brain in the postischemic period are so complicated that PGI<sub>2</sub> with its short half-like and vasodepressor effect will be relinquished for the therapy of vascular diseases, especially as a protective drug in ischemic stroke. Even Ilprost — a chemically and biologically stable analogue of PGI<sub>2</sub> (Stock 1990) with its known inhibitory effect on platelet aggregation, white blood cell adhesion and attenuating secretion of thrombotic and mitogenic factors showed no protective effect on the development of selective damage of Ammon's horn CA<sub>1</sub> neurons, resulting from short-term forebrain ischemia in gerbils (Mossakowski, Gadamski 1987).

Thus, on the basis of results of the present study and data from the literature it seems reasonable to assume that therapy of ischemic stroke will require a multidirectional pharmacological approach.

#### ZMIANY ENDOGENNEJ PROSTACYKLINY W MÓZGU SZCZURA PODZAS ŚMIERCI KLINICZNEJ I PO RESUSCYTACJI

##### Streszczenie

Przy użyciu metody radioimmunologicznej oceniono zmiany stężenia 6-keto-prostaglandyny F<sub>1 $\alpha$</sub>  (PGF<sub>1 $\alpha$</sub> ) — stabilnego metabolitu prostacykliny w mózgu szczura podczas 5 minutowej śmierci klinicznej i do 2 godzin po resuscytacji. Ischemia nie powodowała zmian stężenia 6-keto-PGF<sub>1 $\alpha$</sub>  w mózgu. We wczesnym okresie po resuscytacji wystąpił szybki i bardzo znaczny wzrost stężenia 6-keto-PGF<sub>1 $\alpha$</sub>  w mózgu osiągając w 5 i 15 minucie odpowiednio 8 i 7 razy wartości kontrolne. Następnie stężenie 6-keto-PGF<sub>1 $\alpha$</sub>  w mózgu obniżyło się osiągając w 30 minucie poziom 3 razy wyższy od wartości kontrolnych a w 60 i 120 minucie po resuscytacji uległo normalizacji. Przedyskutowano niektóre przyczyny niepowodzeń w wynikach leczenia prostacykliną niedokrwiennych chorób mózgu.



## REFERENCES

1. Armstrong JM, Lattimer N, Moncada S, Vane JR: Comparison of the vasodepressor effect of prostacyclin and 6-oxo-prostaglandin F<sub>1</sub> with those of prostaglandin F<sub>2</sub> in rats and rabbits. *Br J Pharmacol*, 1978, 62, 125–130.
2. Cho MJ, Allen MA: Chemical stability of prostacyclin (PGI<sub>2</sub>) in aqueous solutions. *Prostaglandins*, 1978, 15, 943–954.
3. Fitzpatrick FA, Stringfellow DA, Maclouf J, Rigaud M: Analytical methods that reveal PGI<sub>2</sub> synthesis by cell cultures: glass capillary gas chromatography with electron capture detection. In: *Prostacyclin*. Eds: JR Vane, S Bergström. Raven Press, New York, 1979, pp 55–64.
4. Gaudet RJ, Levine L: Transient cerebral ischemia and brain prostaglandins. *Biochem Biophys Res Commun*, 1979, 86, 893–901.
5. Gaudet RJ, Alam I, Levine L: Accumulation of cyclooxygenase products of arachidonic acid metabolism in gerbil brain during reperfusion after bilateral common carotid artery occlusion. *J Neurochem*, 1980, 35, 653–658.
6. Gryglewski RJ, Bunting S, Moncada S, Flower RJ, Vane JR: Arterial walls are protected against deposition of platelet thrombi by a substance ( prostaglandin X) which they make from prostaglandin endoperoxides. *Prostaglandins*, 1976, 12, 685–713.
7. Gryglewski RJ, Nowak S, Trąbka-Kostka E, Biedroń K, Kuśmiderski J, Markowska E, Szmatoła S: Clinical use of prostacyclin (PGI<sub>2</sub>) in ischemic stroke. *Pharmacol Res Commun*, 1982, 14, 879–908.
8. Hallenbeck JM, Furlow TW Jr: Prostaglandin I<sub>2</sub> and indomethacin prevent impairment of postischemic brain reperfusion in the dog. *Stroke*, 1979, 10, 629–637.
9. Hamberg M, Svensson J, Samuelsson B: Thromboxanes: A new group of biologically active compounds derived from prostaglandin endoperoxides. *Proc Natl Acad Sci, USA*, 1975, 72, 2992–2998.
10. Huczynski J, Kostka-Trąbka E, Sotowska W, Biedroń K, Grodzienka L, Dembińska-Kieć A, Pykosz-Mazur E, Peczak E, Gryglewski RJ: Double-blind controlled trial of the therapeutic effects of prostacyclin in patients with complete ischemic stroke. *Stroke*, 1985, 16, 810–814.
11. Kapuściński A: Mózgowy przepływ krwi w doświadczalnym modelu śmierci klinicznej u szczurów. *Neuropatol Pol*, 1987, 25, 287–298.
12. Kapuściński A, Hilgier W: Eicosanoids in rat brain and plasma after resuscitation from clinical death. *Neuropatol Pol*, 1989, 27, 519–525.
13. Kempinski O, Shohami E, von Lubitz D, Hallenbeck JM, Feuerstein G: Postischemic production of eicosanoids in gerbil brain. *Stroke*, 1987, 18, 111–119.
14. Kerckhoff van den W, Hossmann KA, Hossmann V: No effect of prostacyclin on blood flow, regulation of blood flow and blood coagulation following global cerebral ischemia. *Stroke*, 1983, 14, 724–730.
15. Korpachev GV, Lysenkov SP, Tiel LZ: Modelowanie klinicznej smierci i postreanimacyjnej boleznij u krysz. *Patol Fizjol Eksp Ter*, 1982, 3, 78–80.
16. Minamisawa H, Terashi A, Katayama Y, Kanda Y, Shimizu J, Shiratori T, Inamura K, Kaseki H, Yoshino Y: Brain eicosanoid levels in spontaneously hypertensive rats after ischemia with reperfusion: Leukotriene as a possible cause of cerebral edema. *Stroke*, 1988, 19, 372–377.
17. Moncada S, Vane JR: Pharmacology and endogenous roles of prostaglandin endoperoxides, thromboxane A<sub>2</sub> and prostacyclin. *Pharmacol Rev*, 1979, 30, 292–331.
18. Mossakowski MJ, Gadamski R: Wpływ indometacyny na niedokrwiennie uszkodzenia sektora CA<sub>1</sub> rogu Amona u chomików mongolskich. *Neuropatol Pol*, 1985, 23, 493–506.
19. Mossakowski MJ, Gadamski R: Wpływ prostacykliny PGI<sub>2</sub> i indometacyny na niedokrwiennie uszkodzenia sektora CA<sub>1</sub> rogu Amona u chomików mongolskich. *Neuropatol Pol*, 1987, 25, 21–34.
20. Orchard MA, Robinson C: Prostacyclin is stabilized by serum albumin. *Br J Pharmacol*, 1981, 74, 206.
21. Pluta R: Influence of prostacyclin on early morphological changes in the rabbit brain after complete 20 min ischemia. *J Neurol Sci*, 1985, 70, 305–316.
22. Pluta R: Influence of prostacyclin on the recovery of bioelectric activity after complete ischemia. *Acta Neurol Scand*, 1986, 73, 44–54.
23. Pluta R: The effects of prostacyclin on early ultrastructural changes in the neuron nuclei of the motor cortex in rabbits after complete 20-min cerebral ischemia. *Exp Mol Pathol*, 1988, 48, 161–173.

24. Pluta R: Experimental treatment with prostacyclin of global cerebral ischemia in rabbit – new data. *Neuropatol Pol*, 1990, 28, 205–215.
25. Powell WS: Rapid extraction of oxygenated metabolites of arachidonic acid from biological samples using octadecylsilyl silica. *Prostaglandins*, 1980, 20, 947–957.
26. Stock G: Ilprost: a stable analogue of prostacyclin. In: *Endothelium-derived relaxing-factors*. Eds: GM Rubanyi, PM Vanhoutte Karger, Basel, 1990, pp 260–264.
27. Svensson J, Hemberg M, Samuelsson B: Prostaglandin endoperoxides IX. Characterisation of rabbit aorta contracting substance from guinea pig lung and human platelets. *Acta Physiol Scand*, 1975, 94, 222–228.

Author's address: Department of Neuropathology, Medical Research Centre, Polish Academy of Sciences, 3 Dworkowa Str, 00-784 Warsaw, Poland

HALINA KROH<sup>1</sup>, ANNA TARASZEWSKA<sup>1</sup>, EDMUND RUZIKOWSKI<sup>2</sup>,  
JERZY BIDZIŃSKI<sup>2</sup>, MIROSLAW J. MOSSAKOWSKI<sup>1</sup>

## NEUROPATHOLOGICAL CHANGES IN RESECTED TEMPORAL LOBE OF PATIENTS WITH CRYPTOGENIC EPILEPSY

<sup>1</sup> Department of Neuropathology, Medical Research Centre, Polish Academy of Sciences, Warsaw,  
<sup>2</sup> Department of Neurosurgery, School of Medicine, Warsaw

The study was performed on cerebral tissue resected during temporal lobectomy in 16 patients whose long-standing cryptogenic epilepsy did not submit to anticonvulsive drugs. Cases presenting definite etiological factors such as CNS trauma, infection or neoplasm were excluded. Neuropathological investigations disclosed microangiomas and focal vascular malformations in the meninges and tissue in 7 patients. Neuronal heterotopias in the white matter and of the white matter in the cortex were observed in 3 cases. Main cortical changes were: neuronal loss, chronic neuronal degeneration, perineuronal satellitosis, and GFAP-positive submeningeal gliosis, especially at the bottom of sulci, perivascular gliosis and laminar or diffuse gliosis. The changes in the hippocampus were most enhanced in the end-plate and in the sector H3 of the pyramidal layer. Astrocytic gliosis in the white matter presented distinct GFAP and S-100 immunostaining; the latter involved in some cases a wider area than the GFAP reaction.

The above named changes are analysed with regard to the presumed epileptogenic factors and to the postepileptic damage.

*Key words: temporal lobectomy, epilepsy, neurons, gliosis.*

The problem of idiopathic epilepsy engaged a good deal of attention, especially devoted to the explanation of the morphological ground of temporal epilepsy. Cases of spontaneous epilepsy raise the question whether morphological alterations are the consequence or the cause of epileptic seizures, a question probably impossible to answer. With the purpose of explaining the origin of temporal epilepsy in a selected group of patients in whom symptomatic epilepsy had been eliminated, we took an interest in patients treated with temporal lobectomy. These patients suffered of long-standing drug-resistant epileptic seizures.

## MATERIAL AND METHODS

## Clinical data

The material under study was obtained from 11 male and 5 female patients. Their age at the time of operation was 8–50 years (mean 21.8) for men and 20–38 (mean 25.4) for women. At the outset of the first temporal seizure the age of patients ranged from 4 months to 28 years (mean 10.3), whereas the duration of the medically treated illness till surgical intervention was 3–22 years. In the majority of cases the etiology of the epilepsy remained obscure; perinatal traumas such as asphyxia, forceps delivery, premature delivery were established in 3 patients. Slight mechanical traumas were discovered in 2 cases, twice in 2-year-old child and once in 28-year-old man with brief period of unconsciousness. In one case meningitis in a 1-year-old baby preceded epilepsy by 8 years. In the early period of the illness generalized maximal seizures were observed in 11 patients, whereas simple partial and complex partial seizures were not frequent and in only 4 cases associated with grand-mal. In this early stage the number of all types of seizures could not be established, the number reported by the patients was 1–70 per year. At the time preceding lobectomy only 7 patients complained of grand-mal but the fits increased in number as well as increased the number of seizures of other types, so the patients complained of 50-1000 seizures per year. Neurological examinations in 3 patients revealed some minor abnormalities but no definite neurological symptoms, whereas psychological tests established emotional and intellectual disturbances in 11 patients. Neuroradiological examination (Rtg, CT) showed also some minor pathological changes without distinct relation to the etiology of epilepsy (5 patients). EEG investigations demonstrated foci of slow waves or foci of sharp waves or both types in all 16 patients. Applied pharmacological treatment consisted of the following anticonvulsant drugs: Amizepam, Dipromal, Phenydantin, Luminal, Tegretol, Mizodin.

Right-side temporal lobectomy was performed in 9 patients, left-sided in 7. The extent of lobectomy in all cases depended on the ECoG results at the outset and during the operation and on the local conditions. Radical lobectomy was performed in 10 cases, in 6 cases it covered the anterior part of the temporal lobe. The majority (8 out of 10) of radical lobectomies was performed in the right hemisphere, whereas resection of anterior parts was done mainly (5 out of 6) in the left lobe. Only in one case temporal lobe resection did not comprise the hippocampus: in 8 cases the lobectomized tissue included total or partial hippocampal structure, in 2 cases temporal lobectomy comprised also the hippocampus and nucleus amygdalae. In 5 cases temporal lobectomy including the hippocampus covered additionally (due to ECoG) other epileptogenic areas (frontal parietal, parieto-occipital and occipital cortex). Two of the patients had to be operated twice because of persistence of epileptic seizures, one after 4 years, another after 10 months.

The cerebral surface was normal in 11 patients whereas in four widening of temporal gyri was distinct; in 2 of them the medial temporal gyrus was twice the normal size.

Opacity of leptomeninges over the temporal lobe was observed in 2 pa-

tients, one of them presented additionally some cortical atrophy. A superficial cyst involving the middle part of the temporal lobe and extending to the parieto-occipital area was found in one case. Adhesions between dura mater and leptomeninges were observed in 3 cases (twice in reoperated patients). The appearance and consistence of the cerebral tissue removed during lobectomies seemed altogether unchanged in nine out of 16 patients.

### Neuropathological methods

Cerebral tissue obtained from 16 patients was fixed in formalin and embedded in paraffin. The 10  $\mu$  thick paraffin sections were stained routinely with HE, Klüver-Barrera method, some also with cresyl violet. Immunohistochemical investigations were performed on mirror sections from the same paraffin blocks. Antisera against protein S-100 and against glial fibrillary acidic protein (GFAP) were obtained from Dacopatts (Copenhagen). The former was used in 1:5000 solution with use the APAAP method, the latter in 1:500 solution by the ABC method.

### RESULTS

In the temporal cortex and subcortical white matter of all 16 patients pathological alterations were present. Most of them took the form of neuronal changes and astrocytic gliosis. The cortex displayed most frequently neuronal loss, dark neurons, chronic neuronal degeneration, sometimes combined with perineuronal satellitosis. In all the cases the enhanced cortical GFAP-positive subpial fibrous gliosis, in particular at the bottom of sulci (Fig. 1), perivascular gliosis (Fig. 2) and gliosis either haphazardly disseminated or distributed in some cortical layers (Figs 3, 4) were observed. GFAP-positive astrocytes were also S-100 immunostained, but in some cases the area of S-100 astrocytic immunoreactivity extended beyond the fields of GFAP-positive astrocytes and involved the whole cortex. In two cases reactive astroglia did not show any GFAP reaction in spite of marked S-100 reactivity.

In the white matter diffuse astrocytic gliosis of various intensity appeared in 11 cases, whereas 3 cases presented only marked fibrous gliosis restricted to the cortical-subcortical junction (Fig. 5). Similarly as in the cortex, perivascular GFAP-positive gliosis was distinct and appeared in all cases and often was most prominent around small lacunae (Fig. 6). As in the cortex, reactive astrocytes showed both GFAP and S-100 immunostaining, the latter spreading over a wider area in 4 cases (Figs 7, 8).

Discrete inflammatory changes such as mononuclear perivascular infiltrations in the meninges, cortex, and in the white matter, and the glial-lymphocytic nodules were found in 2 cases. These changes remain obscure in one case; others concern the patient reoperated after 10 months.

Vascular changes were found in 7 cases. They took the form of meningeal microangiomas (Fig. 9) or microscopical size arterio-venous malformations in the meninges and at the meningo-cerebral interface (Fig. 10). Abnormal arteries with thick hyalinized walls in the cortex and white matter were found in a 50-year-old man with 22 years long history of epilepsy.

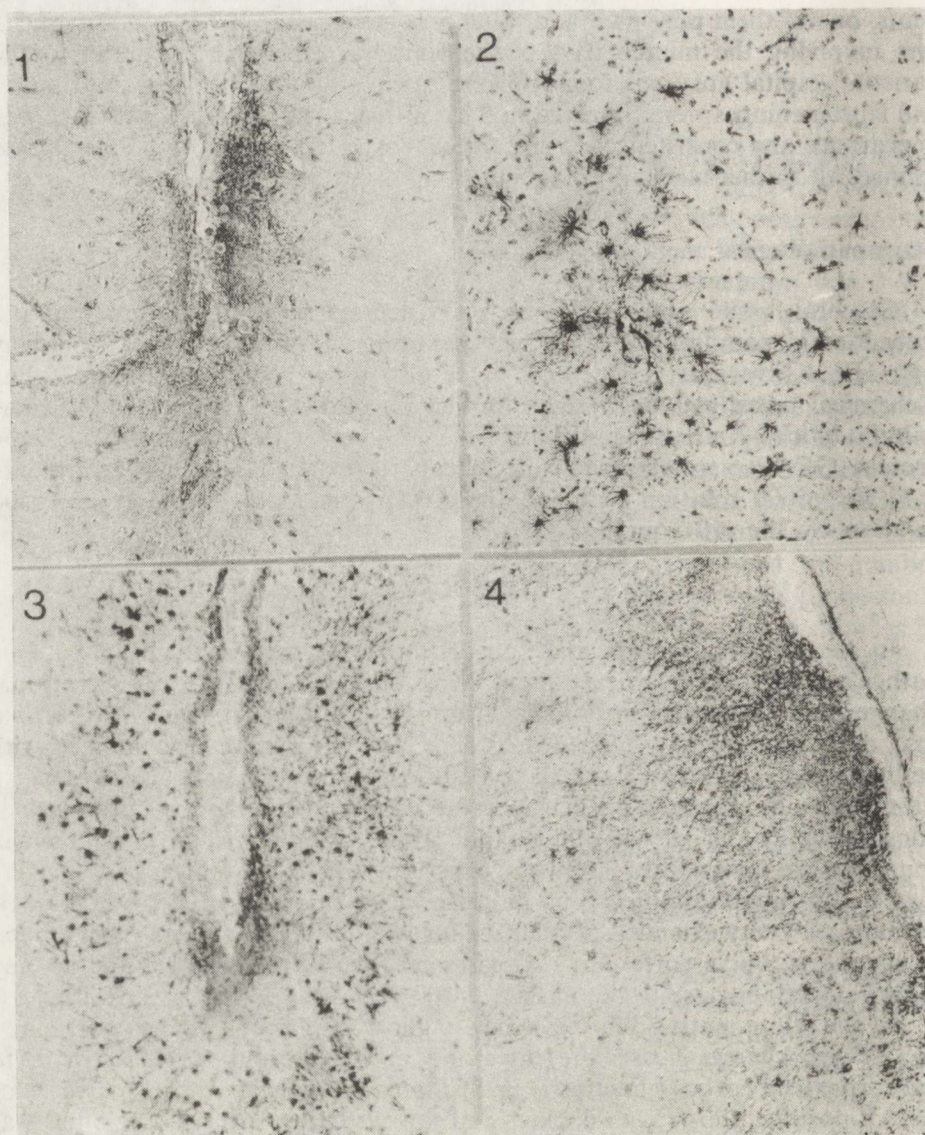


*Fig. 1.* Temporal cortex. Submeningeal GFAP-positive fibrous gliosis at bottom of sulcus.  $\times 100$

*Fig. 2.* Temporal cortex. GFAP-positive perivascular astrocytic gliosis.  $\times 100$

*Fig. 3.* GFAP-positive astrocytic gliosis, mostly in II cortical layer.  $\times 60$

*Fig. 4.* GFAP-positive fibrous gliosis spread from submeningeal region to deeper cortical layers.  $\times 100$

Distinct developmental abnormalities of brain tissue appeared in the case of abortive microgyria in the abnormally wide middle temporal gyrus, associated with white matter heterotopia in the cortex (Fig. 11) and neuronal dystopias in the cortical layers II and III (Fig. 12). In other two cases heterotopias of small groups of neurons occurred in the white matter, but in a 24-year-old patient suffering of temporal epilepsy for 4 years they coexisted with persisting matrix cells.

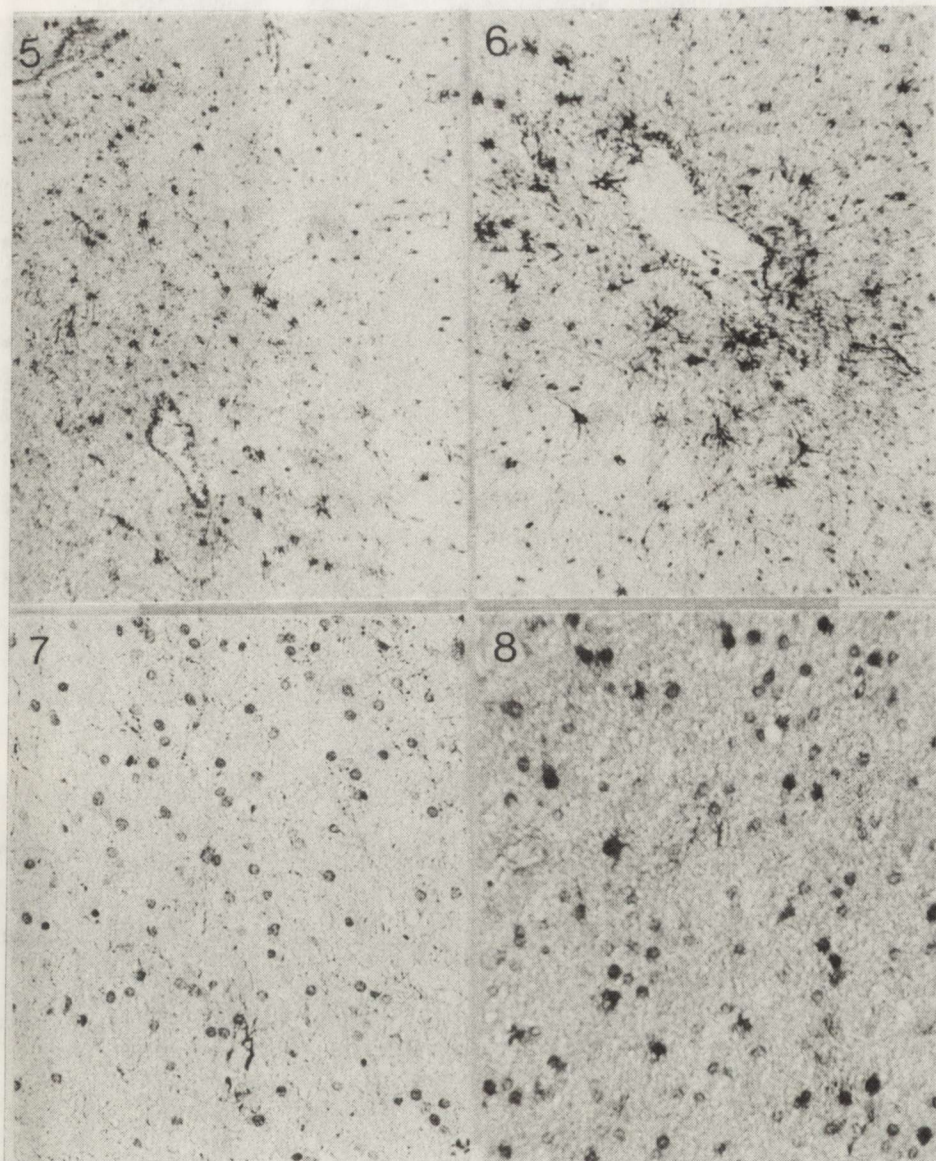


Fig. 5. Cortico-subcortical border. GFAP-positive astrogliosis.  $\times 60$

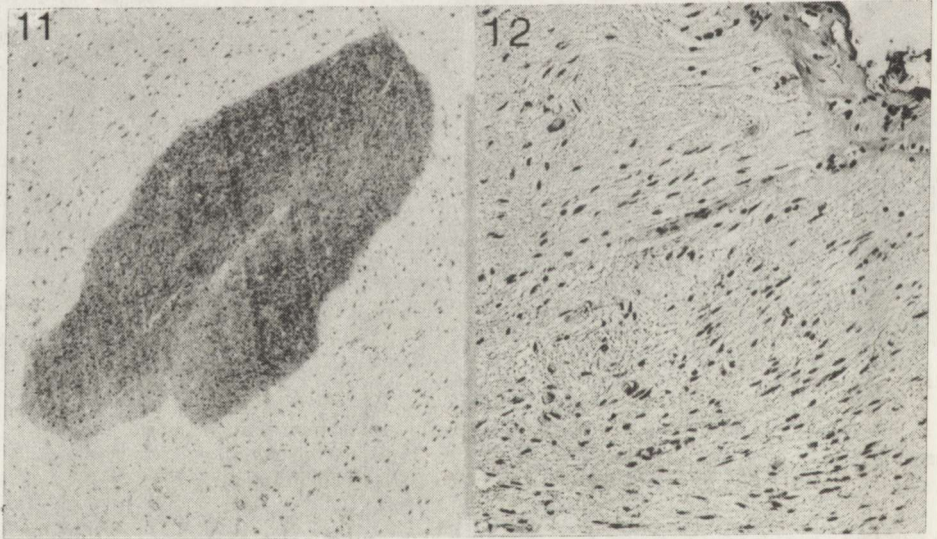
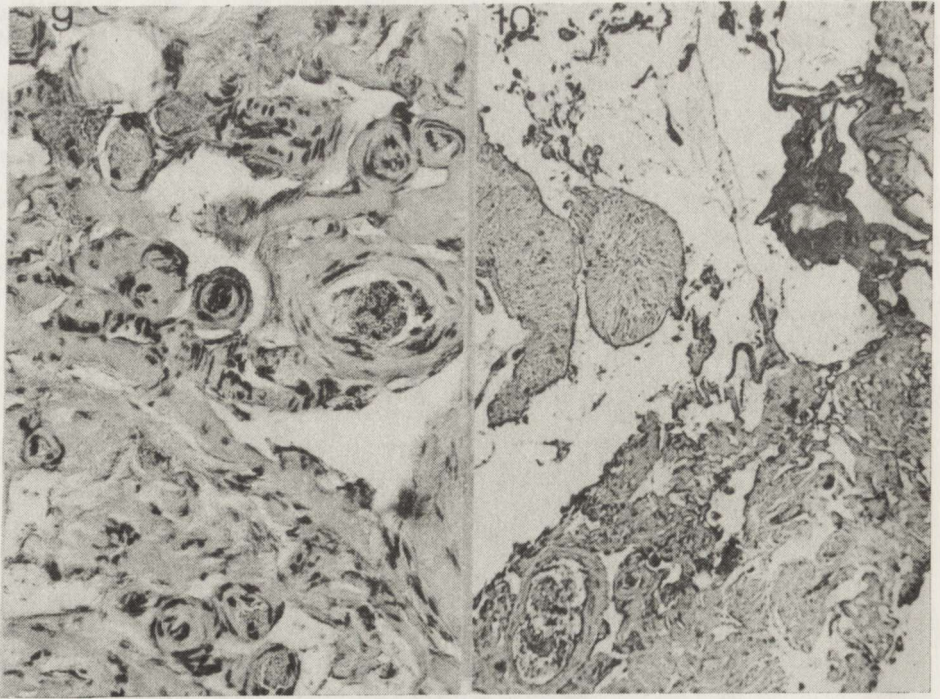
Fig. 6. White matter. GFAP-positive gliosis around perivascular lacuna.  $\times 100$

Fig. 7. White matter. Low GFAP-positive reaction.  $\times 180$

Fig. 8. White matter. Distinct S-100 protein reaction.  $\times 200$

The hippocampus was examined in 9 patients, but fragments of all hippocampal structures were available in 5 cases only, in 3 specimens preserved were only some fragments of *gyrus dentatus* including the *hilus* and in another one — some parts of the *subiculum* and *gyrus dentatus*.

The density of neurons in the hippocampal pyramidal cell layer was either decreased or the neurons revealed neuronal degeneration of chronic type (Fig. 13). In sector H1 and hilus (Fig. 14) beside dark, shrunken neurons, swollen



*Fig. 9.* Angioma in leptomeninges. HE.  $\times 250$

*Fig. 10.* Cortico-meningeal vascular malformation. HE.  $\times 120$

*Fig. 11.* Focal white matter heterotopia in temporal cortex. Klüver-Barrera.  $\times 50$

*Fig. 12.* Cortical layers disturbances. Fibrosis of arachnoidea. HE.  $\times 120$



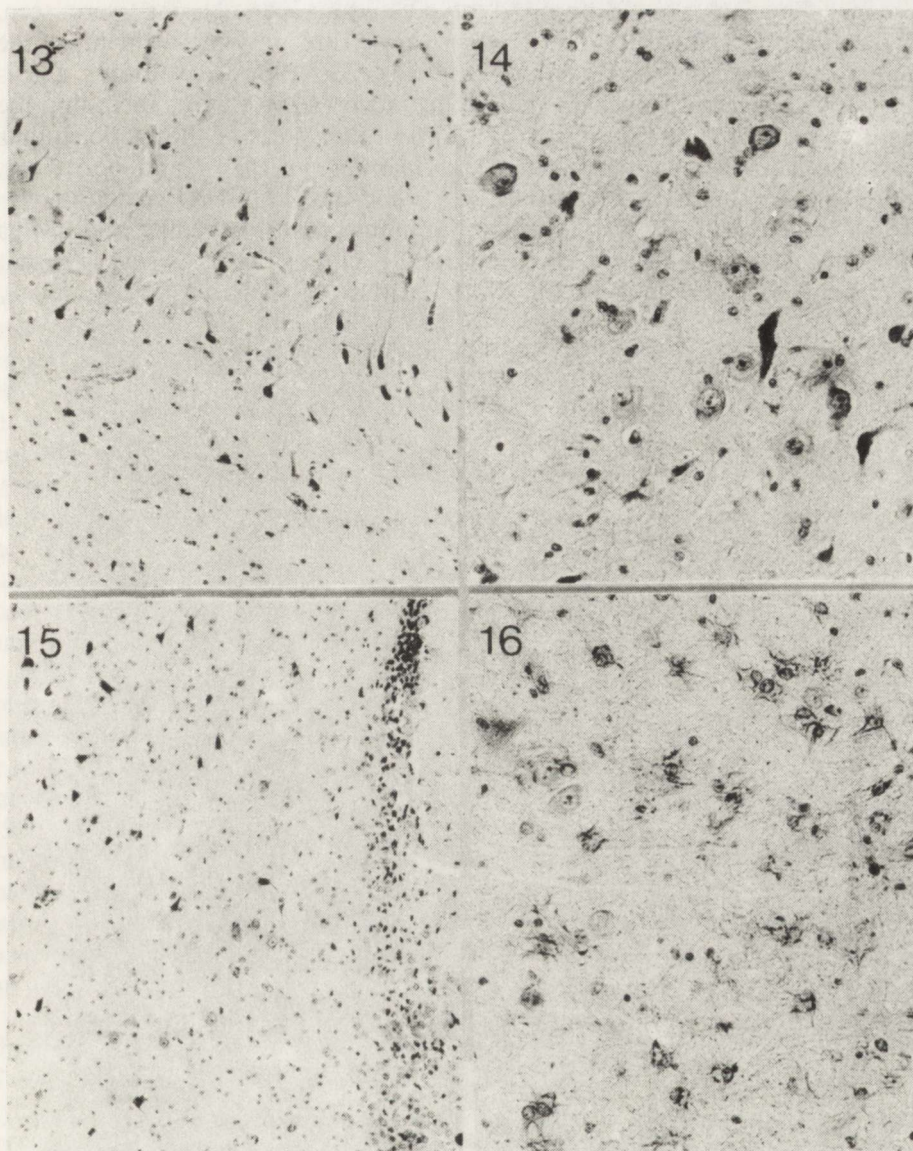


*Fig. 13.* Hippocampus. Neuronal loss and chronic degeneration of pyramidal neurons in H1 sector. HE.  $\times 120$

*Fig. 14.* Hippocampus. Chronic degeneration, swelling and vacuolization of hilar neurons. HE.  $\times 90$

*Fig. 15.* Hippocampus. Segmental loss of granular cells, neuronal chronic degeneration in hilus. HE.  $\times 90$

*Fig. 16.* Hippocampus. Diffuse GFAP-positive astrocytic gliosis in hilus. HE.  $\times 200$

nerve cells against the background of edematous perenchyma were seen. Cellular rarefaction and dark neurons were also visible in some segments of the granular cell layer of *gyrus dentatus* (Fig. 15). GFAP-positive fibrous gliosis was restricted selectively to the whole hilus of the dentate gyrus including the H3 sector of the pyramidal layer (Fig. 16). In other parts of the hippocampus gliosis was observed in the alveus, *s. lacunosum-moleculare* and once in *s. infrapyramidale*. In the H1 sector of *s. pyramidale* the GFAP reaction was almost negative (Fig. 17). S-100 protein immunostaining was enhanced in this sector only twice. Besides, enhanced diffuse GFAP-positive gliosis was present in the neighboring periventricular white matter in 5 cases.



Fig. 17. Hippocampus. Trace of GFAP reaction in pyramidal cell layer in H1 sector.  $\times 120$   
 Fig. 18. *Nucleus amygdalae*. Distinct GFAP-positive astrocytic gliosis.  $\times 120$

Fragments of *nucleus amygdalae* were found in 2 specimens. *N. amygdalae* showed all types of alterations as neuronal loss, chronic neuronal changes, neuronal swelling and cytoplasmic vacuolization. Nerve cell abnormalities were associated with perineuronal satellitosis and diffuse cellular gliosis which in one case was represented by strongly GFAP-positive, astrocytic hypertrophy (Fig. 18).

## DISCUSSION

Our results reveal two types of pathological changes which can be the primary cause of abnormal stimuli releasing epileptic seizures. These are vascular changes (7 cases) and maldevelopment of the nerve tissue of temporal lobes (4 cases). Both kinds of focal lesions were seldom reported in the literature as a cause of long-year standing, drug-resistant epileptic seizures. In a large collection of lobectomized patients both lesions amounted to 10% and 7%, respectively, whereas the preponderance of neoplastic changes (55%) in the temporal lobe has been striking (Plate et al. 1990). According to Cavanagh and Meyer (1956), one third of their lobectomy material showed focal abnormalities. Similar data are reported by other authors (Sager, Oxbury 1987). By initial elimination of the patients suspected of symptomatic epilepsy, our material became enriched in a large number of developmental changes. The vascular changes in meninges and at the meningo-cerebral interface consist mainly of microangiomas and small vascular malformations diagnosed neither clinically nor during lobectomy. The vascular changes together with macro- and micro-heterotopias support the opinion of Alzheimer and Vogt (1907) of maldevelopmental alterations being the ground of epilepsy. However, such observations do not explain late epilepsy in patients with congenital changes characterized by a low degree of evolution (neuronal dystopias).

So far as vascular malformation can be directly responsible for initiation of epileptic focus, the epileptogenic mechanism originating in irregular synaptic terminals between ectopic neurons and regular neurons is unknown. Complex or separate vascular and ectopic malformations have been found in more than half of the examined patients (9) what seems to corroborate Penfield's opinion (1956) about participation of expansive lesions in psychomotor epilepsies. Also studies of Gastaut et al. (1959) presented in autopsy material numerous vascular and atrophic changes underlying temporal lobe epilepsy. Six of our patients did not reveal such obvious changes. We believe their lack can depend to some extent on the surgical procedure or on the way of collecting the tissue for histological processing.

Changes in the cortex of the temporal lobe, in the hippocampus and in the white matter were observed in all patients. Predominated edematous changes of vasogenic origin appearing as perivascular lacunae in white matter and pale myelin accompanied by GFAP-positive fibrous gliosis perivascularly, at the cortico-subcortical border and submeningeal gliosis most intensive at the bottom of sulci. Submeningeal gliosis in sclerosis of Ammon's horn has been well established before (Cavanagh, Meyer 1956). The localization of astrocytic reaction points to the involvement of borderline zones of terminal vascularization. S-100 protein-positive gliosis overlapped the range of GFAP reaction in particular in the white matter, but sometimes appeared separately. This observation endorses the opinion that white matter contains more S-100 protein than gray matter (Moore, Perez 1968). In our material the GFAP-positive perivascular reaction occurred most frequently associated with S-100 protein-labeled astrocytes which extended over a wider zone than the GFAP reaction and this phenomenon was reported around the neoplasms by other authors who suspected production of both proteins as being evoked by

different stimuli (Kimura et al. 1986). The enhanced production of protein S-100 in astrocytes takes place during their hyperplasia and proliferation in response to removal of breakdown products in experimental conditions, its peak between week 2-6 of the process, its resolution together with cessation of an early reaction (Cicero et al. 1970). The intense reaction in our material can indicate a recurrent process. Besides, in an intense glial response in the white matter one can not exclude participation of oligodendroglia, which in normal conditions also contains protein S-100 (Kahn et al. 1983). Some authors express the opinion that intracellular GFAP is attributed mainly to the processes, whereas S-100 to the perikarya and possibly – nuclei (Boyes et al. 1986).

Cortical changes are restricted to irregular neuronal loss in various cortical layers, appearance of dark neurons and neurons with chronic changes intermingled with normal ones. Apart from doubts as to the character of dark neurons (Mouritzen Dam 1979), some authors report that in experimental conditions after 1 h of status epilepticus the majority of dark neurons become normal and only some survive in such a state or degenerate during the next few hours in the cortex and in the hippocampal sectors CA1 and CA3, without glial reaction (Ingvar et al. 1988). In contrast to the moderate cortical changes in the temporal lobe, the cellular changes and loss of neurons in the *nucleus amygdalae* and hippocampus were striking in spite of the difficulties in evaluation of fragmented structures. They consisted of diminished neuronal density and chronic neuronal changes of pyramidal neurons in the H1 sector, loss of hilar neurons and segmental loss of granular cells. These lesions of various intensity occurred in all examined cases. It was reported that neuronal loss in the hippocampus correlates with low density of neurons in particular sectors in the order: H3, H1, H1-2 and H2 (Mouritzen Dam 1979, 1980). The neuronal loss in each sector of the pyramidal cell layer can reach in temporal epilepsy up to 50% of neurons in control human material (Kim et al. 1990).

In our material the lesions in the pyramidal cell layer were accompanied by gliosis in *s. lacunosum-moleculare* and associated with neuronal loss in the hilus with GFAP-positive fibrous gliosis, as already observed in the Mongolian gerbil after short experimental ischemia (Gadamski, Kroh 1992). The sensibility of H1 sector and resistance of H2 sector neurons to the injury is generally accepted (Mouritzen Dam 1990). Other sectors reveal irregular loss of neurons up to 50% in the H3 sector (end-folium) in which cellular density is lowest. If sector H1 is affected there are always changes in other sectors of this layer (Mouritzen Dam 1980, 1988).

The most striking observation in our material is the lack of glial reaction in the impaired H1 sector. We have observed a similar phenomenon in experimental ischemia in the Mongolian gerbil (Gadamski, Kroh 1991, 1992). We believe that the hippocampal sector H1 contains very few astrocytes, this being an explanation for the ready vulnerability of this field to all kinds of injury.

On the basis of hippocampal changes a lack of relationship was established between the rate of neuronal loss and the duration of the illness (Kim et al. 1990). However, there exists a correlation between the loss of neurons in H1 and H1-2 sectors and the duration of illness characterized by frequent clonic-tonic seizures, contrary to the lack of any pattern of changes with

partial seizures (Mouritzen Dam 1980, 1988). Of some significance is the age of the patient, because there exists a relation between neuronal loss in H1, in the end-folium and granular cell layer and seizures in children who suffer of convulsions before the 3rd year of life (Sager, Oxbury 1988). The pattern of changes in our patients suffering of partial seizures evolving to tonic-clonic convulsions does not allow such conclusions.

Many authors found Ammon's horn sclerosis in autopsy material in psychiatric patients without epileptic seizures, and that the changes in Ammon's horn are more frequent in non-epileptic (41%) than in epileptic patients with grand-mal (20.5%), (Morel, Wildi 1954; Cavanagh, Meyer 1956). In our material Ammon's horn was not spared in cases with focal lesions in the temporal lobe, as reported by Cavanagh and Meyer (1956). Gastaut et al. (1959) concluded from their autopsy material that damage to Ammon's horn in temporal epilepsy patients is not a constant lesion but rather "not obligatory" and unfrequent and the mechanism of the damage to Ammon's horn is the same as for other parts of the temporal lobe in psychomotor epilepsy. The authors consider injury of the temporal lobe including Ammon's horn, as being most probably of ischemic origin, and as the cause and not the consequence of the seizures.

Experimental studies on brief ischemia with various survival time in gerbils (Gadamski, Kroh 1991, 1992) point to uni- or bilateral injury of the hippocampus, in particular of the CA1 sector, hilus and *gyrus dentatus*, accompanied by fibrous gliosis analogical to that found in patients with temporal psychomotor epilepsy. Albeit comparison of both conditions: human epileptogenic and experimental ischemic is doubtful, we are inclined to favor the fundamental theory of Spielmeyer (1927) concerning a vasogenic origin of hippocampal changes evoked by epileptic seizures triggered by temporal foci (malformations, ectopias), by perinatal injuries (Earle et al. 1953), or by the other processes like febrile convulsions in children. The exact pathogenesis of neuronal death and hippocampal gliosis is not clear and all theories of delayed neuronal death (Kirino 1982), excitotoxic stimulation of receptors (Olney et al. 1983; Rothman, Olney 1987) or excessive intracellular influx of  $Ca^{2+}$  with membrane depolarization (Meldrum 1987) can only indicate particular stages of superimposed events of a long-lasting process in the brain, conditioned additionally by tissue maturity and medical treatment.

#### ZMIANY NEUROPATOLOGICZNE W RESEKOWANYM PŁACIE SKRONIOWYM PACJENTÓW Z SAMOISTNĄ PADACZKĄ SKRONIOWĄ

##### Streszczenie

Badania oparto na materiale pobranym w trakcie lobektomii skroniowej wykonanej w celu terapeutycznym u 16 pacjentów, u których wieloletnie napady skroniowe i uogólnione nie poddawały się leczeniu zachowawczemu. U pacjentów tych wykluczono uprzednio urazy, choroby zapalne lub nowotworowe mózgu. Badaniem neuropatologicznym stwierdzono w 7 przypadkach mikronaczyniaki i malformacje naczyniowe w oponach miękkich i w tkance mózgu nie wykrywalne makroskopowo. Heterotopie neuronalne w istocie białej i istoty białej w korze obserwowano w 3 przypadkach. Główne zmiany korowe to ubytki neuronalne i schorzenia typu przewlekłego, satelitoza perineuronalna i GFAP-dodatnia glejzoza podoponowa zwłaszcza na dnie rowków,

okołonaczyniowa, warstwowa lub rozlana. W hipokampie zmiany te były wybitnie nasilone szczególnie w płycie końcowej i polu H3. W istocie białej występowała glejoza astrocytarna z żywym odczynem immunohistochemicznym GFAP i odczynem S-100, który w pewnych przypadkach był bardziej rozległy niż odczyn GFAP. Przedstawione zmiany przeanalizowano pod kątem przypuszczalnych przyczyn padaczki i uszkodzeń ponapadowych mózgu.

## REFERENCES

1. Alzheimer A, Vogt H: Die Gruppierung der Epilepsie. *Allg Z Psychiat*, 1907, 418–448.
2. Boyes BE, Kim SV, Lee V, Sung SC: Immunohistochemical co-localization of S100b and the glial fibrillary acidic protein in rat brain. *Neuroscience*, 1986, 17, 857–865.
3. Cavanagh JB, Meyer A: Aetiological aspects of Ammon's horn sclerosis associated with temporal lobe epilepsy. *Brit Med J*, 1956, 2, 1403–1407.
4. Cicero TJ, Cowan WM, Moore BW, Suntzeff V: The cellular localization of the two brain specific proteins S-100 and 14-3-2. *Brain Res*, 1970, 18, 25–34.
5. Earle KM, Baldwin M, Penfield W: Incisural sclerosis and temporal lobe seizures produced by hippocampal herniation at birth. *Arch Neurol Psychiat*, 1953, 69, 27–42.
6. Gadamski R, Kroh H: Astrocytic reaction in dorsal hippocampus after 5 min ischemia in gerbil. *Clin Neuropathol*, 1991, 10, 204 (Abstr).
7. Gadamski R, Kroh H: Immunoreactivity of astroglia after brief ischemia resulting in asymmetrical damage to CA1 hippocampal sector in Mongolian gerbil. *Neuropatol Pol*, 1992, subjected.
8. Gastaut H, Toga M, Roger J, Gibson W: A correlation of clinical, electroencephalographic and anatomical findings in nine autopsied cases of temporal lobe epilepsy. *Epilepsia*, 1959, 1, 56–85.
9. Ingvar M, Morgan PF, Auer RN: The nature and timing of excitotoxic neuronal necrosis in the cerebral cortex, hippocampus and thalamus due to flurothyl-induced status epilepticus. *Acta Neuropathol (Berl)*, 1988, 75, 362–369.
10. Kahn H, Marks A, Thom H, Baumal R: Role of antibody to S-100 protein in diagnostic pathology. *Am J Clin Pathol*, 1983, 79, 341–347.
11. Kim JH, Guimaraes PO, Ihen MY, Masukowa ML, Spencer DD: Hippocampal neuronal density in temporal lobe epilepsy with and without gliomas. *Acta Neuropathol*, 1990, 80, 41–45.
12. Kimura T, Budka H, Soler-Federspiel S: An immunocytochemical comparison of the glia-associated proteins: glial fibrillary acidic protein (GFAP) and S-100 protein (S100P) in human brain tumors. *Clin Neuropathol*, 1986, 5, 21–27.
13. Kirino T: Delayed neuronal death in the gerbil hippocampus following ischemia. *Brain Res*, 1982, 239, 57–69.
14. Meldrum B: Physiological and biochemical mechanisms leading to nerve cell loss in status epilepticus. In: *Advances in epileptology. XVI Epi Int Symp.* Eds: P Wolf, M Dam, D Jouz, F Dreifuss. Raven Press, New York, 1987, 21–25.
15. Moore BW, Perez VJ: Specific acidic proteins of the nervous system. In: *Physiological and biochemical aspects of nervous integration.* Ed: FD Carlsson. Prentice-Hall, Englewood Cliffs, New York, 1968, 343-359.
16. Morel F, Wildi W: Sclérose Ammonienne et épilepsie. *Acta Neurol Psychiat Belg*, 1956, 56, 61–74.
17. Mouritzen Dam A: The density of neurons in the human hippocampus. *Neuropathol Appl Neurobiol*, 1979, 249–264.
18. Mouritzen Dam A: Epilepsy and neuron loss in the hippocampus. *Epilepsia*, 1980, 21, 617–629.
19. Mouritzen Dam A: Consequences of severe epilepsy. Neuropathological aspects. *Acta Neurol Scand, Suppl 117*, 1988, 78, 24–26.
20. Mouritzen Dam A: Neuropathology of epilepsy. *Acta Neurochir, Suppl 50*, 1990, 20–25.
21. Olney JW, de Gulareff T, Sloviter RS: Epileptic brain damage in rats induced by sustained electrical stimulation of the perforant path. II Ultrastructural analysis of acute hippocampal pathology. *Brain Res Bull*, 1983, 10, 669–712.
22. Penfield W: Epileptogenic lesions. *Acta Neurol Psychiat Belg*, 1956, 56, 75–88.

23. Plate KH, Wieser HG, Yasargil MG, Wiestler OD: Neuropathologische Läsionen in selectiven Temporallappen-Resektionen bei complex-partieller Epilepsie: Analyse von 150 Fällen. 35 Jahrestagung der Deutschen Gesellschaft für Neuropathologie und Neuroanatomie, München, 25–28 April, 1990, p 8, (Abstr).
24. Rothman SM, Olney JW: Excitotoxicity and the NMDA receptor. *Trends Neurosci*, 1987, 10, 299–302.
25. Sager HJ, Oxbury JM: Hippocampal neuron loss in temporal lobe epilepsy: correlation with early childhood convulsions. *Ann Neurol*, 1987, 334–340.
26. Spielmeyer W: Die Pathogenesis des epileptischen Krampfes. *Z Dtsch Ges Neurol Psychiat*, 1927, 109, 501–520.

Author's address: Department of Neuropathology, Medical Research Centre, Polish Academy of Sciences, 3 Dworkowa St 00-784 Warsaw, Poland

IRENA NIEBRÓJ-DOBOSZ, JANINA RAFAŁOWSKA, MIROŚLAWA ŁUKASIUŁ,  
WIESŁAWA WIŚNIEWSKA, DOROTA DZIEWULSKA

## INFLUENCE OF AGING ON THE PROTEIN PROFILE OF MYELIN ISOLATED FROM HUMAN BRAIN WHITE MATTER\*

Department of Neurology, School of Medicine, Warsaw, Poland

Myelin proteins composition was examined in material of 20 autoptic cases at ages from 20 to 97 years. The technique of polyacrylamide gel electrophoresis and isotachopheresis was applied. In polyacrylamide gel electrophoresis a progressive increase starting at the age of 60 years of Wolfram protein at the expense of Folch-Lees proteolipid protein and DM-20 protein was observed. The myelin-associated protein started to increase in the 4<sup>th</sup> and 5<sup>th</sup> decade of life, returning thereafter to values observed in younger cases. The isotachopheretic technique did not differentiate the changes observed in myelin protein in the course of aging.

Key words: *myelin, proteins, aging.*

Myelin isolated from senile human brain differs from that of younger subjects in the density of its vesicles (Berlet et al. 1982; Niebrój-Dobosz et al. 1988). It is suggested that the greater heterogeneity of myelin vesicles in old age is the consequence of physicochemical changes in the human brain which appear with age (Berlet et al. 1982). Some contribution to the observed heterogeneity of myelin vesicles in senile subjects may come from lipid changes (Fillerup, Mead 1967; Rouser, Yamamoto 1969; Sun, Samorajski 1972; Niebrój-Dobosz et al. 1986, 1989; Wender et al. 1987). Less is known on the possible influence of aging on the protein composition of human brain myelin.

The aim of this study was to determine if proteins are changed in content and composition in aged human brain myelin, and if so, if they may be responsible, partly at least, for the greater heterogeneity of myelin vesicles in senile subjects.

### MATERIAL AND METHODS

The material consisted of 20 cases aged from 20 to 97 years. There was no clinical and autopsy evidence of central nervous system involvement of the hemispheres taken for further examination. The diagnosis were: *thrombosis a.*

---

\* Study supported by School of Medicine in Warsaw (Grant No. IB/32)



*cerebri med., embolia a. cerebri med., stenosis a. carotis morbus neoplasmaticus, morbus Parkinsoni.* In all cases autopsy was performed within 24 hours after death. For histological examination white matter specimens were formalin-fixed and paraffin-embedded. Sections of the frontal pole in the "healthy" hemisphere were stained with hematoxylin-eosin and Klüver-Barrera method. For biochemical analyses white matter was frozen and preserved at  $-25^{\circ}\text{C}$  during 7 to 14 days. The material was weighed and white matter dry weight was determined in the conventional gravimetric way. Myelin was separated by the method of Norton and Poduslo (1973), as modified by Zgorzalewicz et al. (1974). In the discontinuous sucrose gradient 0.75 M instead of 0.85 M sucrose was used. The isolated myelin was homogenized and total protein content was estimated according to Lowry et al. (1951) after its delipidation in a mixture of ether: alcohol (3:2 v/v) as described by Greenfield et al. (1971). Polyacrylamide gel electrophoresis was run according to Wachneldt and Neuhoff (1974). The concentration of the gel was 12 percent, each lane was loaded with 100  $\mu\text{g}$  of protein. The separated proteins were stained with Coomassie Brilliant Blue R-250. After destaining the gels were scanned with a ISCO Gel Scanner (Model 1310) and Absorbance Monitor (Model UA-5). Molecular weights of the particular protein bands were estimated by comparing their mobilities to those of Sigma protein standards. The protein composition of the isolated myelin was also assessed by analytical isotachopheresis (Delmotte 1977). LKB Tachophor 2127 with UV and thermal detectors was used. The teflon capillary tubing was 23 cm long (0.5 mm I.D.) and was thermostated at  $12^{\circ}\text{C}$ . Absorbance was registered with a LKB 2-channel recorder, type 2210. As amino acid spacers beta-alanine, glycine and valine were used. The densitometric tracings of the Coomassie Blue stained gels and the UV-absorbing peaks in isotachopheresis were integrated by an image analyses system (Mini-Mop M 1100, Opton).

Statistical analyses. The dependence of the proteins content versus the age of the subjects was tested by regression analysis.

## RESULTS

The protein content of the white matter was comparable in all subjects between the age of 20 to 97 years. The values were  $4.8 \pm 1.1$  mg per 1 g of white matter. Changes were, however, observed in the protein pattern resolved by polyacrylamide gel electrophoresis. A representative densitometric tracing of myelin proteins in a young and senile subject is presented in Fig. 1. Among the protein fractions a progressive increase of the myelin-associated glycoprotein (MAG) in the 4<sup>th</sup> and 5<sup>th</sup> decade of life was observed. After the 7<sup>th</sup> decade the content of MAG started to decline, in senile subjects values observed at ages below 40 years of life were present (Fig. 2). Wolfgram protein started to increase between the 6<sup>th</sup> and 7<sup>th</sup> decade of life (Fig. 3). The correlation between the age of the subjects and the content of Wolfgram protein was significant ( $P < 0.001$ ) Folch-Lees proteolipid protein (Fig. 4) and DM-20 protein (Fig. 5)

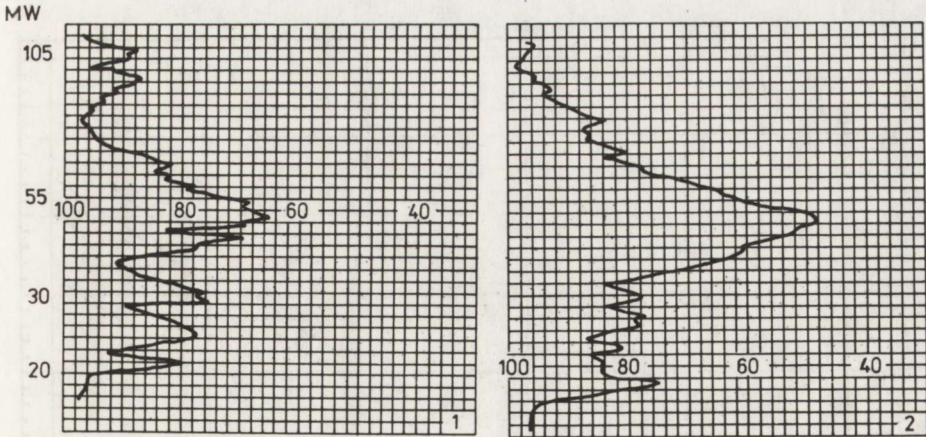


Fig. 1. Densitometric tracing of myelin proteins in 20-year-old (1) and 97-year-old (2) subject

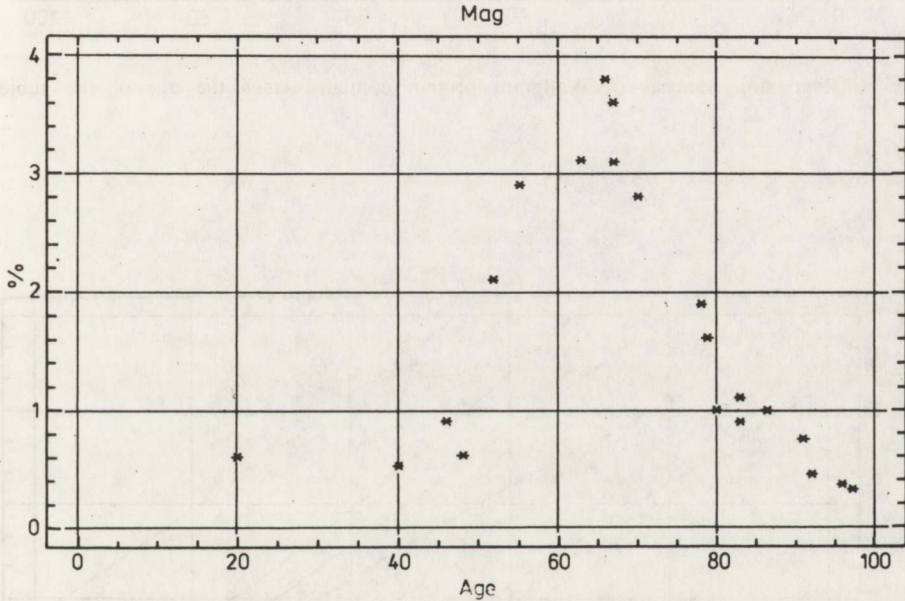


Fig. 2. Myelin glycoprotein content (in percent) versus the age of the subjects

declined at the time when Wolfgram protein started to increase. The latter changes were also age-dependent ( $P < 0.001$ ). Using, however, the capillary isotachopheric technique separating proteins according to their isoelectric points, no dependence between the protein pattern of brain myelin and the age of the subjects was found. A representative tracing of myelin proteins in a 20-year-old subject is presented (Fig. 6).

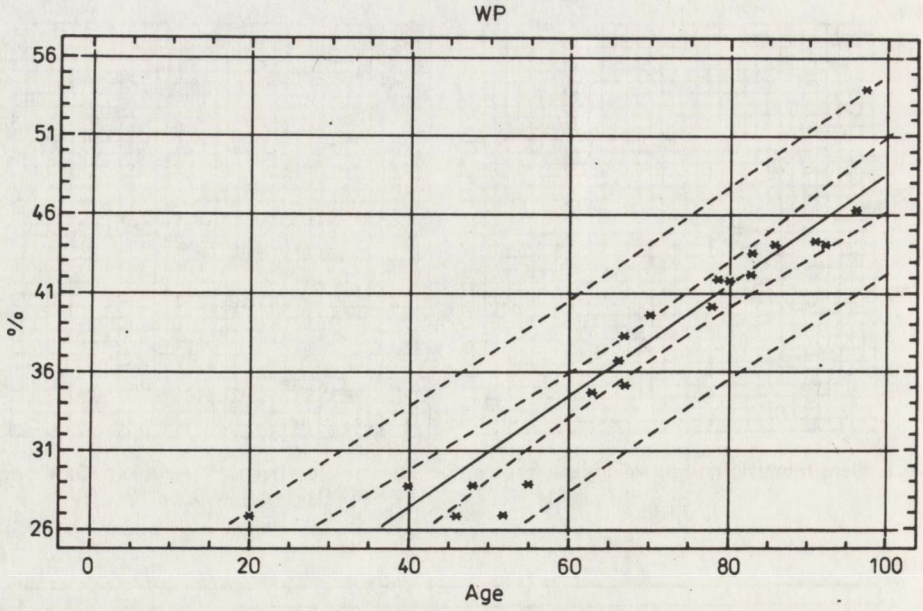


Fig. 3. Regression analysis of Wolfram protein content versus the age of the subjects

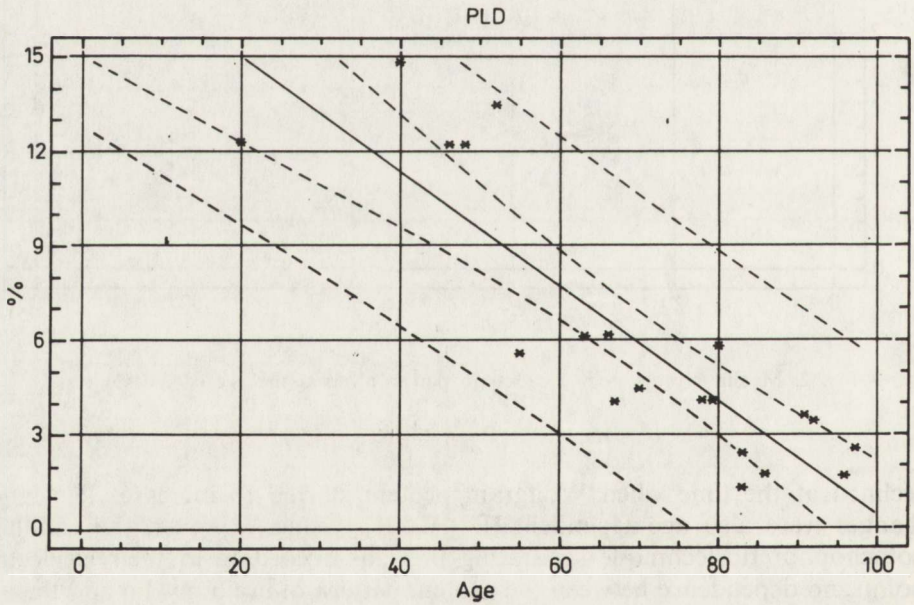


Fig. 4. Regression analysis of Folch-Lees protein content versus the age of the subjects

DM-20

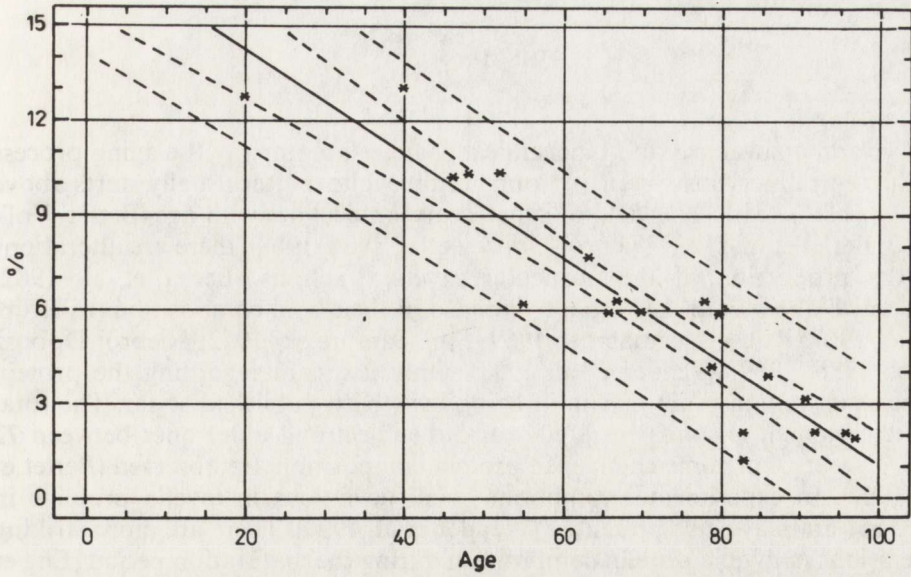


Fig. 5. Regression analysis of DM-20 protein versus the age of the subjects

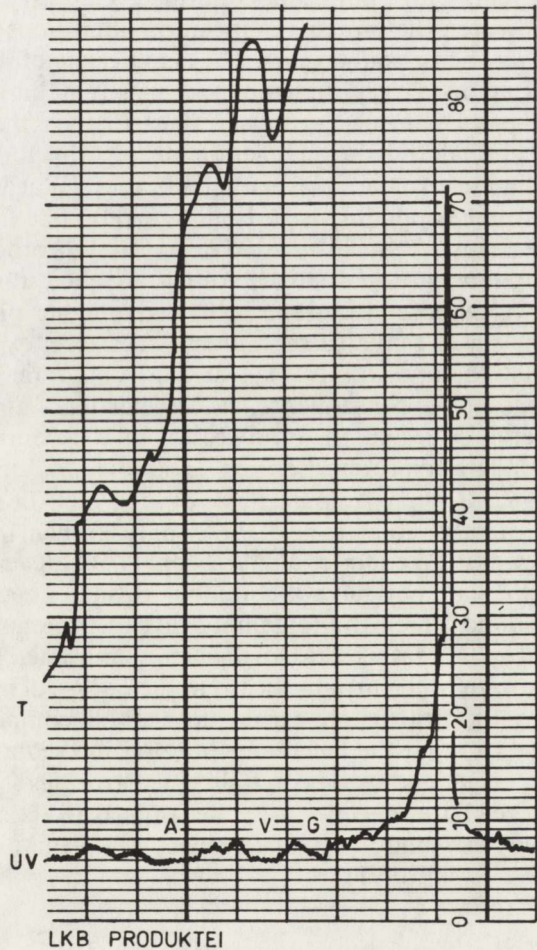


Fig. 6. Capillary isotachopheric tracing of myelin proteins in a 20-year-old subject. A - beta-alanine, V - valine, G - glycine, UV - UV-absorbance, T - thermal detection.

## DISCUSSION

Several anatomical and biochemical changes accompany the aging process of the central nervous system. Atrophy of the white matter usually starts above the age of 70 years. The yield of isolated myelin declines with age (Berlet, Volk 1980; Berlet et al. 1982; Niebrój-Dobosz et al. 1986, 1988), there are alterations in the proportion of the particular myelin fractions (Berlet et al. 1982; Niebrój-Dobosz et al. 1986, 1988) and also in their lipid composition (Fillerup, Mead 1967; Rouser, Yamamoto 1969; Sun, Samorajski 1972; Niebrój-Dobosz et al. 1986, 1989; Wender et al. 1987). Only few data regarding the protein content in human brain myelin in aging have been published so far. The total protein content is similar in a 50-year-old subject and older ones between 72 and 95-years, but some changes in protein composition are observed (Berlet et al. 1982). In experimental conditions small deviations in myelin proteins in aged rat brain are also presented (Wender et al. 1990). There are more striking alterations in myelin protein composition during the maturation period (Eng et al. 1986; Zgorzalewicz et al. 1974).

In the presented report the lack of total protein changes in human brain myelin with aging was confirmed. Contrary to the above mentioned studies, however, the protein composition alterations were more pronounced especially after the age of 60 years. The significance of the observed changes in the course of aging is very difficult to assess. It is known that Wolfgram protein is an integral part of the myelin sheath. It is thought also that this protein has a special transitory function during the formation of compact myelin from oligodendroglial plasma membranes (Wachneldt, Neuhoff 1974). Wolfgram protein is possibly a part of the myelin-like fraction, predominating over other proteins (Agrawal et al. 1970). On the other hand, the myelin-like fraction predominates over the other myelin fractions in senile subjects (Niebrój-Dobosz et al. 1986, 1988). The higher proportion of Wolfgram protein in myelin of senile cases could be therefore, expected. It should also be stressed that the appearance of a higher Wolfgram protein content in senile subjects may be the consequence, at least partly, of atrophy and axonal degeneration of nerve cells and their processes. In the course of Wallerian degeneration the Wolfgram protein content is known to increase (Galas-Zgorzalewicz et al. 1982). The physiological role of the Folch-Lees proteolipid protein and DM-20 protein is not clear yet. It is only known that both proteins are affected in hypoxia (Wender et al. 1989, 1990). Whatever the role of the above mentioned proteins, they have a common feature. They serve primarily as a framework around which the remaining myelin proteins and also lipids can condense to form the rather stable myelin membrane. When compared with the lipids pattern in the myelin sheath in the course of aging (Niebrój-Dobosz et al. 1989), myelin proteins appear as more stable components. It may be connected with the fact that the behaviour of lipids in the myelin sheath is influenced not only by oligodendrocytes, but also by astrocytes (Nakano et al. 1990). The reactivity of the latter declines in senile subjects (Rafałowska et al. 1991) but increases in the remyelination (Goncerzewicz 1988) and myelination processes (Rafałowska, Krajewski 1991).

WPLYW INWOLUCJI  
NA SKŁAD BIAŁEK MIELINY ISTOTY BIAŁEJ MÓZGU

Streszczenie

Badania przeprowadzono na materiale autopsyjnym chorych zmarłych w wieku 20 do 97 lat. Zastosowano technikę rozdziału białek mieliny w żelu poliakrylamidowym i isotachoforetycznie. W wyniku przeprowadzonych badań stwierdzono stopniowy wzrost zawartości białka Wolframa na niekorzyść proteolipidu Folch-Lees i białka DM-20. Zmiany te pojawiły się około 60 roku życia i narastały stopniowo w sposób znamieny. Szczyt zawartości glikoproteidu związanego z mielina przypada między 40 a 50 rokiem życia. Badania białek mieliny oparte na ich rozdziale uzależnionym od punktu izoelektrycznego nie różnicowały mieliny pochodzącej od osobników młodszych i starszych.

REFERENCES

1. Agrawal HC, Banik NL, Bone AH, Davison AN, Mitchell RF, Spohn M: The identity of myelin-like fraction isolated from developing brain. *Biochem J*, 1970, 120, 635–642.
2. Berlet HH, Volk B: Age-related heterogeneity of myelin basic protein isolated from human brain. In: *Aging of the brain and dementia*. Eds: L Amaducci, AN Davison, P Antuono. Raven Press, New York, 1980, pp 81–90.
3. Berlet HH, Ilzenhöfer H, Echtenacher B, Volk B: Old age alters density of myelin isolated from brain. In: *Experimental Brain Research. The aging of the brain. Physiological and pathological aspects*. Ed: S Hoyer. Springer, Berlin, Heidelberg, New York, 1982, suppl, 5, pp 167–174.
4. Delmotte P: Analysis of complex protein mixtures by capillary isotachopheresis: Some quantitative and qualitative aspects. *Sci Tools*, 1977, 24, 33–41.
5. Eng LF, Chao FC, Gerstl B, Pratt D, Tavaststjerna MG: The maturation of human white matter myelin. Fractionation of the myelin membrane proteins. *Biochemistry*, 1968, 7, 4455–4465.
6. Fillerup DL, Mead JF: The lipids of the aging human brain. *Lipids*, 1967, 2, 295–298.
7. Galas-Zgorzalewicz B, Wender M, Piechowski A, Śniatała-Kamasa M: Micro-slab gel electrophoresis. Application to studies on myelination and demyelination. *Electrophoresis Forum*, 1982, 102–106.
8. Goncerzewicz A: The role of astroglia in pathological processes characterized by myelin disintegration. II. Electron, enzyme and immunocytochemistry of the astroglia in experimental injury to white matter. *Neuropatol Pol*, 1988, 26, 127–149.
9. Greenfield S, Norton WT, Morell P: Quaking mouse: Isolation and characterization of myelin proteins. *J Neurochem*, 1971, 18, 2119–2128.
10. Lowry OH, Rosebrough NJ, Farr AL, Randall RJ: Protein measurement with Folin reagent. *J Biol Chem*, 1951, 193, 265–275.
11. Nakano S, Kogure K, Abe K, Yae T: Ischemia-induced alterations in lipid metabolism of the gerbil cerebral cortex: I. Changes in free fatty acid liberation. *J Neurochem*, 1990, 54, 1911–1916.
12. Niebrój-Dobosz I, Rafałowska J, Barcikowska-Litwin M: Brain myelin in senile patients with brain infarction. *Neuropatol Pol*, 1986, 24, 351–364.
13. Niebrój-Dobosz I, Wiśniewska W, Barcikowska-Litwin M: Influence of aging on density of myelin fractions isolated from human brain white matter. Preliminary report. *Neuropatol Pol*, 1988, 26, 19–25.
14. Niebrój-Dobosz I, Rafałowska J, Łukasiuk M: Do lipid changes influence the density of aging human brain myelin. *Neuropatol Pol*, 1989, 27, 427–436.
15. Norton WT, Poduslo SE: Myelination in rat brain: Method of myelin isolation. *J Neurochem*, 1973, 21, 749–757.
16. Rafałowska J, Krajewski S: Do astroglial cells participate in the process of human spinal cord myelination? *Neuropatol Pol*, 1991, 29, 41–47.
17. Rafałowska J, Dolińska E, Dziewulska, Krajewski S: Astrocytic reactivity in various stages of human brain infarct in middle and senile age. *Neuropatol Pol*, 1991, 29, 181–191.

18. Rouser G, Yamamoto A: Chemical architecture in the nervous system. Lipids. In: Handbook of Neurochemistry, vol. 1. Ed: A Lajtha. Plenum Press, New York, 1969, pp 121–169.
19. Sun GY, Samorajski T: Age changes in the lipids composition of whole homogenates and isolated myelin fraction of mouse brain. *J Gerontol*, 1972, 27, 10–17.
20. Wachneldt TV, Neuhoff V: Membrane proteins of rat brain: Compositional changes during postnatal development. *J. Neurochem*, 1974, 23, 71–77.
21. Wender M, Adamczewska-Goncerzewicz Z, Stanisławska J, Szczech J, Godlewski A: Pattern of myelin lipids in ageing brain. *Neuropatol Pol*, 1987, 25, 235–245.
22. Wender M, Adamczewska-Goncerzewicz Z, Talkowska D, Pankrac J, Grochowalska A: Influence of experimental acute hypoxia on myelin proteins. *Neuropatol Pol*, 1989, 27, 169–175.
23. Wender M, Adamczewska-Goncerzewicz Z, Talkowska D, Pankrac J: Myelin proteins of senile rat brain. *Neuropatol Pol*, 1990, 28, 287–292.
24. Zgorzalewicz B, Neukoff V, Wachneldt TV: Rat myelin proteins. Compositional changes in various regions of the nervous system during ontogenetic development. *Neurobiology*, 1974, 4, 265–276.

Correspondence address: Dr Irena Niebrój-Dobosz, Department of Neurology, School of Medicine, 1A Banacha Str, 02-097 Warsaw, Poland

MARIA BARCIKOWSKA<sup>1</sup>, ELŻBIETA KIDA<sup>1</sup>, EWA JOACHIMOWICZ<sup>2</sup>,  
ALICJA SIEKIERZYŃSKA<sup>3</sup>

## CEREBELLAR GRANULAR LAYER DEGENERATION IN SMALL CELL LUNG CANCER: PARANEOPLASTIC CEREBELLOPATHY OR ARTIFACT?

<sup>1</sup> Department of Neuropathology, Medical Research Centre, Polish Academy of Sciences, Warsaw, <sup>2</sup> IInd Department of Neurology, School of Medicine, Warsaw, <sup>3</sup> Institute of Tuberculosis and Chest Diseases, Warsaw, Poland

The aim of our study was to ascertain whether granular cell degeneration represents uniquely an artifactual or a supravital event in patients with oat cell carcinoma. The material includes 52 cases of small cell lung cancer (SCLC). Formalin fixed and paraffin embedded representative cerebellar slides were stained routinely (HE, Klüver-Barrera), and some of them served as material for immunohistochemical study. The following antibodies were used: anti-ferritin, anti-GFAP, anti-IgG and anti-C3 complement fraction. Finally 5 cases out of our material could be diagnosed as paraneoplastic cerebellar degeneration (PCD), on the basis of lack of metastases within the CNS and concomitant intensive loss of Purkinje and granule cells. Clinically the cerebellar syndrome was disclosed in 3 cases. In the granular layer prevalence of microglial cell reaction was noted. GFAP-labeled astroglia were not demonstrated in the same intensity. Antisera to the C3 complement fraction showed moderate staining of Purkinje cell cytoplasm and in some cases also of granule cells. IgG immunostaining was disclosed in Purkinje cell cytoplasm and in 4 cases also in granule cell nuclei. The immunopathological changes presently observed and glial cell proliferation could be evidence for a nonartifactual origin of PCD.

*Key words: small cell lung cancer, paraneoplastic cerebellopathy, immunohistochemistry.*

Cerebellopathy is known to occur in various pathological conditions such as alcoholic encephalopathy, side effect of drug treatment, nutritional and metabolic deficiencies or chronic vascular diseases. The peculiar sensitivity of cerebellar cortex to different factors including endo- and exotoxins, anoxia or hypoglycemia, gave reason to believe that atrophy of the cerebellar cortex is almost nonspecific (Wessel et al. 1988).

Degeneration of the cerebellar cortex in patients with internal malignant neoplasms represents one of paraneoplastic syndromes (Henson, Ulrich 1982; Laure-Kamionowska 1990). Most often it accompanies lung, breast and ovarian carcinoma. Paraneoplastic cerebellar degeneration (PCD), regardless if presenting purely degenerative or inflammatory type lesions, affects predominantly



Purkinje cells (Henson, Ulrich 1982). Only in some cases Purkinje cell loss was accompanied by a marked reduction of granule cells. Cases showing damage confined to the granular layer exclusively were reported sporadically (Leigh, Meyer 1949; Morton et al. 1966) and this type of damage was rather ascribed to acute lysis occurring as terminal event (Mc Donald 1961; Steven et al. 1982).

The aim of our study was to establish whether granule cell degeneration in patients with lung carcinoma represents an uniquely artifactual or a supravital event. To exclude its artifactual origin, an immunohistochemical study was undertaken with special emphasis focused on the glial cell reaction. Proliferation of glia within atrophied cerebellar tissue is believed to be an obvious argument for an *in vivo* lesion. The material under consideration includes 52 cases with small cell lung cancer (SCLC) and is representative for elucidation of this problem.

#### MATERIAL AND METHODS

Fifty two cases with small cell lung cancer died in the Institute of Tuberculosis and Chest Diseases in Warsaw during 5 years (1986–1990), were the subject of our study. The material consisted of 20 women and 32 men aged 35–69 (mean age 56.8 years). All patients were assessed neurologically at the beginning of the disease, before starting therapy, and some of them also in the end period of life. All patients were treated with various regimes of chemo- and radiotherapy.

Clinically, the cerebellar syndrome was disclosed in 3 cases, but in one of them obviously caused by metastasis. However, clinical data were not always reliable, because not all patients were examined in the terminal stage of the disease.

In all cases routine neuropathological examination of the central (CNS) and peripheral nervous system (PNS) was performed. From each case cerebellar hemisphere, vermis and nucleus dentatus were routinely taken for microscopical study.

Formalin fixed and paraffin embedded slicedes were stained with HE and Klüver-Barrera method, and silver impregnated according to Yamamoto et al. (1986) modification of Bielschowsky method. After examination based on routine stainings 10 selected cases (5 with PCD and 5 without any sings of granular cell layer atrophy) constituted material for immunohistochemical study. The following antibodies were used; anti-ferritin (Sigma) and anti-GFAP (DAKO), as specific markers for microglia and astroglia, respectively, and antibodies against IgG (DAKO) and C3 complement fraction (Sigma). Immunocytochemistry was applied to paraffin sections using the extravidin-biotin-peroxidase complex method (reagents from Amersham and Sigma) and diaminobenzidine (Sigma) as chromogen. The sections were counterstained with hematoxylin.

#### RESULTS

Granule cell loss was found in 10 cases. In all of them distinct atrophy of Purkinje cells was also encountered. No signs of inflammation were disclosed in any of the cases studied. The intensity of granule cell atrophy varied: in

4 cases it was severe; in 2 cases moderate, and in 4 cases slight. In the cases with severe granular layer atrophy the loss of granule cells involved cerebellar folia uniformly (Fig. 1). In 4 cases with less intense and in 2 cases with moderate damage was rather confined to the vermis and a focal pattern of lesions was found. In some cases in the same cerebellar hemisphere patchy lesions were observed and closely to the cerebellar folia with well preserved granule cells, folia with marked reduction of granule cells were seen. Only in one case (22/89) was marked degeneration of dentate nuclei with demyelination of dentate hili found.

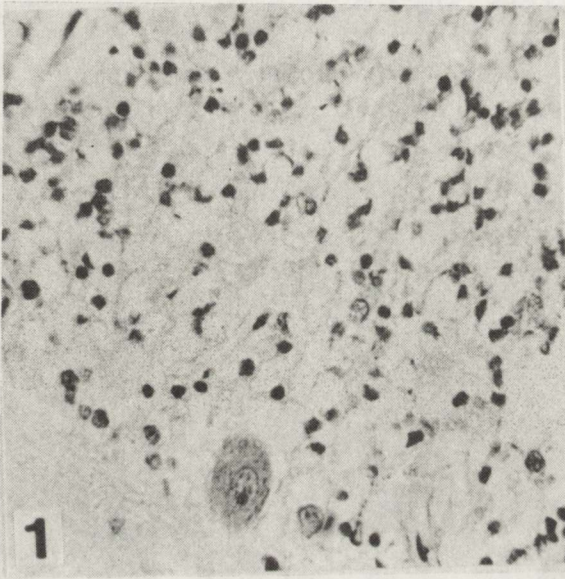


Fig. 1. PCD case. Severe granular cell layer atrophy with concomitant loss of Purkinje cells. HE,  $\times 400$

Table 1. Results of neuropathological and immunohistochemical examination in PCD cases from examined material

No of cases	Age yrs	Sex	Cerebellar symptoms	Granule cell loss	Positive staining for IgG			
					Pc	Gc	C 3	Gc
102/87	64	F	+	(Hemisph) +	0	0	+	0
18/88	57	M	++	(Vermis) +	+	+	+	+
62/88	63	F	+	(Vermis) +++	++	++	+	0
22/89	68	M	0	(Hemisph) ++	+	+++	+	0
18/90	49	M	0	(Hemisph) +	+	0	+	0

Explanations: F-female, M-male, Hemisph - hemispheres, + - slight, ++ - moderate, +++ - severe, Pc - Purkinje cells, Gc - granular cells

In 3 cases with cerebellar damage metastatic foci within the cerebellum were noted. In another case metastatic lesions were found in other CNS structures. One case showed a minute metastatic focus in the pons. Only one case among ten showing cerebellar damage revealed morphological changes of the CNS which could have been attributed to radiotherapy.

The results of neuropathological and immunohistochemical examination of selected cases are presented in Table 1.

Antisera to the C3 complement fraction showed moderate staining of Purkinje cell cytoplasm (Fig. 2) and in some cases also of granule cells (Fig. 3)

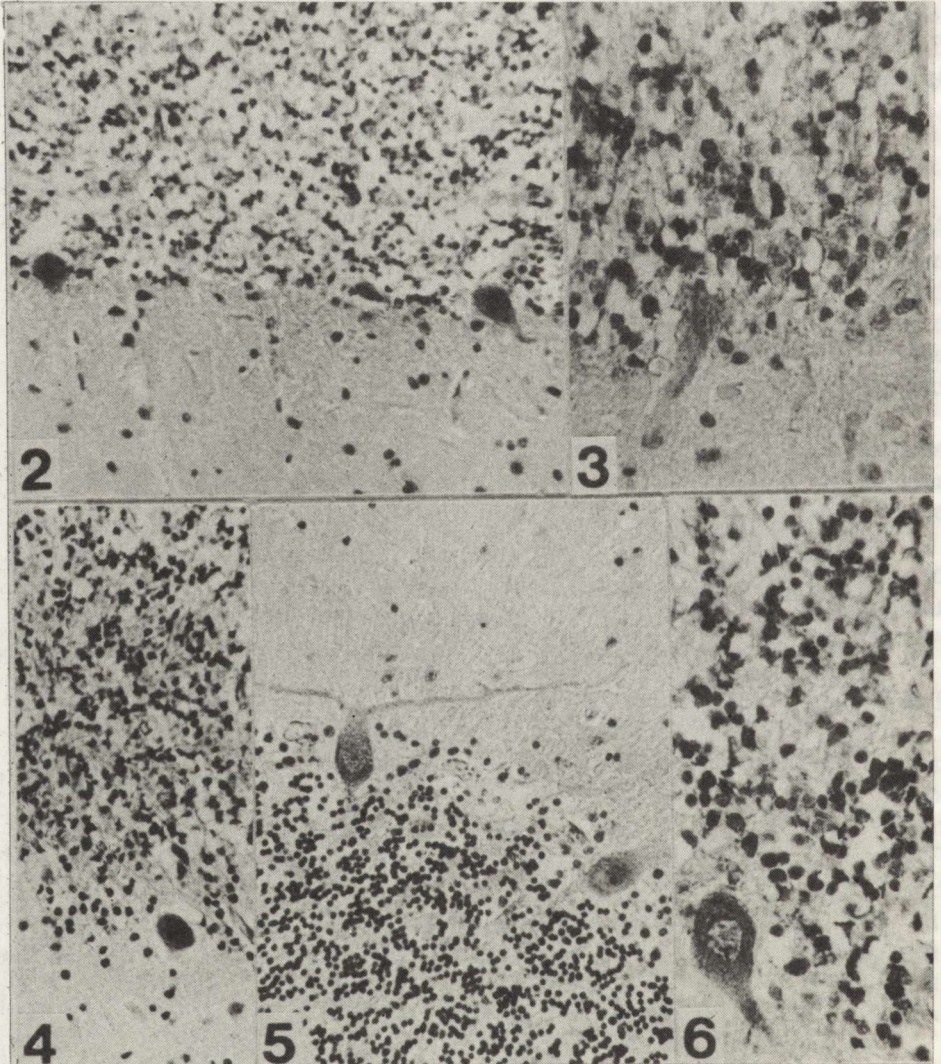


Fig. 2. PCD case. Purkinje cells positive for anti-C3 complement fraction.  $\times 200$

Fig. 3. The same case. Granular cells labeled by anti-C3 complement antibody.  $\times 400$

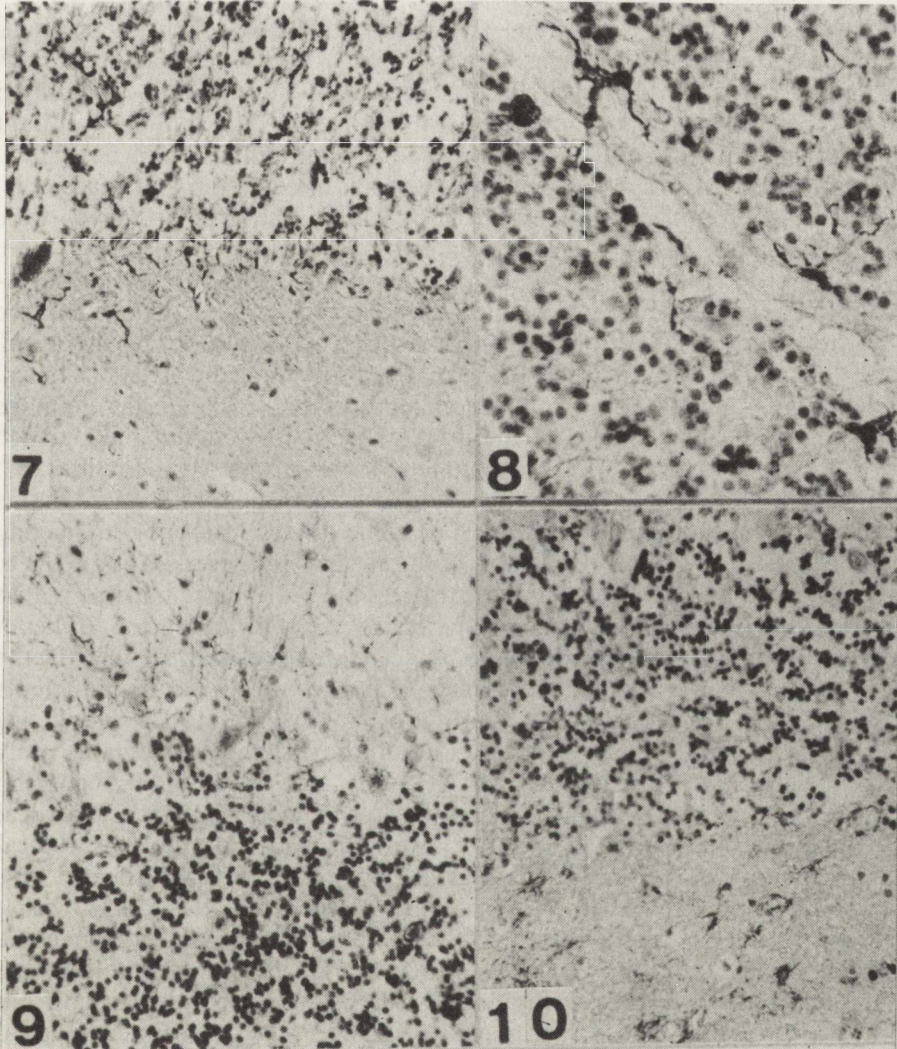
Fig. 4. PCD case. Immunohistochemistry with anti-IgG. Purkinje cells are decorated.  $\times 100$

Fig. 5. PCD case. Anti-IgG serum. Weak staining within Purkinje cells cytoplasm.  $\times 210$

Fig. 6. PCD case. Some of granular cells are also positive with anti-IgG antibody.  $\times 400$

IgG immunostaining was disclosed in Purkinje cell cytoplasm (Figs. 4, 5) and in 4 cases also on granule cell nuclei (Fig. 6).

Immunohistochemical studies showed glial cell proliferation mainly in white matter in the cases with granular layer atrophy. To some extent involvement of the molecular layer was also observed. Gliosis in the Purkinje cell layer seemed to parallel the extent of neuronal atrophy. In the granular layer prevalence of microglia cells was noted (Figs 7, 8). In cases with granular layer damage numerous ferritin-positive cells were seen within the affected



*Fig. 7.* PCD case. Anti-ferritin immunohistochemistry. Microglial cells in granular layer in a border of molecular layer.  $\times 200$

*Fig. 8.* PCD case. Ferritin-positive microglial cells within granular layer.  $\times 400$

*Fig. 9.* PCD case. Anti-GFAP staining. Astroglial cell proliferation visible only within molecular layer.  $\times 200$

*Fig. 10.* GFAP-positive astroglial cells in cerebellar white matter in PCD case.  $\times 200$

tissue. Some microglial cells, however, showed regressive changes, and in some cases a network of delicate, fragmented ferritin-positive fibers was observed. GFAP labeled astroglia was rather scanty. Usually only a few GFAP-positive cells were visible within the granular cell layer, irrespective of the degree of tissue damage (Figs 9, 10).

## DISCUSSION

Metastatic foci in the cerebellum were found in 18 cases, without any signs of accompanying granule cell layer damage or any other cerebellar pathology. From among the 52 cases with SCLC examined, finally five could be diagnosed as PCD, on the basis of lack of metastases within the CNS, and concomitant loss of Purkinje and granule cells. The changes were either focal or diffuse. Severe, diffuse granular layer degeneration was observed in one PCD case only. No features of prominent glial proliferation within the granular layer were demonstrated in our cases, similarly as in some previously reported (Bertrand, Godet Guillain 1942; Leigh, Meyer 1949; Osetowska 1963). Glial cell proliferation should be anticipated in cases with chronic cerebellar dysfunction and the cases without glial proliferation might represent recent cerebellar degeneration. However, generally, the absence of the glial cell reaction and lack of clinical cerebellar signs, inclined rather to conclude that the cerebellar damage occurred in the terminal phase of the disease, evoked or aggravated by such additional factors as anoxia/ischemia (Leigh, Meyer 1949; Mc Donald 1961; Wessel et al. 1988). In our cases intensive gliosis (astroglial and microglia as well) has been seen mainly in cerebellar white matter probably reflecting a secondary response of the glia to Purkinje cell neurites degeneration. It is of interest, that in some cases cerebellar cortical damage was more marked within the vermis, than in the cerebellar hemispheres. Torvik et al. (1986) and Koller et al. (1981) observed a similar distribution of cerebellar cellular atrophy in the aging process. However, similar prevalence of changes within brains of patients with SCLC and other neoplastic pathology was also noticed previously (Meyer, Foley 1953). Severe degeneration of the granular layer was only sporadically encountered in our study what seems to be uncommon. According to Schmid and Riede (1974) is granular cell atrophy characteristic for cortical cerebellar degeneration in SCLC contrary to the loss of Purkinje cells, typical rather for ovarian carcinoma (Steven et al. 1982; Greenlee, Brashear 1983).

The highest incidence of PCD previously reported was 5.1%, being observed in series of patients with bronchogenic carcinoma (Morton et al. 1966). According to Brain and Wilkinson (1965) the period of time between discovery of the tumor and development of cerebellar symptoms ranged from 3 months to 2 years, if that is the order of events. However, when neurological symptoms precede those of the tumor, the interval between the two events is from 2 months to 3 years.

The pathogenesis of PCD remains unclear, but detection of circulating antineuronal antibodies directed against Purkinje cells strongly support the role of the autoimmune process (Kearsley et al. 1985; Cunningham et al. 1986; Greenlee et al. 1983, 1986; Tanaka et al. 1986, 1987; Hammack et al. 1990).

Sera from patients with SCLC produced nuclear and cytoplasmic staining of neurons throughout the CNS. In the cytoplasm of Purkinje cells antibodies were found bounded to clusters of ribosomes, rough endoplasmic reticulum and the Golgi compartments complex (Rodriguez et al. 1988). However, anti-Purkinje cell antibodies are specific rather for SCLC, but not for paraneoplastic neurological disorders (Grisold et al. 1989). It is of interest that plasmapheresis reduced the level of the autoantibodies in the serum, without affecting their level in the cerebrospinal fluid (CSF). These data indicate that autoantibodies in PCD may be produced in the CNS (Furieux et al. 1990). The demonstration that IgG can be picked up by nerve endings and transported to the cell perikaryon provided a potential means whereby an antibody could reach and damage an intracerebellar neuronal structure (Borges et al. 1985; Smith et al. 1988). We had no opportunity to study anti-Purkinje cell antibodies in serum or CSF. However, *post mortem*, we did observe altered immunoreactivity of the nervous tissue, suggesting the participation of humoral immunity in the development of cerebellar damage. In our PCD cases we noted IgG deposits and C3 complement fraction in numerous Purkinje cells and also those of the granular layer.

Therefore, although the presence of IgG in the cell cytoplasm may not have necessarily pathological consequences (Dhib-Jalbut, Liwnicz 1986), we would like to underline that in the non PCD cases examined we have found remarkably weaker immunostaining with IgG and the complement fractions. According to the suggestion of Kamolvarin et al. (1991), the plasma C3 level may be useful for differentiating immune from non-immune neurological diseases. Evidence for IgG and the C3 fraction of complement expression within degenerating cerebellar cells seems to be promising for elucidation of the pathomechanism of PCD. Even so, and even without the possibility of detecting the specific antibody, serum and/or CSF, IgG and complement fractions level could be an early exponent for the occurrence of SCLC in cases with cerebellar signs. The question whether PCD seems to be the effect of autoaggression, as the result of presence of malignancy, or is caused by other factors, such as hypoxia, cachexia or autolytic post mortem changes is still open and requires further investigations. The immunopathological changes presently observed and glial cell proliferation could be an evidence for the non artifactual origin of PCD.

ZWYRODNIENIE WARSTWY ZIARNISTEJ MOZDZKU W PRZEBIEGU  
RAKA OWSIANOKOMÓRKOWEGO:  
ZESPÓŁ PARANOWOTWOROWY CZY ARTEFAKT?

Streszczenie

Celem pracy była próba wyjaśnienia, czy zanik warstwy ziarnistej mózdzku w przebiegu raka owsianokomórkowego jest artefaktem, czy charakterystycznym objawem dla tego nowotworu.

Oceniono mózgi 52 chorych, zmarłych w przebiegu raka drobnokomórkowego płuc. Utrwalone w formalinie i zatopione w parafinie skrawki najpierw barwiono rutynowo (HE, Klüver-Barrera), a następnie w wybranych 10 przypadkach wykonano badanie immunohistochemiczne. Użyto następujące przeciwciała: przeciw ferrytynie, GFAP, IgG i frakcji C3 dopełniacza. Ostatecznie w 5 przypadkach rozpoznano paranowotworowe zwyrodnienie mózdzku.

Trzech chorych wykazywało objawy zespołu mózdkowego w badaniu klinicznym. Odczyn komórek glejowych wydawał się ważnym wykładnikiem dla przyżyciowego rozwoju procesu patologicznego. W uszkodzonej warstwie ziarnistej stwierdzano głównie rozplam komórek mikroglejowych, natomiast w mniejszym stopniu obecność GFAP-dodatnich komórek astrogleju. Przeciwciała przeciw frakcji C3 dopełniacza barwiły cytoplazmę komórek Purkiniego, a niekiedy także neurony warstwy ziarnistej. Surowice skierowane przeciw IgG były wyraźnie dodatnie w cytoplazmie komórek Purkiniego, a w 4 przypadkach barwiły również jądra komórek warstwy ziarnistej. Wydaje się, że zmiany stwierdzone w badaniu immunohistochemicznym, a także pomnożenie komórek glejowych wskazują na przyżyciowe powstanie uszkodzeń i świadczą przeciwko artefaktycznemu pochodzeniu opisywanych zmian.

## REFERENCES

1. Bertrand I, Godet-Guillain J: Etude anatomoclinique d'un cas d'atrophie lamellaire cerebelleuse. *Rev Neurol*, 1942, 74, 287.
2. Borges LF, Elliot PJ, Gill R, Iversen LL: Selective extraction of small and large molecules from the cerebrospinal fluid by Purkinje neurons. *Science*, 1985, 228, 346–348.
3. Brain WR, Wilkinson M: Subacute cerebellar degeneration associated with neoplasm. *Brain*, 1965, 88, 465–478.
4. Cunningham J, Graus F, Anderson N, Posner JB: Partial characterisation of the Purkinje cell antigens in paraneoplastic cerebellar degeneration. *Neurology*, 1986, 36, 1163–1168.
5. Dhib-Jalbut S, Liwnicz BH: Immunocytochemical binding of serum IgG from a patient with oat cell tumor and paraneoplastic motoneuron disease to normal human cerebral cortex and molecular layer of the cerebellum. *Act Neuropathol (Berl.)* 1986, 69, 96–102.
6. Furneaux HF, Reich L, Posner JB: Autoantibody synthesis in the central nervous system of patients with paraneoplastic syndromes. *Neurology*, 1990, 40, 1085–1091.
7. Greenlee JE, Brashear HR: Antibodies to cerebellar Purkinje cells in patient with paraneoplastic cerebellar degeneration and ovarian carcinoma. *Ann Neurol*, 1983, 14, 609–613.
8. Greenlee JE, Lipton HL: Anticerebellar antibodies in serum and cerebrospinal fluid of a patient with oat cell carcinoma of the lung and paraneoplastic cerebellar degeneration. *Ann Neurol*, 1986, 1, 82–85.
9. Greenlee JE, Brashear HR, Herndon RM: Immunoperoxidase labeling of rat brain sera from patients with paraneoplastic cerebellar degeneration and systemic neoplasia. *J Neuropathol Exp Neurol*. 1988, 47, 561–571.
10. Grisold W, Drlicek M, Liszka U, Popp W: Anti-Purkinje cell antibodies are specific for small-cell lung cancer but not for paraneoplastic neurological disorders. *J Neurol*, 1989, 236, 64.
11. Hammack JE, Kimmel DW, O'Neill BP, Lennon VA: Paraneoplastic cerebellar degeneration; A clinical comparison of patients with and without Purkinje cell cytoplasmic antibodies. *Mayo Clin Proc*, 1990, 65, 1423–1431.
12. Henson RA, Urich H: Peripheral neuropathy associated with malignant neoplasm. In: *Cancer and the nervous system*. Eds: RA Henson, H Urich. Blackwell Scientific Publications, Oxford, 1982.
13. Kamolvarin N, Hemachudha T, Ongpipattanakul B, Phanthumchinda K, Sueblinvong T: Plasma C3 c in immune – mediated neurological diseases: a preliminary report. *Acta Neurol Scand*. 1991, 83, 382–387.
14. Kearsley JH, Johnson P, Halmagyi M: Paraneoplastic cerebellar disease remission with excision of the primary tumor. *Arch Neurol*. 1985, 42, 1208–1210.
15. Koller WC, Glatt SL, Fox JH, Kaszniak AW, Wilson RS, Huckman MS: Cerebellar atrophy; relationship to aging and cerebral atrophy. *Neurology*, 1981, 31, 1486–1488.
16. Laure-Kamionowska M: Cerebellopatie paranowotworowe w materiale dziecięcym. *Neuropatol Pol*, 1990, 28, 161–167.
17. Leigh AD, Meyer A: Degeneration of the granular layer of the cerebellum. *J Neurol Neurosurg Psychiatry*, 1949, 12, 287–296.
18. Mc Donald WI: Cortical cerebellar degeneration with ovarian carcinoma. *Neurology*, 1961, 11, 329–334.
19. Meyer JS, Foley JM: The encephalopathy produced by extracts of eosinophils and bone marrow. *J Neuropathol Exp Neurol*, 1953, 12, 349–362.
20. Morton DL, Itabashi HH, Grimes OI: Non-metastatic neurological complications of bronchogenic carcinoma. The carcinomatous neuropathies. *J Thorac Cardiovasc Surg*, 1966, 51, 14–29.

21. Osetowska E: Zaniki kory mózdzku w przebiegu raka narządów wewnętrznych. *Neuropatol Pol*, 1963, 1, 91–100.
22. Rodriguez M, Truh LI, O'Neill BP, Lennon VA: Autoimmune paraneoplastic cerebellar degeneration. Ultrastructural localization of antibody-binding sites in Purkinje cells. *Neurology*, 1988, 38, 1380–1386.
23. Schmid AH, Riede UN: A morphometric study of the cerebellar cortex from cerebellar atrophy. *Acta Neuropathol (Berl.)*, 1974, 28, 343–352.
24. Smith JL, Finley JC, Lennon VA: Autoantibodies in paraneoplastic cerebellar degeneration bind to cytoplasmic antigens of Purkinje cells in humans, rats and mice and are of multiple immunoglobulin classes. *J Neuroimmunol*, 1988, 19, 37–48.
25. Steven MM, Mackay IR, Carnegie PR, Bhathal PS: Cerebellar cortical degeneration with ovarian carcinoma. *Postgr ad Med J*, 1982, 58, 47–51.
26. Tanaka K, Yamazaki M, Sato S, Tyoshima I, Yamamoto A, Miyatake T: Antibodies to brain proteins in paraneoplastic cerebellar degeneration. *Neurology*, 1986, 36, 1169–1172.
27. Tanaka K, Tanaka M, Miyatake T, Yamamoto A, Kurahashi K, Matsuanga M: Antibodies to brain proteins in a patient with subacute cerebellar degeneration and Lambert-Eaton myasthenic syndrome. *Tohoku J Exp Med*, 1987, 153, 161–167.
28. Torvik A, Torp S, Lindboe CF: Atrophy of the cerebellar vermis in ageing: a morphometric and histologic study. *J Neurol Sci*, 1986, 76, 283–294.
29. Wessel K, Diener HC, Dichgans J, Thorn A: Cerebellar dysfunction in patients with bronchogenic carcinoma; clinical and posturographic findings. *J Neurol*, 1988, 235, 290–296.
30. Yamamoto T, Hirano A: A comparative study of modified Bielschowsky, Bodian and thioflavin S stains on Alzheimer's neurofibrillary tangles. *Neuropathol Appl Neurobiol*, 1986, 12, 3–9.

Correspondence address: Dr M. Barcikowska, Department of Neuropathology, Medical Research Centre, Polish Academy of Sciences, 3 Dworkowa Str, 00-784 Warsaw, Poland



EWA MATYJA<sup>1</sup>, IZABELA KUCHNA<sup>2</sup>, MIROSLAW ZĄBEK<sup>3</sup>

## CEREBRAL GANGLIOGLIOMA WITH LONG HISTORY AND UNUSUAL PROMINENCE OF THE MESENCHYMAL ELEMENTS. CASE REPORT

<sup>1</sup> Department of Neuropathology and <sup>2</sup> Laboratory of Developmental Neuropathology, Medical Research Centre, Polish Academy of Sciences, Warsaw, <sup>3</sup> Department of Neurosurgery, Bródnowski Hospital, Warsaw

A case of cerebral ganglioglioma, a relatively rare and controversial tumor of the central nervous system, is reported. The histological pattern of the tumor consisted of differentiated neuronal cells and glial elements displaying a various extent of cytologic abnormalities. Beside these two typical components for ganglioglioma, an abundance of collagen fibrils and numerous blood vessels were encountered. The long clinical course manifested by temporal epilepsy preceding clinical diagnosis of brain tumor and peculiar histological appearance seem to be of considerable interest.

Key words: *ganglioglioma, mesenchymal tissue.*

Ganglioglioma of the central nervous system (CNS) is a relatively rare tumor composed of a mixture of differentiated neuronal and glial cells (Courville 1930; Courville, Anderson 1941; Kernohan et al. 1932; Anderson, Adelstein 1942; Russel, Rubinstein 1977; Henry et al. 1978; Johannsson et al. 1981). These tumors are most often of relatively low-grade malignancy and slow clinical course, they occur in children and/or young adults under the age of 30. The terminology and histogenesis of this type of tumors still remain controversial, they are considered most often as hamartomatous with tendency to neoplastic changes (Steggmann, Winer 1961; Russel, Rubinstein 1962, 1977).

### CASE REPORT

A 48-year old male patient had suffered from focal seizures since the age of 26. The diagnose was temporal epilepsy and the patient had been treated with anticonvulsant drugs for 22 years. At the age of 38 he was hospitalized with diagnosis of epilepsy and hysteric mutism. At the age of 48 severe headache without nausea and vomiting, moreover apathy and occasionally disturbances of balance occurred. Neurological examination revealed enhanced deep tendon

reflexes on the left side, and visual assessment left temporal hemianopsia. The CT scan showed a large cystic lesion in the right temporal lobe (Fig. 1). The cerebrospinal fluid contained 181 mg% of protein. Right temporal craniotomy was performed. A widespread mass of tumor was present in the right temporal lobe accompanied by a large cyst connected with the lateral ventricle and containing yellow fluid. Inside the lateral ventricle a mass of rich-vascularized neoplastic tissue associated with tela choroidea was encountered. The tumor extended to deep parts of the temporal lobe and was subtotally removed.

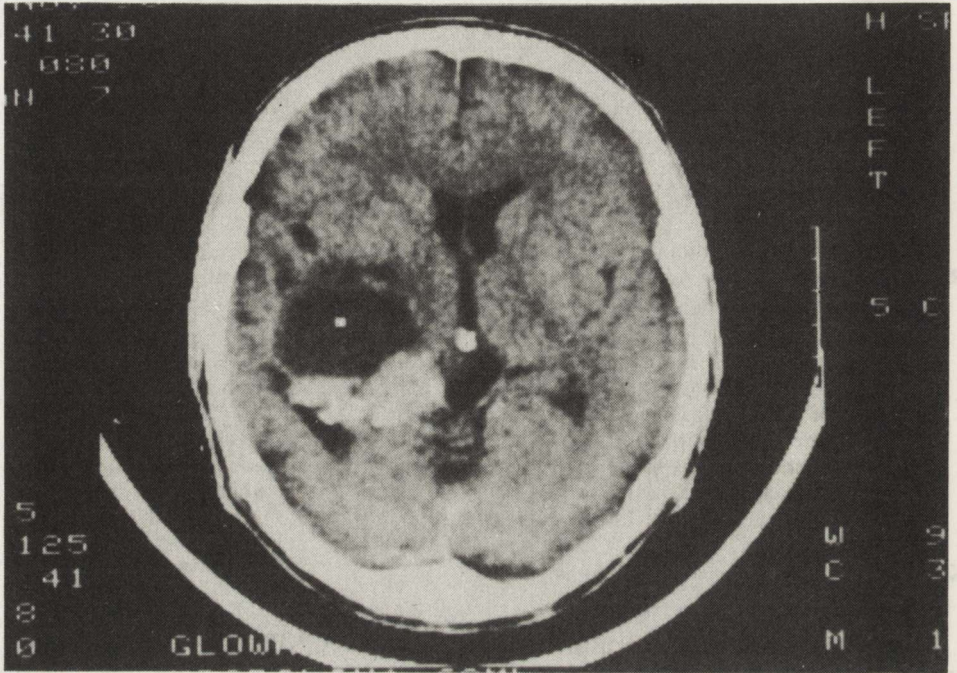


*Fig. 1.* CT scan demonstrating mass lesion in the right hemisphere composed of a solid part with focal fibrosis and cystic part at the base of the temporal lobe

The biopsy material was fixed in 4% paraformaldehyde and embedded in paraffin. The sections were stained with hematoxylin-eosin, Klüver-Barrera, van Gieson and Gridley method. Immunohistochemical studies for the presence of glial fibrillary acidic protein (GFAP) were performed on paraffin sections with antisera for GFAP (Dakopatts) using the extravidin-biotin-peroxidase complex method with diaminobenzidine as chromogen.

#### NEUROPATHOLOGICAL EXAMINATION

Light microscopy examination revealed a variable histological picture from field to field. The tumor tissue displayed poor to moderate cellular density. The cells were usually dispersed in an background rich in fine cell processes. Some

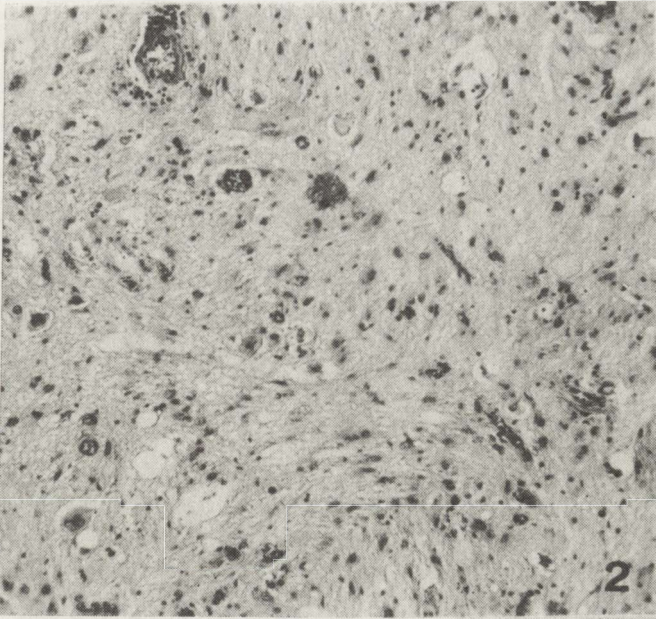
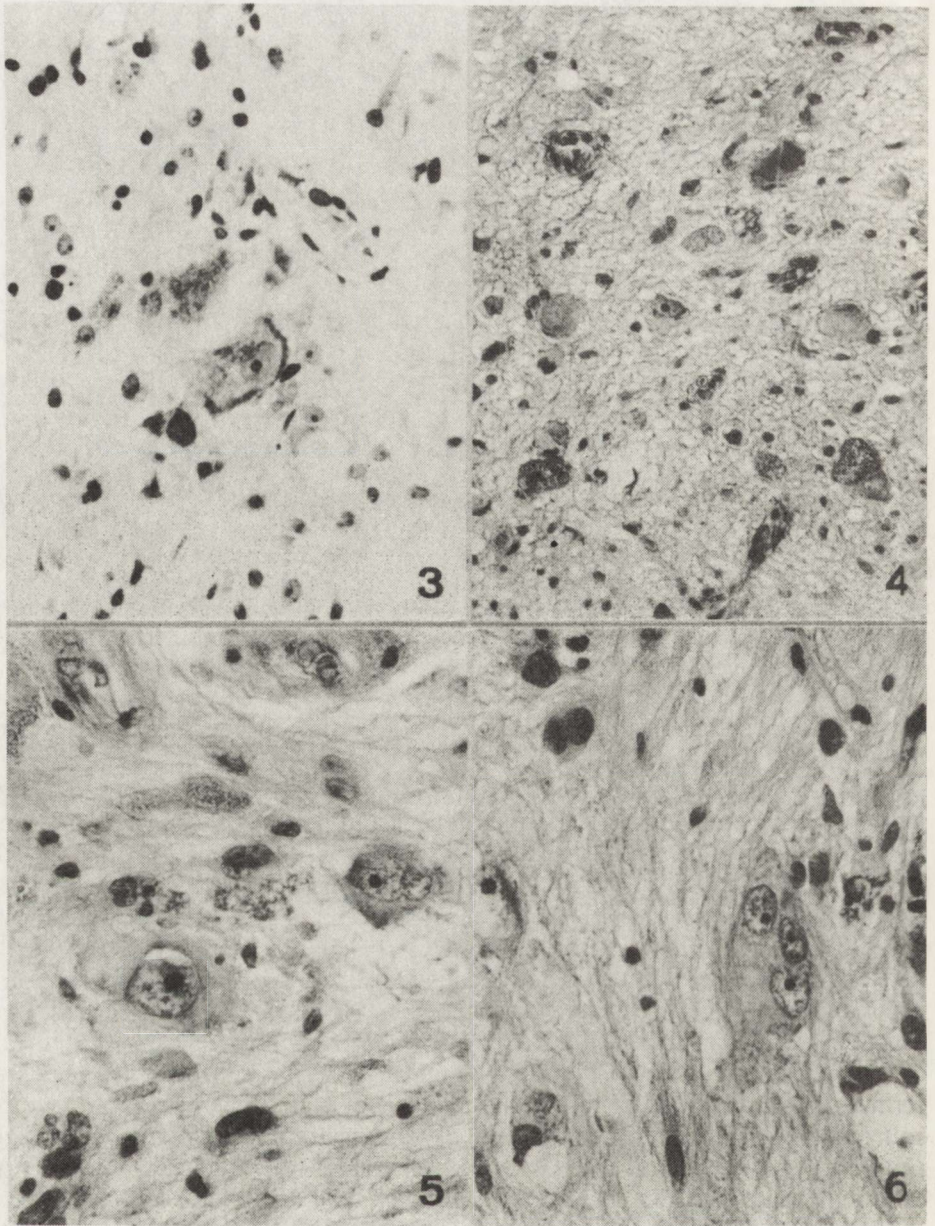


Fig. 2. Compact tumor tissue with fields composed of neuronal and glial cells. H-E.  $\times 100$

areas were occupied by collagen-rich tissue and/or numerous blood vessels with thickened walls.

The infiltrative tissue was essentially composed of two types of cell elements: atypical neuronal or ganglion cells and neuroglial cells. The neuronal cells were scattered without any particular arrangement throughout the infiltrated cerebral tissue (Fig. 2). The nerve cells showed marked variability of size and shape. In some of them various amounts of Nissl substance were unevenly distributed, most often irregularly or on the periphery of the perikaryon (Fig. 3). Numerous nerve cells revealed degenerative changes and appeared as eosinophilic and homogeneous (Fig. 4). Some large cells had a round, vesicular nucleus limited by a well-defined nuclear membrane and containing small nucleoli typical for ganglion cells (Fig. 5). Bi- or tri-nucleated forms of ganglion cells were occasionally encountered (Fig. 6). Scant stromal neuroglial elements were represented by both astrocytes and oligodendroglia (Fig. 7). The astrocytic cells were pilocytic as demonstrated by GFAP immunohistochemistry (Fig. 8). The glial elements exhibited scant evidence of neoplastic transformation expressed by anaplastic cellular forms, but without marked increase of cellular density and mitoses. In some areas of infiltrated tissue numerous tiny calcospherites were present. In some fragments of biopsy material abundant connective tissue and thickened walls of blood vessels predominated in the histological picture (Fig. 9). Hyaline thickening of the vessel walls and hyalinization or calcification of the bands of connective tissue could be observed. In the fibrous parts exhibiting a dense network of reticulin fibers (Fig. 10) the sparse cells were compressed by mesenchymal elements so it was difficult to determine their morphology.



*Fig. 3.* Neuronal cell with round nucleus containing nucleolus and peripherally distributed Nissl substance in the perikaryon. Klüver-Barrera  $\times 400$

*Fig. 4.* Some neuronal cells revealing degenerative changes. H-E.  $\times 200$

*Fig. 5.* Large ganglion cells with vesicular nucleus and prominent nucleoli. H-E.  $\times 400$

*Fig. 6.* Multinucleated ganglion cells. H-E.  $\times 400$

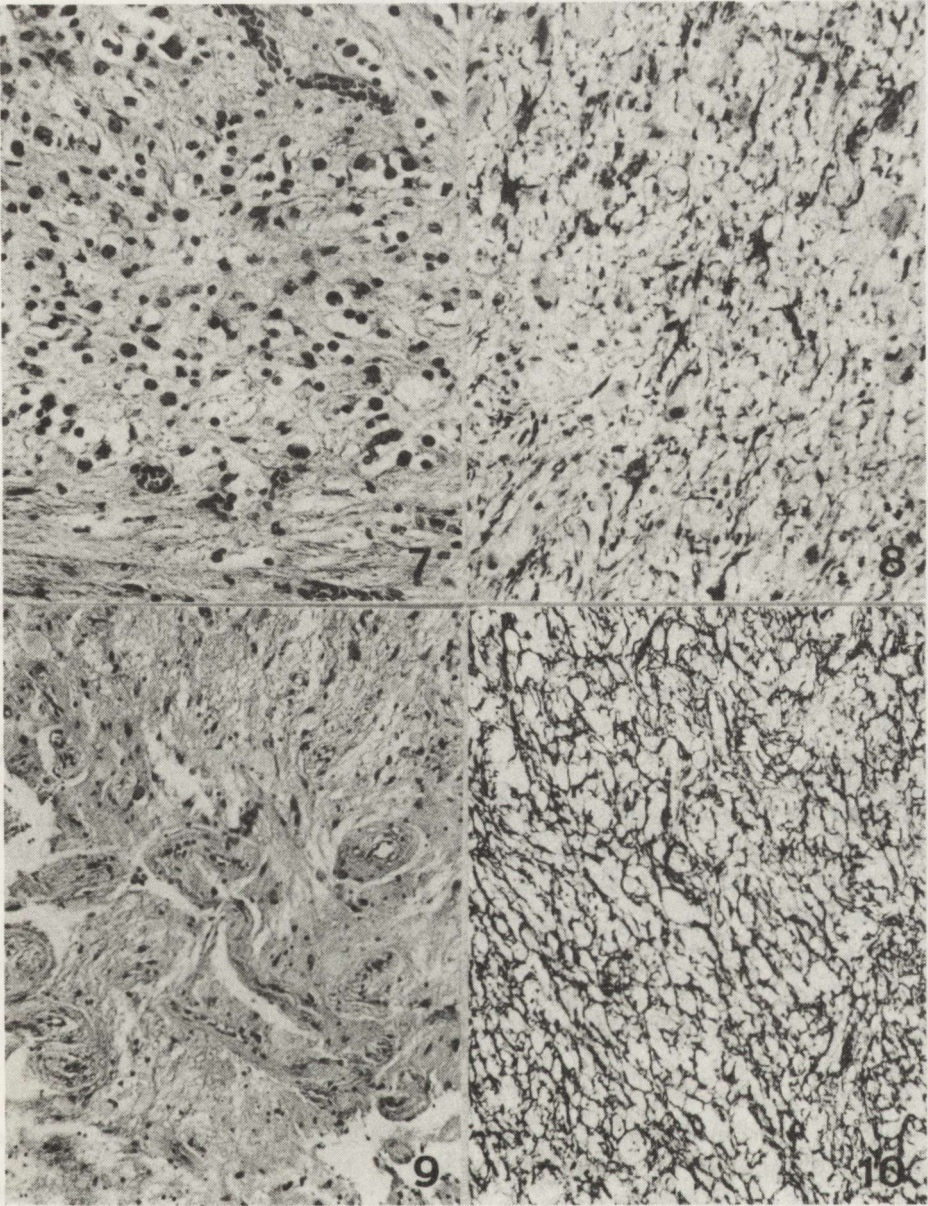


*Fig. 7.* Highly-cellular area of the tumor composed of neuroglial cell with predominant oligodendroglial component. H-E.  $\times 200$

*Fig. 8.* Astroglial cells with fibrous and pilocytic features. GFAP immunocytochemical staining.  $\times 200$

*Fig. 9.* Numerous vessels exhibit thick, fibrous walls. H-E.  $\times 100$

*Fig. 10.* Dense network of reticulin fibers. Gridley  $\times 100$

## DISCUSSION

The tumor in our case revealed neuronal, glial and mesenchymal elements forming a complex of proliferative tissue. The neuronal cells similar to those of peripheral ganglia showed marked features of cytologic abnormalities concerning difference in size and shape. Multinucleated neuronal cells were seen also in this like in other reported cases (Johannsson et al. 1981; Takahashi et al. 1989). It is difficult to determine whether the observed cells participated actually in the neoplastic process or represented only different stages of maturation. However, the number and degree of neuronal abnormalities may support the diagnosis of ganglioglioma. The glial elements seemed to be more engaged in the neoplastic process. Nevertheless, scanty anaplasia and mild cellular proliferation without mitoses justify the repeated opinion that nosological classification of this type of tumor could be controversial (Russell, Rubinstein 1977).

The tumor cells were encompassed by a rich network of fibrous connective tissue and in some areas collagen fibres dominated in the histological appearance of the tumor. Such an unusual abundance of fibrous connective tissue has been previously found in some central ganglionic tumors (Russell, Rubinstein 1962; Robertson et al. 1964; Miller, Ramsden 1966; Rubinstein, Herman 1972; Vandenberg et al. 1987). Some similarity was suggested to the structure of peripheral ganglia and this supports the hypothesis of hamartomatous origin of ganglionic CNS tumors (Rubinstein, Herman 1972). On the basis of slow evolution of the tumor and histological picture, this group of tumors is often considered as of maldevelopmental nature with the possibility to undergo anaplastic changes during further growth. In the present case, the exceptionally long clinical course preceding diagnosis of CNS tumor may have been connected with slow growth of the tumor owing to mild anaplasia of neuronal and glial elements.

PRZYPADEK *GANGLIOGLIOMA* MÓZGU O DŁUGIM PRZEBIEGU KLINICZNYM,  
Z DUŻYM UDZIAŁEM TKANKI ŁĄCZNEJ  
W OBRAZIE MORFOLOGICZNYM

## Streszczenie

Przedstawiono przypadek *ganglioglioma*, rzadkiego guza ośrodkowego układu nerwowego, którego histogeneza jest nadal kontrowersyjna.

Utkanie guza składało się z dojrzałych komórek nerwowych rozrzuconych w podścielisku glejowym. Znamienną cechą obrazu histologicznego była obfitość elementów mezenchymalnych w postaci pasm tkanki łącznej i pogrubiałych ścian naczyń. W obrębie podścieliska glejowego stwierdzono niewielki stopień anaplazji. Długi przebieg kliniczny oraz obraz histologiczny utkania zdają się potwierdzać udział zaburzeń różnicowania komórek typu hamartoma w patomechanizmie rozwoju *ganglioglioma* z potencjalną możliwością ich rozrostu nowotworowego.

## REFERENCES

1. Anderson FM, Adelstein LJ: Ganglion cell tumor (*ganglioglioma*) in the third ventricle. Operative removal with clinical recovery. Arch Surg, 1942, 45, 129–139.

2. Courville CB: Ganglioglioma. Tumor of the central nervous system: review of the literature and report of two cases. *Arch Neurol Psychiat*, 1930, 24, 439–491.
3. Courville CB, Anderson FM: Neuro-gliogenic tumors of the central nervous system. Report of two additional cases of ganglioglioma of the brain. *Bull Los Angeles Neurol Soc*, 1941, 6, 154–176.
4. Henry JM, Heffner RR, Earle KM: Gangliogliomas of CNS: a clinicopathological study of 50 cases. *J Neuropathol Exp Neurol*, 1978, 37, 626 (Abst).
5. Johannsson JH, Reikate HL, Roessmann U: Gangliogliomas: pathological and clinical correlation. *J Neurosurg*, 1981, 54, 58–63.
6. Kernohan JW, Learmonth JR, Doyle JB: Neuroblastomas and gangliogliomas of the central nervous system. *Brain*, 1932, 55, 287–310.
7. Miller AA, Ramsden FR: A cerebral neuroblastoma with unusual fibrous tissue reaction. *J Neuropathol Exp Neurol*, 1966, 25, 328–340.
8. Robertson DM, Hendry WS, Vogel FS: Central gangliioneuroma: a case study using electron microscopy. *J Neuropathol Exp Neurol*, 1964, 23, 692–705.
9. Rubinstein LJ, Herman MM: A light- and electron-microscopic study of a temporal lobe ganglioglioma. *J Neurol Sci*, 1972, 16, 27–48.
10. Russell DS, Rubinstein LJ: Ganglioglioma: a case with long history and malignant evolution. *J Neuropathol Exp Neurol*, 1962, 21, 185–193.
11. Russel DS, Rubinstein LJ: Pathology of the tumors of the nervous system. Williams and Wilkins, Baltimore, 1977, pp. 261–262.
12. Steegmann AT, Winer B: Temporal lobe epilepsy resulting from ganglioglioma. *Neurology*, 1961, 11, 406–412.
13. Takahashi H, Wakabayashi K, Kawai K, Ikuta F, Tanaka R, Takeda N, Washiyama K: Neuroendocrine markers in central nervous system neuronal tumors (gangliocytoma and ganglioglioma). *Acta Neuropathol*, 1989, 77, 237–243.
14. Vandenberg SR, May EE, Rubinstein LJ, Herman MM, Perents E, Vinores SA, Collins VP, Park TS: Desmoplastic supratentorial neuroepithelial tumors of infancy with divergent differentiation potential (“desmoplastic infantile gangliogliomas”). Report on 11 cases of distinctive embryonal tumor with favorable prognosis. *J Neurosurg*, 1987, 66, 58–71.

Authors' address: Department of Neuropathology, Medical Research Centre, Polish Academy of Sciences, 3 Dworkowa Str, 00-784 Warsaw, Poland

BOGDAN GOETZEN, ELŻBIETA SZTAMSKA

## COMPARATIVE ANATOMY OF THE ARTERIAL VASCULARIZATION OF THE HIPPOCAMPUS IN MAN AND IN EXPERIMENTAL ANIMALS (CAT, RABBIT AND SHEEP)

Laboratory of Angiology of the Central Nervous System, Department of Neurology, School of  
Medicine, Łódź, Poland

The studies were performed by the authors' injection method on 30 human brains and 80 animal ones. The cerebral arteries were injected with synthetic coloured latex and then prepared in an operating microscope. It was found that the main source of arterial supply of both the human and animal hippocampus is the posterior cerebral artery. However, this artery has different origins in the arterial circle of the brain in man, cat, rabbit and sheep. Comparative investigations have also proved that the hippocampal vascular system in man and animals is very similar. It is formed by branches of the posterior cerebral artery and of the anterior choroidal artery, called the hippocampal arteries, and by numerous internal hippocampal arterioles arising from them at right angle. The regional distribution of these arterioles is impossible to describe because of their variable course in the hippocampal cortex and of the similar vascularization of different cortical areas of the hippocampus. The studies have also shown that the hippocampal arterial system is very well developed and makes collateral circulation possible. Extracerebral segments of the hippocampal arterioles in human senile brains, and chiefly in brains with atherosclerosis, showed different deformations in the form of siphon-like structures, knot-loops and vascular glomeruli.

*Key words: arterial vascularization, hippocampus, comparative anatomy.*

In anatomical studies on the telencephalon structures called the limbic system both in man and animals, including the phylogenetically oldest cortical formations, and performing the basic function in evoking emotional reactions, the vascular system and its role are still insufficiently known. The progress of the research on brain pathology, mainly on cerebral vascular pathology, prompted the need to study more precisely also the arterial vascularization of the limbic system in man and experimental animals. There is particularly a lack of comparative investigations of the insufficiently known arterial vascularization of the hippocampus in man and animals.

Only few studies are devoted to arterial vascularization of the hippocampus in man (Uchimura 1928; Heiman 1938; Lindenberg 1957; Lierse 1963; Muller, Show 1965), and authors do not describe in detail all the hippocampal arteries and their sources of supply, giving different informations about the origins, topography and number of primary hippocampal arteries, their course,



vascular regions and classification of the secondary (internal) hippocampal arterioles. However, since the time of Spielmeyer's (1925) and Uchimura's (1928) studies, various histopathological lesions of the individual cortical areas of the hippocampus, appearing e.g. in cases of carbon monoxide poisoning, epilepsy, ischemia and inflammatory processes of the brain, are related to the specific hippocampal angioarchitectonics and cerebral circulatory insufficiency.

The aim of the present study was to investigate anatomically and comparatively the sources of arterial vascularization, structure, topography and courses of the extra- and intracerebral segments of the hippocampal arteries in man, cat, rabbit and sheep, as well as the possibilities of collateral circulation in the hippocampus.

#### MATERIAL AND METHODS

Studies were carried out with the use of the injection method by Goetzen (1957) on 30 human brains with more or less developed atheromatosis, with or without arterial hypertension, and 30 cat, 30 rabbit and 20 sheep brains. Macrosmatic mammals were chosen representing animal groups with different levels of phylogenetic development.

The arterial systems of the human brains were injected with synthetic many-coloured latex (Hycar, Revinex and Perbunan N) through the internal carotid arteries or through the main trunks of the arterial circle of the brain, after perfusion of the vessels with distilled water. In animals latex was injected through the common carotid arteries of cat, rabbit and sheep brains *in situ*, and then the brains were removed from the skulls. The specimens were fixed in ethanol. Trunks of the latex-filled arterial circles of the brains, their cortical branches and the extracerebral segments of the deep arteries were subjected to anatomical evaluation by means of an operating microscope. Intracerebral segments of the deep cerebral arteries were dissected with microsurgical instruments, under an operating microscope at a magnification of 8–32 times. The shape, course, extent of vascularization and kinds of branches and anastomoses of the studied arteries were established as well as their deformations, number and diameters.

#### RESULTS

##### Sources of arterial vascularization of the hippocampus in man, cat, rabbit and sheep

The main and constant vessel carrying the blood to the hippocampus in human, cat, rabbit and sheep brains is the posterior cerebral artery. However, the sources of supply of this artery in man and the studied animals are different.

The sources of supply of the posterior cerebral arteries in the human brain depend on the structure of the arterial circle of the brain. In cases when the posterior cerebral arteries branch out from the basilar artery, they receive blood from the vertebral arteries. In modifications of the structure of the posterior part of the arterial circle of the brain, occurring in 26% of cases

according to our studies, they receive blood mainly from the internal carotid arteries, symmetrically in both cerebral hemispheres in 16% of cases.

Contrary to the human posterior cerebral arteries, the cerebral arteries corresponding to them in cat and sheep are the main, strongly developed branches of the posterior ramifications of the internal carotid artery and always receive blood from the internal carotid arteries (Fig. 1). However, in the rabbit brain the posterior cerebral artery originates from the junction of the posterior ramification of the internal carotid artery with the terminal ramification of the basilar artery. An additional source of arterial supply to the anterior part of the hippocampus in man and the studied animals is the anterior choroidal artery. The vascular extent of this artery in the hippocampus is variable. In man, the anterior choroidal artery supplies the foot of the hippocampus in 11% of cases. Superficial ramifications of the anterior



Fig. 1. Typical structure and topography of the trunks and branches of the arterial circle of the cat brain.  $\times 5$

Aca — arteria cerebri anterior, Acm — arteria cerebri media, Cra-, Crp — crura arteriae cerebri internae, anterior et posterior, Acp — arteria cerebri posterior, Ab — arteria basilaris, Ch — chiasma opticum, Lpr — lobus pyriformis, Pc — pedunculus cerebri

choroidal artery in man in 28% of cases anastomose in the uncus region with branches of the posterior cerebral artery leading to the hippocampus. These anastomoses make collateral circulation possible.

#### Arterial vascularization of the human hippocampus

The human hippocampus has its own specific arterial system, formed by the collateral branches of the posterior cerebral artery, and also quite often of the anterior choroidal artery, called (primary) hippocampal arteries, and by the internal (secondary) hippocampal arterioles arising from them.

The hippocampal arteries of the posterior cerebral artery are derived from the terminal segment beyond the postanastomosed part of their maternal trunk surrounding the cerebral peduncle (25%) or from the proximal segments of its cortical branches (75%) (Fig. 2), often close to the thalamochoroidal arteries. There are usually 2–5 single hippocampal arteries, from 400 to 800  $\mu\text{m}$  in diameter. In rare cases they start in a common trunk as a pedicle containing 2–3 branches. The hippocampal arteries after leaving the maternal trunks run in the leptomeninx of the hippocampal gyrus and the subiculum with arches in the hippocampal direction. Then they bend in L shape or divide into two branches in Y, rarely T-shape and run diverging from one another along the hippocampal sulcus. Quite often, in 30% of cases, the hippocampal arteries fuse in the hippocampal sulcus forming vascular arcades. Few hippocampal arteries

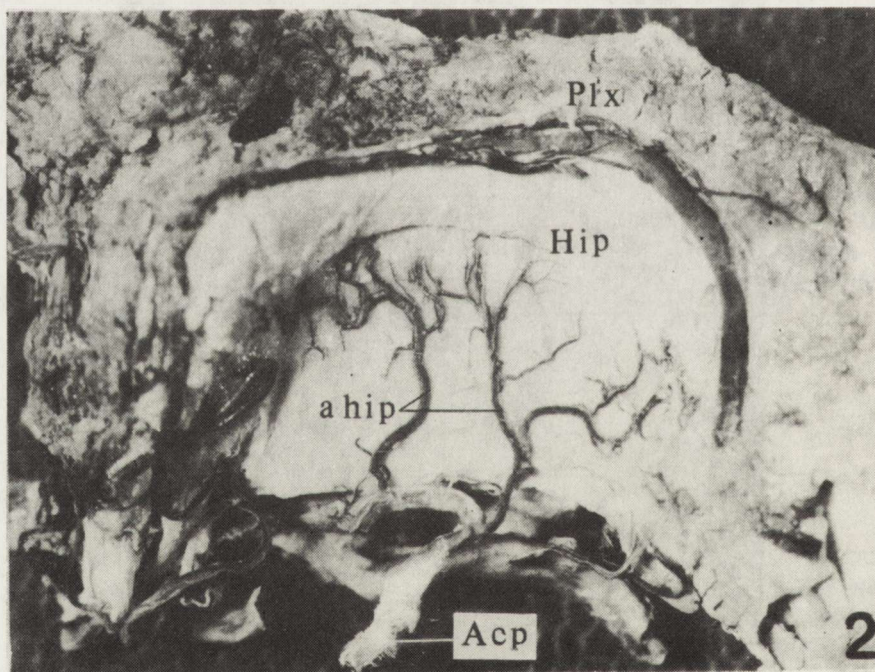


Fig. 2. Origin, structure and course of the hippocampal arteries (ahip) of the posterior cerebral artery (Acp) in man. The hippocampal arteries arise as two single trunks from the proximal segment of the main cortical branch of the Acp. Hip – hippocampus, Plx – *plexus choroideus*. View on the side of the thalamus.  $\times 4$

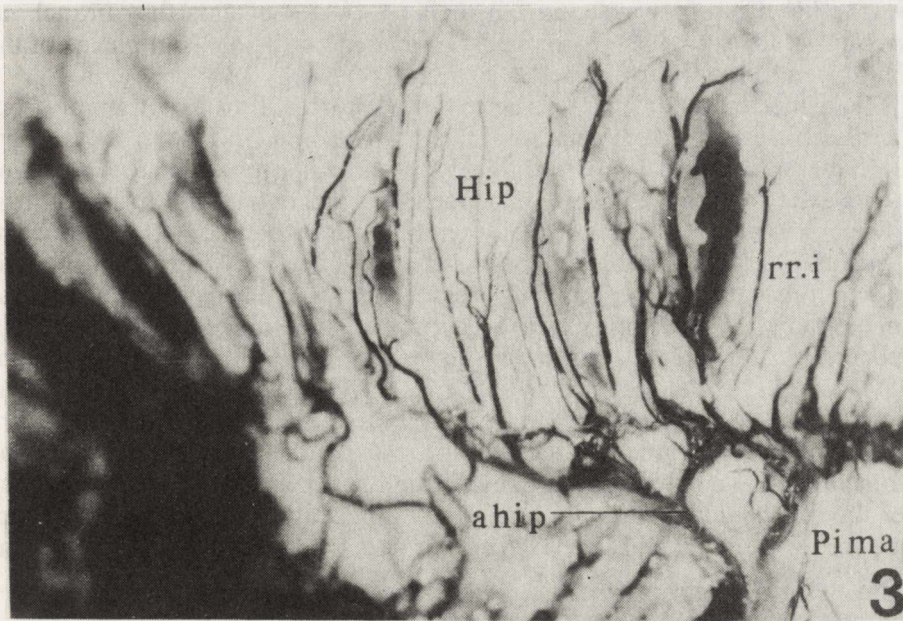


Fig. 3. Structure, course and supplying region of the internal arterioles of the human hippocampus (Hip); ahip - arteria hippocampi, rri - rami interni, Pima - pia mater. View on the side of the inferior horn of the lateral ventricle.  $\times 8.5$

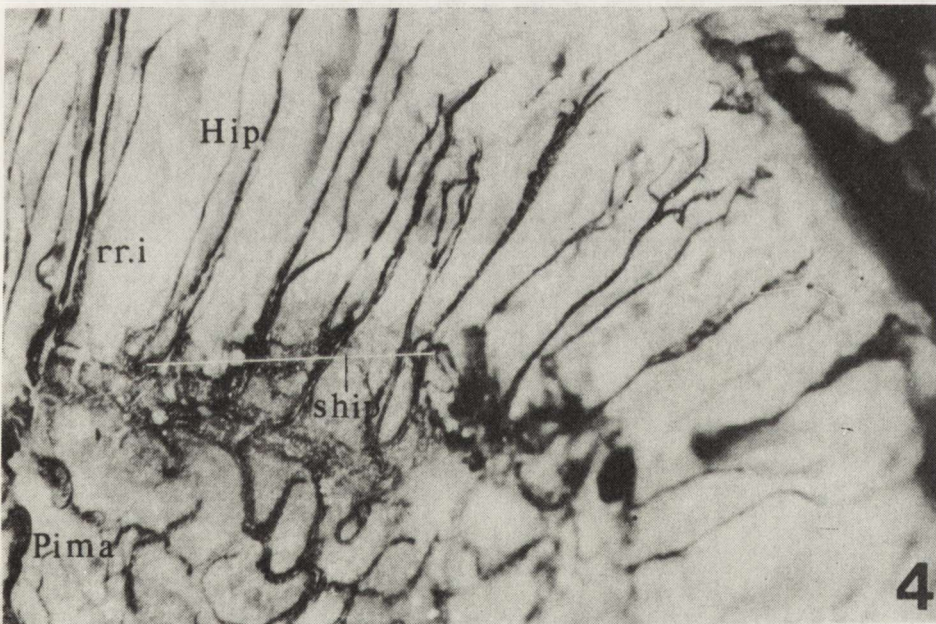


Fig. 4. Topography of the internal arterioles (rri) in longitudinal section of the human hippocampus (Hip); ship - sulcus hippocampi, Pima - pia mater.  $\times 8.5$

leave the hippocampal sulcus and in their terminal segments they branch on the temporal lobe surface (7% of cases) or enter into the choroid plexus of the cerebral ventricles (5% of cases).

The hippocampal arteries of the anterior choroidal artery originate from the proximal segment of the maternal trunk in the number of 1 to 3 branches. They have a structure similar to the hippocampal arteries of the posterior cerebral artery and run in the hippocampal sulcus in the region of the uncus.

The hippocampal arteries give off their main branches along the hippocampal sulcus — the internal hippocampal arterioles. However, on all their extracerebral segments they give off some few, small collateral leptomeningeal branches supplying the hippocampal gyrus and the subiculum. The internal hippocampal arterioles arise from the hippocampal arteries at an almost right angle, usually at equal distance as single trunks or pedicles, less frequently as bundles of two to five vessels 50 to 180  $\mu\text{m}$  in diameter. In their proximal, very short extracerebral segments they run straight, parallel to one another in the leptomeninx of the subiculum giving off small superficial branches. Then they enter the hippocampus variably along the hippocampal sulcus. Some of them divide into 2–3 trunks just before or after penetrating into the hippocampal

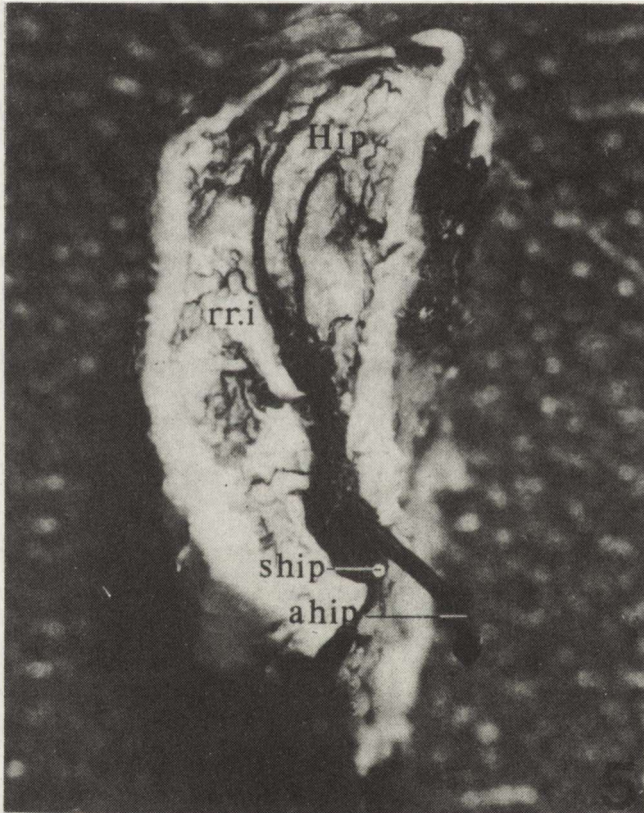


Fig. 5. Topography of the internal arterioles (rr.i) and their vascular areas in transversal section of the human hippocampus (Hip); ahip — arteria hippocampi, ship — sulcus hippocampi.  $\times 10$

6

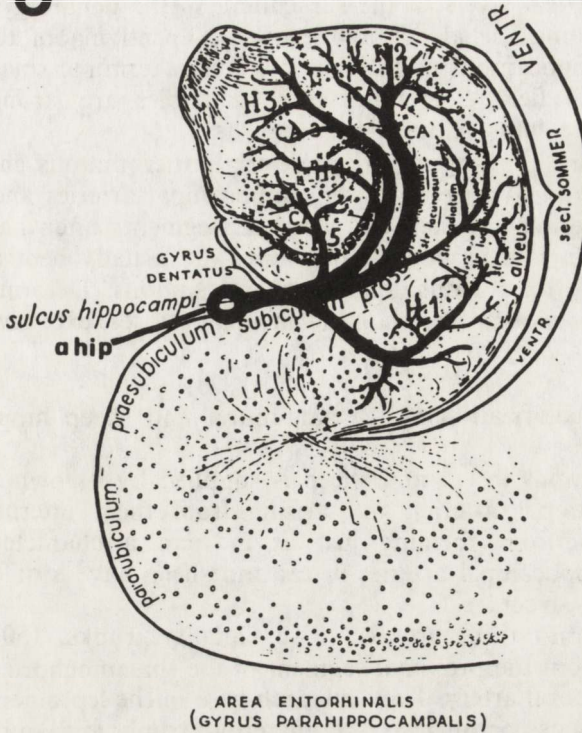


Fig. 6. Diagram illustrating the typical course of the internal arterioles in the hippocampal cortex in man, drafted on the illustration of the hippocampal microscopic appearance by Gastaut and Lammers (1961); ahip — arteria hippocampi

sulcus. The internal hippocampal arterioles do not form anastomoses in their course, so that anatomically they are terminal vessels.

Detailed delimitation of the vascular areas and division of the internal hippocampal arterioles into vessels groups is impossible in view of their variable course and structure. The internal hippocampal arterioles differ much in size, shape, branches and supplying regions between themselves, so it is impossible to differentiate among them special branches for each cortical area of the hippocampus proper and also for the dentate gyrus. In the hippocampus these arterioles run variably from their various entrances in the hippocampal sulcus, in the direction of the CA1, CA2 and CA3 fields in different layers of the archicortex, giving off small arboreal branches in successive regions and cortical fields through which they run (Figs 3–5). One should emphasize that the course of the internal hippocampal arterioles in the hippocampus is topographically related to the folding and microscopic structure of the archicortex. These arterioles mostly run parallel along cortical hippocampal layers. Strongly developed, thick arterioles often run between the dentate gyrus and the hippocampus proper, in the molecular layer containing the fewest nerve cells bodies and most numerous nerve fibers in comparison with the

other layers (Fig. 6). The arterioles running this way, give off small branches to neighbouring cortical layers of the subiculum, to the dentate gyrus and CA1, CA2 fields, reaching the alveus and even the ependyma of the ventricular surface of the hippocampus and divide into bushy terminal small branches in the CA2 or CA3 field. Sometimes these arterioles are strongly bent and penetrate into the hilus of the dentate gyrus.

In senile brains showing advanced arterial atheromatous changes, and in people with arterial hypertension, the hippocampal arteries and the internal hippocampal arterioles in their extracerebral segments often have a changed shape and course. The hippocampal arteries are usually bent arcuately and serpentinely, they form elongated loops and siphons. Deformations of the internal arterioles assume the shape of lacunar ectases, excessively elongated arches and loops.

#### Arterial vascularization of the cat, rabbit and sheep hippocampus

The hippocampus in cat and sheep is supplied by its own vessels — the primary hippocampal arteries and arising from them internal, secondary hippocampal arterioles, forming just as in man a characteristic system. However, the hippocampal arteries in cat and sheep have a different, than in man, origin and structure.

In the cat brain these arteries, 1–3 singular trunks, 150–200  $\mu\text{m}$  in diameter, arise from the proximal segment of the thalamochochoidal branch of the posterior cerebral artery. They run arch-wise in the leptomeninx along the hippocampal sulcus, parallel to the maternal trunk and quite often they anastomose with one another. They give off many small internal arterioles at right angles as singular trunks or pedicles comprising 2–4 branches, which penetrate directly into the hippocampus along the hippocampal sulcus. They give off also thicker, but much fewer cortical branches running in the leptomeninx of the pyriform and occipital lobes. In cat, moreover, a singular hippocampal artery arises from the proximal segment of the anterior chorooidal artery and runs backward arch-wise to the inferior part of the hippocampus. In the superior part of the cat hippocampus the internal hippocampal arterioles arise with singular trunks at right angle directly from the trunk of the thalamochochoidal branch of the posterior cerebral artery.

In the sheep brain, the hippocampal arteries, 3–4 trunks, 250–300  $\mu\text{m}$  in diameter, arise at right angles from the proximal segments of the main cortical branches of the posterior cerebral artery and from the proximal segment of the anterior chorooidal artery. They run with singular straight trunks in the hippocampal sulcus and divide into many single trunks or grouped in pedicles of two to four, internal arterioles which penetrate directly into the hippocampus along the hippocampal sulcus.

In the rabbit brain, all internal arterioles as the singular or 2–4 trunks pedicles, arise at right angles directly from the main branch of the posterior cerebral artery surrounding the brain stem along the hippocampal sulcus. This branch, 200–250  $\mu\text{m}$  in diameter, also gives off many arterioles supplying the pulvinar and the geniculate bodies, and in its terminal segment it also supplies the occipital lobe cortex. The internal hippocampal arterioles are characterized



Fig. 7. Structure, course and supplying region of the internal arterioles (rri) in the cat hippocampus (Hip); ship — *sulcus hippocampi*, Plx — *plexus chorioideus*, Pima — *pia mater*. The right cerebral hemisphere, view on the postero-lateral side.  $\times 8.5$

by a long, loop-shape extracerebral course in the leptomeninx of the subiculum.

According to our results there are strong similarities in structure, course, topography and vascular extent of the internal hippocampal arteries in man, cat, rabbit and sheep. In these animal brains the arterioles penetrate into the hippocampus at right angle variably along the hippocampal sulcus and run in the direction of the CA1, CA2 and CA3 fields in different layers of the archicortex, however, mostly in the molecular layer (particularly in rabbit and sheep), almost parallel to one another, giving of small arborescent collateral branches to the subiculum, dentate gyrus and various neighbouring cortical areas. In their terminal segments they divide shaggily and bend arcuately in the direction of the concave surface of the hippocampus (Figs 7, 8). Cat, rabbit and sheep internal hippocampal arterioles, like human ones, comprise in their vascular regions different fields and layers of the hippocampal cortex in individual cases, so it is difficult to distinguish cytoarchitectonic groups of vessels among them. The diameter of the internal hippocampal arterioles fluctuates from 30 to 80  $\mu\text{m}$  in cat, from 40 to 100  $\mu\text{m}$  in rabbit and from 50 to 120  $\mu\text{m}$  in sheep.



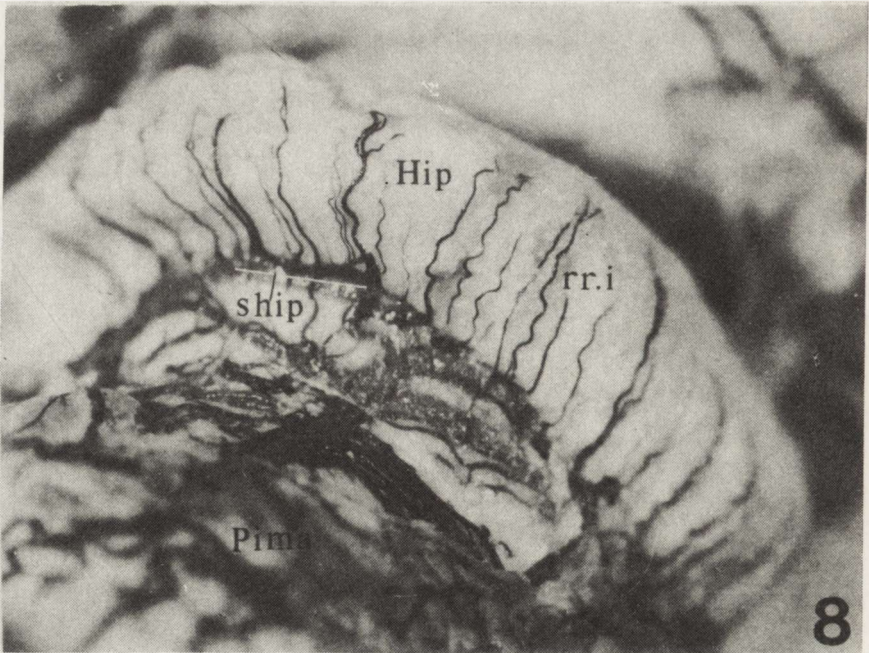


Fig. 8. Similar structure and topography of the internal arterioles (rri) in the sheep hippocampus (Hip); ship – *sulcus hippocampi*, Pima – *pia mater*. Right cerebral hemisphere, view on the side of the inferior horn of the lateral ventricle.  $\times 6.5$

#### DISCUSSION

Our studies have shown that both in man and in cat and sheep the hippocampus is supplied by the hippocampal arteries of the posterior cerebral artery, running along the hippocampal sulcus, and by the internal hippocampal arterioles arising from them at right angle. However, the studies of Scharrer (1940) and Nilgels (1944) did not prove the contribution of analogical arteries to the supply of the animal hippocampus. According to Nilgels (1944) the internal arterioles supplying the animal hippocampus with blood arise directly from the trunk of the posterior cerebral artery or from its main cortical branches. In our studies we have found this kind of origin of the internal hippocampal arterioles in the rabbit and also in the superior part of the cat hippocampus. Research performed on the topography and origin of the human hippocampal arteries allowed to distinguish the hippocampal segment in the course of the posterior cerebral artery. It lies in the ambient cistern, on the medial surface of the hippocampus in the region of the lateral geniculate body.

In our earlier results (Goetzen, Sztamska 1990; Sztamska 1991), the very similar structure and topography of the internal hippocampal arterioles both in man and in animals should be emphasized. These similarities are probably related to the very similar microscopic structure of the cortical hippocampal formations in all mammals (Gastaut, Lammers 1961).

Our studies have confirm the opinion of Uchimura (1928) who ascertained that the human internal hippocampal arterioles are anatomically terminal vessels. We have also shown, contrary to Nilgels' (1944) studies, animal internal hippocampal arterioles to also be anatomically terminal ones. However, unlike the results of Uchimura (1928), Nilgels (1944), Lindenberg (1957) and Gastaut and Lammers (1961), we have found that each cortical area of the hippocampus and dentate gyrus, both in man and in animals, is vascularized more or less equally and one cannot distinguish among the internal hippocampal arterioles the topographic groups of vessels. It is difficult to determine the anatomical criteria of their classification in view of their highly variable structure, topography and vascular regions.

The performed studies of the internal vascularization of the human and animal hippocampus allow the statement that it is supplied by very numerous, usually abundantly branched arterioles. Morphometric studies of the capillary vessels of the limbic system in man and animals (Lierse 1963; Kraszpulski, Wrzołkova 1987) also testify to the particularly reach vascularization of the hippocampus. According to our studies, the hippocampus in man and in cat has usually a well developed own system of arterial anastomoses in the form of the arterial arcades, making collateral circulation possible. The hippocampal arteries derived from the anterior choroidal artery are an additional protection for the circulation in the human hippocampus — they lead blood to the hippocampus from the supplementary anterior arterial source of the brain.

On the ground of the performed studies one can conclude that, considering the arterial vascularization of the hippocampus in man, cat, rabbit and sheep, these animals can serve as experimental models for study of blood circulation in the hippocampus and angiogenic pathologic lesions of the latter. However, in these experiments one should take into consideration the differences in the sources of the arterial supply to the hippocampus in man and animals, related to the different structures of their brain arterial circles. A cat is more suitable model for the cerebral circulation study with reference to man than rabbit and sheep.

#### CONCLUSIONS

1. The posterior cerebral arteries, the main source of the vascularization of the hippocampus, arise from different maternal trunks in the human, cat, rabbit and sheep brains.
2. The arterial vascularization of the hippocampus in man, cat, sheep and rabbit is similar especially in its internal area.
3. There are not significant anatomical differences in the angioarchitectonics of the different fields and cortical regions of the hippocampus.
4. The internal arterioles penetrating into the hippocampal cortex in man, cat, rabbit and sheep are anatomically terminal vessels.
5. The human and animal arterial hippocampal system, in comparison with the other vascular areas of their cerebral cortex, distinguish itself with stronger developed structure and, moreover, it creates anatomical conditions for the collateral circulation.

## ANATOMIA PORÓWNAWCZA UNACZYNIENIA TĘTNICZEGO HIPOKAMPA U CZŁOWIEKA I ZWIERZĄT DOŚWIADCZALNYCH (KOTA, KRÓLIKA I OWCY)

### Streszczenie

Badania wykonano własną metodą iniekcijną na 30 mózgach ludzi i 80 mózgach zwierząt. Tętnice mózgowe nastrzyknięto barwnymi lateksami syntetycznymi i preparowano pod mikroskopem operacyjnym.

Stwierdzono, że główne źródło zaopatrzenia tętniczego hipokampa, zarówno u człowieka, jak i u zwierząt, stanowi tętnica tylna mózgu. Tętnica ta w kołach tętniczych mózgow człowieka, kota, królika i owcy ma jednakże różne miejsca odejścia. Badania porównawcze wykazały ponadto, że układ naczyniowy hipokampa u człowieka i zwierząt jest bardzo podobny. Jest on utworzony przez gałęzie tętnicy tylnej mózgu i tętnicy naczyniówkowej przedniej, zwane tętnicami hipokampa oraz przez odchodzące od nich pod kątem prostym liczne wewnętrzne tętniczki hipokampa. Opisany w piśmiennictwie topograficzny podział tych tętniczek jest niemożliwy ze względu na ich zmienny przebieg w korze hipokampa oraz podobne unaczynienie różnych obszarów korowych hipokampa. Badania wykazały także, że układ tętniczy hipokampa jest bardzo dobrze wyształcony i stwarza możliwość krążenia obocznego. W mózgach starczych, a zwłaszcza w mózgach ze zmianami miażdżycowymi naczyń, zewnątrz- i wewnątrz-mózgowe odcinki tętnic i tętniczek hipokampa wykazują zniekształcenia w postaci wydłużonych syfonów, pętli i kłębków naczyniowych.

### REFERENCES

1. Gastaut H, Lammers HJ: Anatomie du rhinencéphale. Les grandes activités du rhinencéphale. V 1. Masson et Cie, Paris, 1961.
2. Goetzen B: Zastosowanie lateksów syntetycznych w anatomicznych badaniach naczyń i przewodów. Pol. Tyg Lek, 1957, 12, 296–301.
3. Goetzen B, Sztamska E: Vascularisation de l'hippocampe ventral chez l'homme et les animaux d' experimentation. Bull Soc. Anat Paris 1990, 14, 79–85.
4. Heiman M: Über Gefäßstudien am aufgehellten Gehirn: I. Die Gefäße des Ammonshornes. Schweiz Arch Neurol Psychiat, 1938, 40, 277–301.
5. Kraszpulski M, Wrzołkowska T: Blood-brain exchange in various regions of the limbic system. Morphologic studies. Neuropatol Pol, 1987, 25, 265, 271.
6. Lierse W: Die Kapillardichte im Rhinencephalon verschiedener Wirbeltiere und Menschen. In: The rhinencephalon and related structures. Eds: W Bargman, JP Schade. Prog Brain Res, V 3, Elsevier, Amsterdam, 1963.
7. Linderberg R: Die Gefäßversorgung und ihre Bedeutung für Gewebsschäden. Die eigentlichen Hirnarterien. In: Handbuch der speziellen pathologischen Anatomie und Histologie. Bdt 13/1B. Eds: O Lubarsch, R Rössle, F Henke. Springer, Berlin, 1957.
8. Muller J, Shaw L: Arterial vascularization of the human hippocampus. Arch Neurol, 1965, 13, 45–47.
9. Nilgels RG: The arteries of the mammalian *cornu ammonis*. J Comp Neurol, 1944, 80, 197–190.
10. Scharrer E: Vascularization and vulnerability of the *cornu ammonis* in the opossum. Arch Neurol Psychiat, 1940, 44, 486–506.
11. Spielmeier W: Zur Pathogenese örtlich elektiver Gehirnveränderungen. Ztschr Neurol Psychiat, 1925.
12. Sztamska E: Unaczynienie tętnicze wężomózgowia i hipokampa człowieka oraz zwierząt doświadczalnych (kota i owcy). PhD-thesis, School of Medicine, Łódź, 1991.
13. Uchimura I: Zur Pathogenese der örtlich elektiven Ammonshornerkrankung. Ztschr Neurol Psychiat, 1928, 114, 567–601.

Authors' address: Laboratory of Angiology of the Central Nervous System, Department of Neurology, School of Medicine, 20 Kopcińskiego Str., 90–153 Łódź, Poland

NAJKORZYSTNIEJSZE CENY I NAJBOGATSZA OFERTA  
W PLACÓWKACH WŁASNYCH WYDAWNICTWA OSSOLINEUM

- 50-106 WROCŁAW, Rynek 6, tel. 336-66  
50-227 WROCŁAW, ul. Kleczkowska 44, tel. 214-861 (magazyn hurtowy i księgarnia wysyłkowa)  
31-110 KRAKÓW, ul. Św. Jana 28, tel. 225-844 (sprzedaż detaliczna i hurtowa)  
00-634 WARSZAWA, ul. Jaworzyńska 4, tel. 254-366  
90-447 ŁÓDŹ, ul. Piotrkowska 181, tel. 361-943  
61-745 POZNAŃ, al. Marcinkowskiego 30, tel. 521-916  
80-855 GDAŃSK, ul. Łagiewniki 56, tel. 315-133 (książki i muzykalia)  
70-551 SZCZECIN, pl. Żołnierza Polskiego 1, tel. 345-65  
44-100 GLIWICE, al. Zwycięstwa 37 (w organizacji)

Pełny asortyment wydawnictw ossolińskich oferują też księgarnie Ośrodka Rozpowszechniania Wydawnictw Naukowych PAN:

- 00-901 Warszawa, Pałac Kultury i Nauki  
31-020 Kraków, ul. Św. Marka 22  
61-725 Poznań, ul. Mielżyńskiego 27/29  
15-082 Białystok, ul. Świętojańska 13  
40-077 Katowice, ul. Bankowa 14, paw. D, I p.  
20-031 Lublin, pl. M. Curie-Skłodowskiej 5.

Ponadto sprzedaż edycji Ossolineum prowadzą większe księgarnie: 00-068 WARSZAWA, ul. Krakowskie Przedmieście 7, Główna Księgarnia Naukowa im. Bolesława Prusa; 31-118 KRAKÓW, ul. Podwale 6, Księgarnia „Elefant”; 87-100 TORUŃ, ul. Kościuszki 9, Księgarnia „Indeks”; 45-015 OPOLE, Rynek 19/20, Księgarnia „Omega”.

Zapraszamy do współpracy księgarzy, agencje kolporterskie i odbiorców indywidualnych. Hurtownicy mogą kupić nasze książki po cenach zbytu bezpośrednio w Wydawnictwie. Odbiór następuje transportem własnym lub przesyłką pocztową na koszt odbiorcy. Rozliczenie należności dopuszczamy w różnych formach: wpłaty gotówką lub czekiem potwierdzonym w banku bezpośrednio do kasy Wydawnictwa, albo przelewem na nasze konto w Wielkopolskim Banku Kredytowym S.A. O/Wrocław nr 359209-1078 (w terminie 14 dni od otrzymania towaru).

OSSOLINEUM – YOUR CHEAPEST AND MOST RELIABLE SUPPLIER  
OF ACADEMIC BOOKS AND PERIODICALS

You can send orders directly at the Export Department of the Ossolineum Publishing House, Rynek 9, 50-106 Wrocław, Poland. No advance payment is required. For orders containing more than 10 titles a considerable discount will be granted. Our bank account: Wielkopolski Bank Kredytowy S.A. O/Wrocław, 359209-1078.

Zakład Narodowy im. Ossolińskich – Wydawnictwo. Wrocław 1992.  
Objętość: ark. wyd. 6,80; ark. druk. 6,0; ark. A<sub>1</sub>–8.  
Wrocławska Drukarnia Naukowa. Zam. 2201/92.

CONTENTS

M. Dąbska: Perinatal damage of brain stem depending on the maturity of its structures	91
G. Szumańska, R. Gadamski: Lectin histochemistry and alkaline phosphatase activity in the pia mater vessels of spontaneously hypertensive rats (SHR)	99
B. Gajkowska, M. J. Mossakowski: Calcium accumulation in synapses of the rat hippocampus after cerebral ischemia	111
A. Kapuściński: Changes in endogenous prostacyclin in the rat brain during clinical death and after resuscitation	127
H. Kroh, A. Taraszewska, E. Ruzikowski, J. Bidziński, M. J. Mossakowski: Neuropathological changes in resected temporal lobe of patients with cryptogenic epilepsy	133
I. Niebrój-Dobosz, J. Rafałowska, M. Łukasiuk, W. Wiśniewska, D. Dziewulska: Influence of aging on the protein profile of myelin isolated from human brain white matter	147
M. Barcikowska, E. Kida, E. Joachimowicz, A. Siekierzyńska: Cerebellar granular layer degeneration in small cell lung cancer: paraneoplastic cerebellopathy or artifact?	155
E. Matyja, I. Kuchna, M. Ząbek: Cerebral ganglioglioma with long history and unusual prominence of the mesenchymal elements. Case report	165
B. Goetzen, E. Sztamska: Comparative anatomy of the arterial vascularization of the hippocampus in man and in experimental animals (cat, rabbit and sheep)	173